Inside Track with Klaus Werner, RF Energy Alliance | 24

Smart Homes Delivering Sustainability | 33

Boosting Public Safety via Communications | 45

Microwaves & RF®

MARCH 2017 TRUSTED ENGINEERING RESOURCE FOR OVER 50 YEARS www.mwrf.com

Impedance Tuners IN CONTROL

p| 100

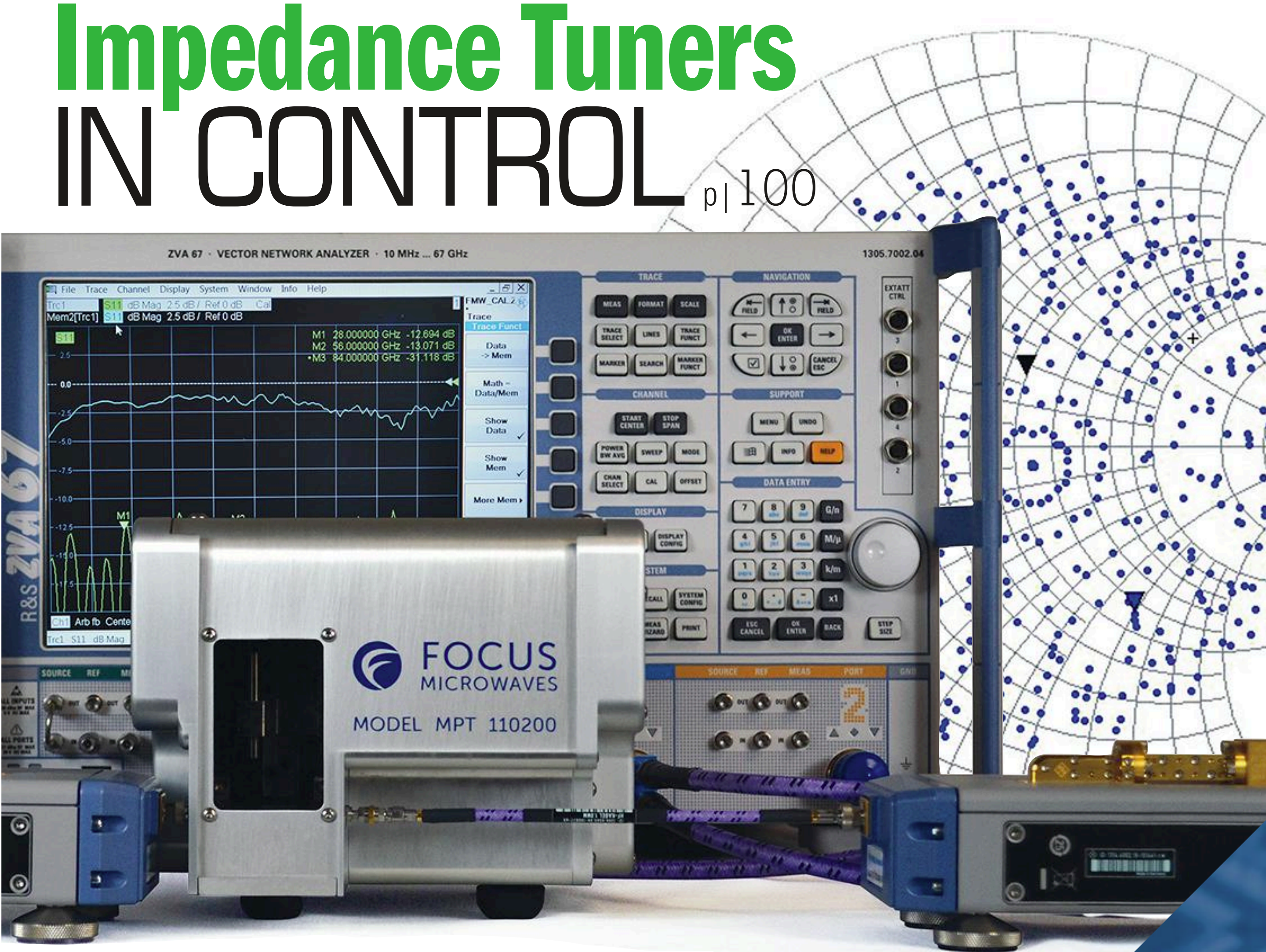

$10.00 Powered by Penton
Periodicals Postage Paid • USPS 100 Approved Poly

- Amplifiers – Solid State
- Attenuators – Variable/ Programmable
- Couplers (Quadrature, 180° & Directional)
- Detectors – RF/Microwave
- DLVAs, ERDLVAs & SDLVAs
- DTOs, VCOs, PLO, DROs, & Frequency Synthesizers
- Filters & Switched Filter Banks
- Form, Fit, Functional Products & Services
- Frequency Discriminators & IFMs
- Integrated MIC/MMIC Assemblies (IMAs)
- IQ Vector Modulators
- Limiters – RF/Microwave
- Log Amplifiers
- Millimeter Wave Components (Up to 50 GHz)
- Miscellaneous Products
- Monopulse Comparators
- Multifunction Integrated Assemblies (MIAs)
- Phase Shifters & Bi-Phase Modulators
- Power Dividers/Combiners (Passive & Active)
- Pulse Modulators (SPST)
- Rack & Chassis Mount Products
- Receiver Front Ends & Transceivers
- SDLVAs, ERDLVAs & DLVAs
- Single Side Band Modulators
- SMT & QFN Products
- Switch Matrices
- Switched Filter Banks
- Switches – Solid State
- Systems – Fly Eye Radars
- Threshold Detectors
- USB Products

Planar Monolithics Industries, Inc.

Ultra Broadband State-Of-The-Art 360° Digital Phase Shifters

PMI offers the highest quality phase shifters for industrial and military applications in the frequency range of 85 MHz to 10 GHz. These models offer a 360° phase shift with various options available.

Model: PS-200M10G-8B-SFF

http://www.pmi-rf.com/products/phaseshift-biphasemod/phaseshifters/PS-200M10G-8B-SFF.htm

Frequency	200 MHz to 10.0 GHz
Insertion Loss	10.5 dB Typ - Measured 8.0 dB
VSWR	2.4:1 Output, 1.5:1 Input
Amplitude Error	±1 dB Typ. - Measured ±0.1 dB
Phase Accuracy	±0.5° Typ. - Measured ±0.35°
Control	8-BIT TTL Compatible: 15 Pin Sub-D (Male)
Temperature	-55 °C to +85 °C

Package Size: 3.25" X 3.25" X 0.84"
DC Voltage: -15 VDC @ 21 mA
+15 VDC @ 189 mA
Switching Speed: Measured <250 ns

Model: PS-85M4G-9B-SFF

http://www.pmi-rf.com/Products/phaseshift-biphasemod/phaseshifters/PS-85M4G-9B-SFF.htm

Frequency	85 MHz to 4.0 GHz
Insertion Loss	13 dB Max - Measured 10.1 dB
VSWR	1.75:1 Typ - Measured 1.65:1
Amplitude Error	±1 dB Typ. - Measured ±1.91 dB
Phase Shift Error	±10° Max - Measured +13.4°/ -13.1°
Control	10-Bit TTL Compatible: 15 Pin Sub-D (Male)
Temperature	0 °C to +50 °C (Operating)

Package Size: 4.95" X 3.38" X 1.0"
DC Voltage: -15 VDC @ 38 mA
+15 VDC @ 265 mA
Switching Speed: Measured <300 ns

Model: PS-2G6G-8B-SFF

http://www.pmi-rf.com/Products/phaseshift-biphasemod/phaseshifters/PS-2G6G-8B-SFF.htm

Frequency	2.0 to 6.0 GHz
Insertion Loss	10.5 dB Typ - Measured 8.0 dB
VSWR	2.4:1 Output, 1.5:1 Input
Amplitude Error	±1 dB Typ. - Measured ±0.1 dB
Phase Accuracy	±0.5° Typ. - Measured ±0.35°
Control	8-BIT TTL Compatible: 15 Pin Sub-D (Male)
Temperature	-55 °C to +85 °C

Package Size: 3.25" X 3.25" X 0.84"
DC Voltage: -15 VDC @ 21 mA
+15 VDC @ 189 mA
Switching Speed: Measured <250 ns

Model: PS-500M2G-8B-SFF & PS-500M2G-10B-SFF

http://www.pmi-rf.com/Products/phaseshift-biphasemod/phaseshifters/PS-500M2G-8B-SFF.htm
http://www.pmi-rf.com/Products/phaseshift-biphasemod/phaseshifters/PS-500M2G-10B-SFF.htm

Frequency	0.5 to 2.0 GHz	PS-500M2G-8B-SFF	PS-500M2G-10B-SFF
Insertion Loss	13 dB Typ	9.77 dB	8.20 dB
VSWR	1.75:1	1.61:1	1.65:1
Amplitude Error	±1 dB Typ.	±0.61 dB	±0.23 dB
Phase Shift Error	±10° Max	±0.48°	±0.34°
Control	8-BIT TTL 15 Pin Sub-D (Male): PS-500M2G-8B-SFF 10-BIT TTL 15 Pin Sub-D (Male): PS-500M2G-10B-SFF		
Temperature	0 °C to +50 °C (Operating)		

Package Size: 4.95" X 3.38" X 1.0"
DC Voltage: -15 VDC @ 18 mA
+15 VDC @ 249 mA
Switching Speed: Measured <300 ns

West Coast Operation:
4921 Robert J. Mathews Pkwy, Suite 1
El Dorado Hills, CA 95762 USA
Tel: 916-542-1401, Fax: 916-265-2597

East Coast Operation:
7311-F Grove Road
Frederick, MD 21704 USA
Tel: 301-662-5019, Fax: 301-662-1731

sales@pmi-rf.com • www.pmi-rf.com

ISO9001-2008 REGISTERED

VOLUME 56, ISSUE 3

In This Issue

FEATURES

100 **COVER STORY:**
MULTIPURPOSE TUNERS CONTROL IMPEDANCES FROM 20 TO 110 GHz
These versatile electromechanical tuners can create impedances using three independently adjustable wideband probes at three harmonic frequencies continuously from 20 to 110 GHz.

33 HOW SMART HOMES CAN DELIVER SUSTAINABILITY AS A SERVICE
Smart-home services have the potential to impact households in a profound way.

39 MODULATION AND DEMODULATION, PART 2
Digital modulation/demodulation formats provide options in terms of bandwidth efficiency, power efficiency, and complexity/cost when meeting a modern communications system's data-transfer needs.

45 DEVICE-TO-DEVICE COMMUNICATION AIDS PUBLIC SAFETY
LTE technology is enabling a wave of public safety communication networks.

50 LOW-NOISE AMPLIFIER SPANS DC TO 17 GHz
This pHEMT LNA design combines low-frequency and high-frequency circuit techniques to achieve extremely low noise levels over a wide frequency range.

54 DESIGNING A STEP-RECOVERY-DIODE-BASED COMB GENERATOR
By leveraging advanced software, accurate results were obtained in the design and testing of a comb generator.

56 METAMATERIALS SCULPT UWB BANDPASS FILTER
By combining left- and right-handed transmission lines with conventional microstrip circuitry, it is possible to achieve a wide passband for a UWB bandpass filter.

65 WHAT'S THE DIFFERENCE BETWEEN OPTICAL AND WIRELESS COMMUNICATIONS?
Wireless and optical communications technologies are often found on the same cellular communications tower, supporting modern communications using different wavelengths.

100

33

65

PRODUCT TECHNOLOGY

103 Vector Network Analyzers
108 Oscilloscopes for Complex Signals
110 Wideband Mixers
112 Coaxial Terminations
114 Modeling and Simulation Software
116 Module Evaluation Kits

JOIN US ONLINE

follow us @MicrowavesRF

become a fan at facebook.com/microwavesRF

NEWS & COLUMNS

10 ON MWRF.COM
13 EDITORIAL
18 FEEDBACK
20 NEWS
24 INSIDE TRACK with Klaus Werner, RF Energy Alliance

28 R&D ROUNDUP
98 APPLICATION NOTES
118 NEW PRODUCTS
120 ADVERTISERS INDEX

defense electronics

Starts on p. **79**

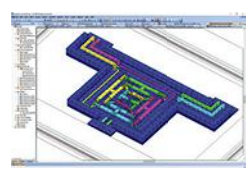

The Trusted Name in RF, Microwave & Millimeterwave ICs

Featured MACOM MMIC Devices

Application	Function	Part Number
Aerospace & Defense	Low Noise Amplifier Octave Band VCO Power Amplifier	MAAM-011229, 0.05 - 4 GHz MAOC-415000, 10 - 20 GHz MAAP-011232, 0.1 - 3 GHz
SATCOM	Ka-Band Power Amplifier Doubler Power Amplifier L-Band Power Amplifier Module	MAAP-011289, 28 - 30.5 GHz MAFC-011009, 28 - 30 GHz MAAP-011060, 1616 - 1627 MHz
Test & Measurement	Wideband Power Amplifier Wideband Low Noise Amplifier Wideband DBL BAL Mixer	MAAP-011247, DC - 22 GHz MAAL-011141, DC - 26.5 GHz MAMX-011036, 8 - 43 GHz
Industrial, Scientific & Medical	Low Noise Amplifier Gain Block	MAAL-011129, 18 - 32 GHz MAAM-011206, DC - 15 GHz
Wired Broadband	Variable Gain Amplifier Gain Block Very Low Noise Amplifier	MAAM-011194, 45 - 1218 MHz MAAM-011220, 45 - 1218 MHz MAAL-011136, 45 - 1218 MHz

onMicrowaves&RF.com

REVERSING 25 YEARS OF ANTENNA DEGRADATION

http://mwrf.com/passive-components/reversing-25-years-antenna-degradation

Does anyone remember pulling out the antenna on your first mobile phone to make a call? Over the past 25 years, antenna design has changed radically for cell phones. While transitioning from 2G to 3G to LTE, we have incrementally and gradually sacrificed as much as 10 dB of link budget in some cases. It's shocking but true: The network has improved dramatically, so we've been able to compromise performance in the handset antenna without much backlash from consumers.

BASICS OF MODULATION AND DEMODULATION

http://mwrf.com/systems/basics-modulation-and-demodulation

Information can be sent from a transmitter to a receiver by means of modulation and demodulation, respectively, whether those signals are light waves moving through optical cables, radio waves through metallic cables, or radio waves propagating through the air. The electromagnetic (EM) waves that transport the information are referred to as carrier signals, while the information they carry may be in the form of audio, video, or data. Find out more in Part 1 of this two-part report.

IoT GROWTH BANKS ON RELIABLE COMMUNICATION

http://mwrf.com/iot/iot-growth-banks-reliable-communication

According to technology industry researcher Gartner, the number of "things" in the Internet of Things (IoT) increases by 5.5 million each day. By 2020, the total number is expected to reach 20.8 billion. Given such explosive growth, it's imperative to examine the internet that will connect and enable communication between all of these things. Creating reliable wireless connectivity among devices is proving to be one of the IoT's greatest challenges.

7 KEY ELEMENTS OF LEO AND GEO SPACE SATELLITES

http://mwrf.com/blog/7-key-elements-leo-and-geo-space-satellites

Innovations in the small satellite industry have been increasing at a tremendous rate in recent years. This growth can be attributed to exponential increases in technology and the demand for broadband connectivity in remote locations all around the world. Low earth orbit (LEO) and geostationary (GEO) satellites are big players in this skyrocketing industry, and the future for both is looking bright. Here are the top seven criteria you should review when trying to understand both.

join us online

twitter.com/MicrowavesRF facebook.com/microwavesrf

Editorial

CHRIS DeMARTINO
Technical Editor
chris.demartino@penton.com

LoRa's Got Game

A few months back, I wrote a column titled, "Narrowband-IoT Proves its Worth" (*http://mwrf.com/blog/narrowband-iot-proves-its-worth*), explaining how Narrowband-IoT (NB-IoT) technology is shaping up to be a key player in the Internet of Things (IoT) game. But of course, NB-IoT is not the only game in town. Another technology that is clearly making a name for itself is LoRa..

As I wrote last year, LoRa derives its name from its ability to enable "long-range" communications. It essentially achieves longer range at the expense of lower data rates. In North America, LoRaWAN networks operate in the industrial, scientific, and medical (ISM) frequency band from 902 to 928 MHz, while Europe uses the frequency band from 867 to 869 MHz.

LoRa, which was developed by Semtech, is based on spread spectrum technology. Currently, Semtech offers the SX127X LoRa transceiver product line, as well as the SX1301 digital baseband chip. More information regarding LoRa can be found on the company's IoT page at *http://www.semtech.com/wireless-rf/internet-of-things/*.

The LoRa Alliance is an open, non-profit association of members. Its goal is to standardize low-power-wide-area-networks (LPWANs) that are being deployed worldwide. Currently, the Alliance consists of hundreds of member from all across the world.

Two companies—both of which are LoRa Alliance members—recently made announcements regarding LoRa. For one, Anritsu announced it intends to create new test and measurement solutions for research and development, certification, and manufacturing of LoRa-equipped IoT devices. Some of the company's general-purpose test instruments can be adapted to meet IoT requirements.

In addition, Ethertronics recently made news by announcing its plug-and-play LoRa module for LPWAN connectivity. It takes advantage of the company's Active Steering technology to bring long-range performance to IoT/M2M applications.

On a final note, anyone interested in learning more about NB-IoT and LoRa may want to check out the white paper, *"NB-IoT vs. LoRa Technology: Which Could Take Gold?"* The paper discusses technical differences between both technologies and reviews how each fits into different IoT applications. mw

EDITOR'S NOTE: On another topic, those in the Long Island, N.Y., area should take note of the Long Island RF/Microwave Symposium & Exhibits on April 6. The event will consist of an exhibition along with technical lectures. Visit www.ieee.li/microwave/.

JOIN US ONLINE twitter.com/MicrowavesRF
become a fan at facebook.com/MicrowavesRF

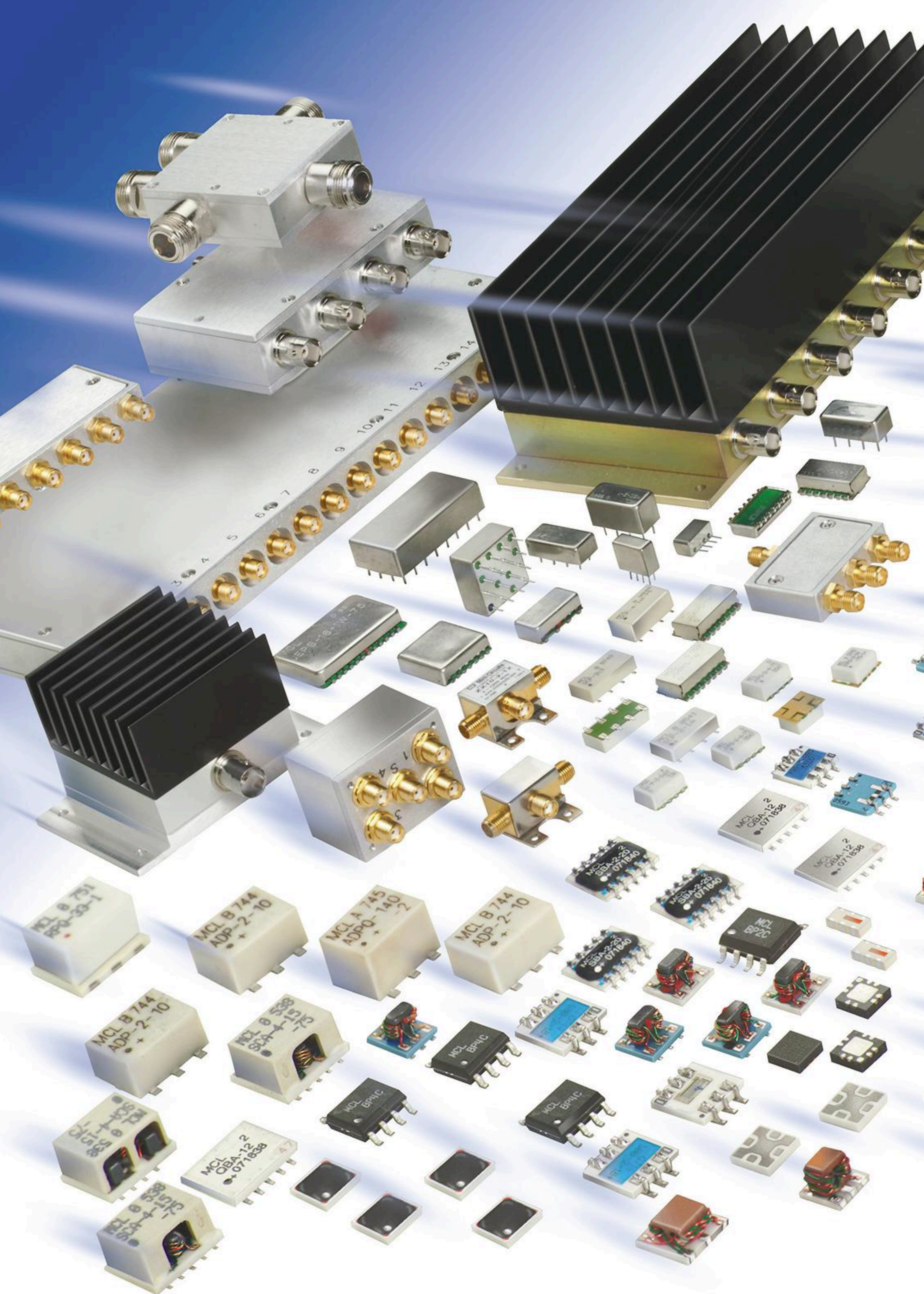
MCL B 744
ADP-2-10
MCL A 745
ADPQ-140 -2
MCL B 538
SCA-4-15 -75
MCL QBA-12 2
071838
MCL SBA-2-20
071640
MCL BP2C
MCL BPNC

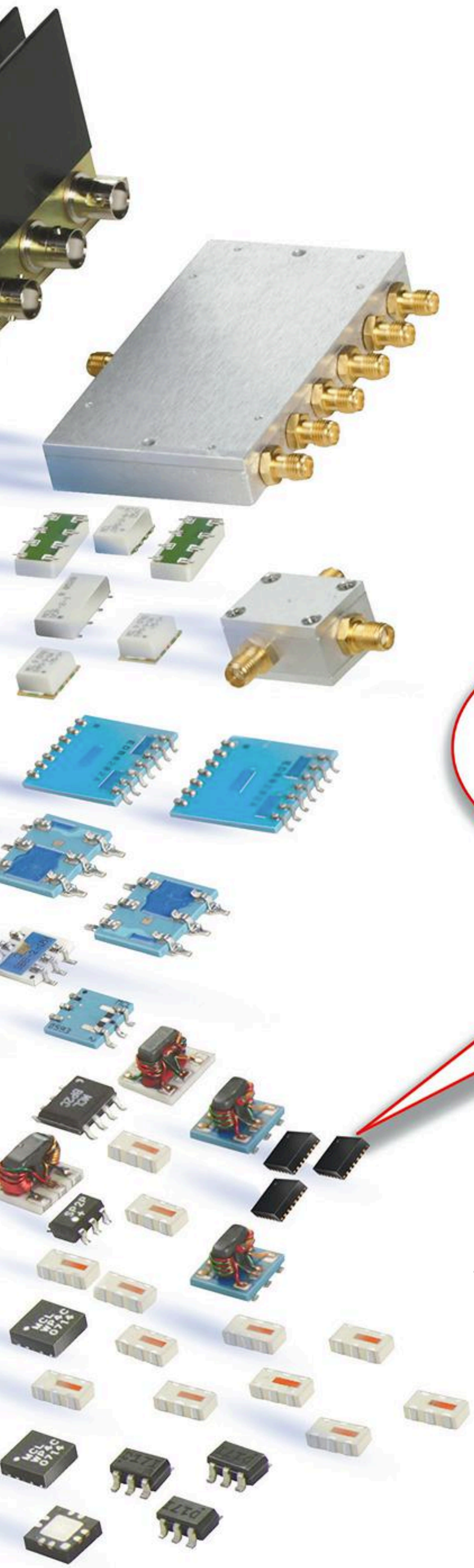

MARCH | 2017 **Microwaves&RF**

Powered by Penton

EDITORIAL

CONTENT DIRECTOR: **NANCY K. FRIEDRICH** nancy.friedrich@penton.com
TECHNICAL CONTRIBUTOR: **JACK BROWNE** jack.browne@penton.com
TECHNICAL ENGINEERING EDITOR: **CHRIS DeMARTINO** chris.demartino@penton.com
CONTENT PRODUCTION DIRECTOR: **MICHAEL BROWNE** michael.browne@penton.com
PRODUCTION EDITOR: **JEREMY COHEN** jeremy.cohen@penton.com
CONTENT PRODUCTION SPECIALIST: **ROGER ENGELKE** roger.engelke@penton.com
CONTENT OPTIMIZATION SPECIALIST: **WES SHOCKLEY** wes.shockley@penton.com
ASSOCIATE CONTENT PRODUCER: **LEAH SCULLY** leah.scully@penton.com
ASSOCIATE CONTENT PRODUCER: **JAMES MORRA** james.morra@penton.com

ART DEPARTMENT

GROUP DESIGN DIRECTOR: **ANTHONY VITOLO** tony.vitolo@penton.com
SENIOR ARTIST: **JIM MILLER** jim.miller@penton.com
CONTENT DESIGN SPECIALIST: **JOCELYN HARTZOG** jocelyn.hartzog@penton.com
CONTENT DESIGN SPECIALIST: **TIM DRIVER** tim.driver@penton.com
CONTENT & DESIGN PRODUCTION MANAGER: **JULIE JANTZER-WARD** julie.jantzer-ward@penton.com

PRODUCTION

GROUP PRODUCTION MANAGER: **CAREY SWEETEN** carey.sweeten@penton.com
PRODUCTION MANAGER: **VICKI MCCARTY** vicki.mccarty@penton.com
CLASSIFIED PRODUCTION COORDINATOR: **LINDA SARGENT** linda.sargent@penton.com

AUDIENCE MARKETING

USER MARKETING DIRECTOR: **BRENDA ROODE** brenda.roode@penton.com
USER MARKETING MANAGER: **DEBBIE BRADY** debbie.brady@penton.com
FREE SUBSCRIPTION/STATUS OF SUBSCRIPTION/ADDRESS CHANGE/MISSING BACK ISSUES
OMEDA **T** | 847.513.6022 **TOLL FREE** | 866.505.7173

SALES & MARKETING

MANAGING DIRECTOR: **TRACY SMITH** **T** | 913.967.1324 **F** | 913.514.6881 tracy.smith@penton.com

REGIONAL SALES REPRESENTATIVES

AZ, NM, TX: **GREGORY MONTGOMERY** **T** | 480.254.5540 gregory.montgomery@penton.com
AK, CA, CO, ID, MT, ND, NV, OR, SD, UT, WA, WI, WY, W/CANADA: **JAMIE ALLEN** **T** | 415.608.1959 **F** | 913.514.3667 jamie.allen@penton.com
AL, AR, IA, IL, IN, KS, KY, LA, MI, MN, MO, MS, NE, OH, OK, TN: **PAUL MILNAMOW** **T** | 312.840.8462 paul.milnamow@penton.com
CT, DE, FL, GA, MA, MD, ME, NC, NH, NJ, NY, RI, PA, SC, VA, VT, WV, EASTERN CANADA: **SHANNON ALO-MENDOSA** **T** | 978.501.7303 shannon.alo-mendosa@penton.com

INTERNATIONAL SALES

GERMANY, AUSTRIA, SWITZERLAND: **CHRISTIAN HOELSCHER** **T** | 011.49.89.95002778 christian.hoelscher@husonmedia.com
BELGIUM, NETHERLANDS, LUXEMBURG UNITED KINGDOM, SCANDINAVIA, FRANCE, SPAIN, PORTUGAL: **JAMES RHOADES-BROWN** **T** | +011 44 1932 564999 **M** | +011 44 1932 564998 james.rhoadesbrown@husonmedia.com
PAN-ASIA: **HELEN LAI** **T** | 886 2-2727 7799 helen@twoway-com.com

PLEASE SEND INSERTION ORDERS TO: orders@penton.com
PENTON REPRINTS: **WRIGHT'S MEDIA** **T** | 877.652.5295 penton@wrightsmedia.com

LIST RENTALS:
SMARTREACH CLIENT SERVICES MANAGER: **JAMES ADDISON** **T** | 212.204.4318 james.addison@penton.com

ONLINE

PRODUCT DEVELOPMENT DIRECTOR: **RYAN MALEC** ryan.malec@penton.com

DESIGN ENGINEERING & SOURCING GROUP

EXECUTIVE DIRECTOR OF CONTENT AND USER ENGAGEMENT: **NANCY K. FRIEDRICH**
GROUP DIRECTOR OF OPERATIONS: **CHRISTINA CAVANO**
GROUP DIRECTOR OF MARKETING: **JANE COOPER**

PENTON

1166 AVENUE OF THE AMERICAS, 10TH FLOOR, NEW YORK, NY 10036 **T** | 212.204.4200

Penton

Electronic Design | Machine Design | Microwaves & RF | Source ESB | Hydraulics & Pneumatics | Global Purchasing | Distribution Resource | Power Electronics | Defense Electronics

PENTON IS AN INFORMA BUSINESS

RF Amplifiers and Sub-Assemblies for Every Application

Delivery from Stock to 2 Weeks ARO from the catalog or built to your specifications!

- Competitive Pricing & Fast Delivery
- Military Reliability & Qualification
- Various Options: Temperature Compensation, Input Limiter Protection, Detectors/TTL & More
- Unconditionally Stable (100% tested)

ISO 9001:2000 and AS9100B CERTIFIED

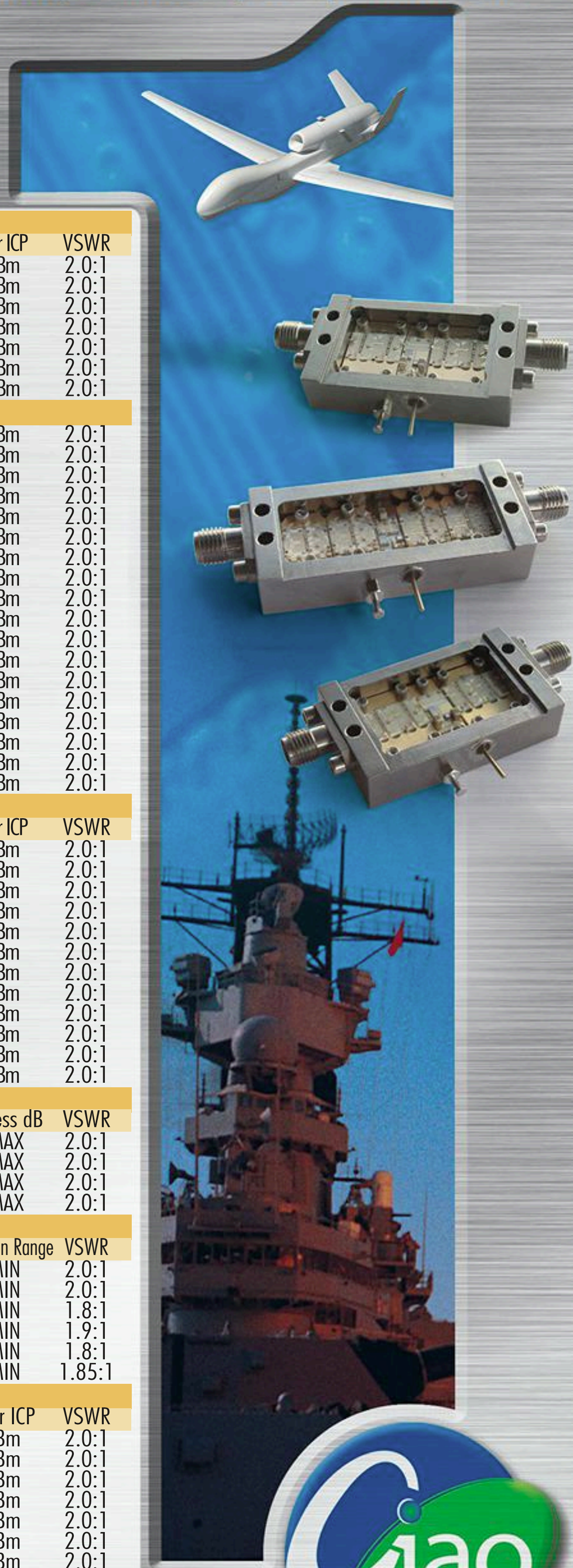

OCTAVE BAND LOW NOISE AMPLIFIERS

Model No.	Freq (GHz)	Gain (dB) MIN	Noise Figure (dB)	Power-out @ P1-dB	3rd Order ICP	VSWR
CA01-2110	0.5-1.0	28	1.0 MAX, 0.7 TYP	+10 MIN	+20 dBm	2.0:1
CA12-2110	1.0-2.0	30	1.0 MAX, 0.7 TYP	+10 MIN	+20 dBm	2.0:1
CA24-2111	2.0-4.0	29	1.1 MAX, 0.95 TYP	+10 MIN	+20 dBm	2.0:1
CA48-2111	4.0-8.0	29	1.3 MAX, 1.0 TYP	+10 MIN	+20 dBm	2.0:1
CA812-3111	8.0-12.0	27	1.6 MAX, 1.4 TYP	+10 MIN	+20 dBm	2.0:1
CA1218-4111	12.0-18.0	25	1.9 MAX, 1.7 TYP	+10 MIN	+20 dBm	2.0:1
CA1826-2110	18.0-26.5	32	3.0 MAX, 2.5 TYP	+10 MIN	+20 dBm	2.0:1

NARROW BAND LOW NOISE AND MEDIUM POWER AMPLIFIERS

Model No.	Freq (GHz)	Gain (dB) MIN	Noise Figure (dB)	Power-out @ P1-dB	3rd Order ICP	VSWR
CA01-2111	0.4 - 0.5	28	0.6 MAX, 0.4 TYP	+10 MIN	+20 dBm	2.0:1
CA01-2113	0.8 - 1.0	28	0.6 MAX, 0.4 TYP	+10 MIN	+20 dBm	2.0:1
CA12-3117	1.2 - 1.6	25	0.6 MAX, 0.4 TYP	+10 MIN	+20 dBm	2.0:1
CA23-3111	2.2 - 2.4	30	0.6 MAX, 0.45 TYP	+10 MIN	+20 dBm	2.0:1
CA23-3116	2.7 - 2.9	29	0.7 MAX, 0.5 TYP	+10 MIN	+20 dBm	2.0:1
CA34-2110	3.7 - 4.2	28	1.0 MAX, 0.5 TYP	+10 MIN	+20 dBm	2.0:1
CA56-3110	5.4 - 5.9	40	1.0 MAX, 0.5 TYP	+10 MIN	+20 dBm	2.0:1
CA78-4110	7.25 - 7.75	32	1.2 MAX, 1.0 TYP	+10 MIN	+20 dBm	2.0:1
CA910-3110	9.0 - 10.6	25	1.4 MAX, 1.2 TYP	+10 MIN	+20 dBm	2.0:1
CA1315-3110	13.75 - 15.4	25	1.6 MAX, 1.4 TYP	+10 MIN	+20 dBm	2.0:1
CA12-3114	1.35 - 1.85	30	4.0 MAX, 3.0 TYP	+33 MIN	+41 dBm	2.0:1
CA34-6116	3.1 - 3.5	40	4.5 MAX, 3.5 TYP	+35 MIN	+43 dBm	2.0:1
CA56-5114	5.9 - 6.4	30	5.0 MAX, 4.0 TYP	+30 MIN	+40 dBm	2.0:1
CA812-6115	8.0 - 12.0	30	4.5 MAX, 3.5 TYP	+30 MIN	+40 dBm	2.0:1
CA812-6116	8.0 - 12.0	30	5.0 MAX, 4.0 TYP	+33 MIN	+41 dBm	2.0:1
CA1213-7110	12.2 - 13.25	28	6.0 MAX, 5.5 TYP	+33 MIN	+42 dBm	2.0:1
CA1415-7110	14.0 - 15.0	30	5.0 MAX, 4.0 TYP	+30 MIN	+40 dBm	2.0:1
CA1722-4110	17.0 - 22.0	25	3.5 MAX, 2.8 TYP	+21 MIN	+31 dBm	2.0:1

ULTRA-BROADBAND & MULTI-OCTAVE BAND AMPLIFIERS

Model No.	Freq (GHz)	Gain (dB) MIN	Noise Figure (dB)	Power-out @ P1-dB	3rd Order ICP	VSWR
CA0102-3111	0.1-2.0	28	1.6 Max, 1.2 TYP	+10 MIN	+20 dBm	2.0:1
CA0106-3111	0.1-6.0	28	1.9 Max, 1.5 TYP	+10 MIN	+20 dBm	2.0:1
CA0108-3110	0.1-8.0	26	2.2 Max, 1.8 TYP	+10 MIN	+20 dBm	2.0:1
CA0108-4112	0.1-8.0	32	3.0 MAX, 1.8 TYP	+22 MIN	+32 dBm	2.0:1
CA02-3112	0.5-2.0	36	4.5 MAX, 2.5 TYP	+30 MIN	+40 dBm	2.0:1
CA26-3110	2.0-6.0	26	2.0 MAX, 1.5 TYP	+10 MIN	+20 dBm	2.0:1
CA26-4114	2.0-6.0	22	5.0 MAX, 3.5 TYP	+30 MIN	+40 dBm	2.0:1
CA618-4112	6.0-18.0	25	5.0 MAX, 3.5 TYP	+23 MIN	+33 dBm	2.0:1
CA618-6114	6.0-18.0	35	5.0 MAX, 3.5 TYP	+30 MIN	+40 dBm	2.0:1
CA218-4116	2.0-18.0	30	3.5 MAX, 2.8 TYP	+10 MIN	+20 dBm	2.0:1
CA218-4110	2.0-18.0	30	5.0 MAX, 3.5 TYP	+20 MIN	+30 dBm	2.0:1
CA218-4112	2.0-18.0	29	5.0 MAX, 3.5 TYP	+24 MIN	+34 dBm	2.0:1

LIMITING AMPLIFIERS

Model No.	Freq (GHz)	Input Dynamic Range	Output Power Range Psat	Power Flatness dB	VSWR
CLA24-4001	2.0 - 4.0	-28 to +10 dBm	+7 to +11 dBm	+/- 1.5 MAX	2.0:1
CLA26-8001	2.0 - 6.0	-50 to +20 dBm	+14 to +18 dBm	+/- 1.5 MAX	2.0:1
CLA712-5001	7.0 - 12.4	-21 to +10 dBm	+14 to +19 dBm	+/- 1.5 MAX	2.0:1
CLA618-1201	6.0 - 18.0	-50 to +20 dBm	+14 to +19 dBm	+/- 1.5 MAX	2.0:1

AMPLIFIERS WITH INTEGRATED GAIN ATTENUATION

Model No.	Freq (GHz)	Gain (dB) MIN	Noise Figure (dB)	Power-out @ P1-dB	Gain Attenuation Range	VSWR
CA001-2511A	0.025-0.150	21	5.0 MAX, 3.5 TYP	+12 MIN	30 dB MIN	2.0:1
CA05-3110A	0.5-5.5	23	2.5 MAX, 1.5 TYP	+18 MIN	20 dB MIN	2.0:1
CA56-3110A	5.85-6.425	28	2.5 MAX, 1.5 TYP	+16 MIN	22 dB MIN	1.8:1
CA612-4110A	6.0-12.0	24	2.5 MAX, 1.5 TYP	+12 MIN	15 dB MIN	1.9:1
CA1315-4110A	13.75-15.4	25	2.2 MAX, 1.6 TYP	+16 MIN	20 dB MIN	1.8:1
CA1518-4110A	15.0-18.0	30	3.0 MAX, 2.0 TYP	+18 MIN	20 dB MIN	1.85:1

LOW FREQUENCY AMPLIFIERS

Model No.	Freq (GHz)	Gain (dB) MIN	Noise Figure dB	Power-out @ P1-dB	3rd Order ICP	VSWR
CA001-2110	0.01-0.10	18	4.0 MAX, 2.2 TYP	+10 MIN	+20 dBm	2.0:1
CA001-2211	0.04-0.15	24	3.5 MAX, 2.2 TYP	+13 MIN	+23 dBm	2.0:1
CA001-2215	0.04-0.15	23	4.0 MAX, 2.2 TYP	+23 MIN	+33 dBm	2.0:1
CA001-3113	0.01-1.0	28	4.0 MAX, 2.8 TYP	+17 MIN	+27 dBm	2.0:1
CA002-3114	0.01-2.0	27	4.0 MAX, 2.8 TYP	+20 MIN	+30 dBm	2.0:1
CA003-3116	0.01-3.0	18	4.0 MAX, 2.8 TYP	+25 MIN	+35 dBm	2.0:1
CA004-3112	0.01-4.0	32	4.0 MAX, 2.8 TYP	+15 MIN	+25 dBm	2.0:1

CIAO Wireless can easily modify any of its standard models to meet your "exact" requirements at the Catalog Pricing.

Visit our web site at **www.ciaowireless.com** for our complete product offering.

Ciao wireless

Ciao Wireless, Inc. 4000 Via Pescador, Camarillo, CA 93012

Tel (805) 389-3224 Fax (805) 389-3629 sales@ciaowireless.com

FINDING A FAST SWITCH FOR AUTOMOTIVE SYSTEMS

I read with great interest the "Design Feature" by Mouqun Dong in your February 2017 issue (p. 56) on transient delays in GaAs MMIC switches, especially where it analyzes the effects of step functions on RF switch output power. The author makes many excellent points about RF switches and cautions against simply accepting certain performance parameters from a data sheet. Much of the advice presented in that article can apply to the use of lower-frequency power switching in the emerging electric-vehicle and hybrid-electric-vehicle markets. Manufacturers of vehicles for these markets envision future charging stations replacing many of the locations currently occupied by fueling stations for gasoline-powered vehicles.

Certainly, EVs and HEVs promise minimal side-effects detrimental to the environment, with potentially lower operating costs than gas-powered vehicles. But before such vehicles can become widespread, they must become more affordable, and methods for transferring electric power to those vehicles must dramatically improve. Most drivers will not be willing to wait an hour at a charging station for their electric vehicle to "refuel." Switching technologies will play a role in how fast power can be transferred from storage devices in a charging station to the storage devices (such as capacitor and battery arrays) in an EV.

Understandably, these power-switching applications are at considerably lower frequency applications than typically found in your magazine. But many of the phenomena that exist for various types of switches apply from DC through microwave and even millimeter-wave frequencies. Unfortunately, I see a general lack of editorial coverage on switches in your magazine and believe your staff can perform a much-needed service with greater coverage of current RF switch technologies and applications. Whether articles are from switch manufacturers such as Mr. Dong or from your staff, this is an important RF component that is often ignored in many system designs. And as Mr. Dong pointed out, even small delays can add up.

William Brockhurst

EDITOR'S NOTE

Thank you for reading and for your thoughtful note. The article you referenced did address general switching circuits in its first several figures, and many of the phenomena detailed in the article do apply at lower frequencies as well as at microwave frequencies. But your point about switches being important components is well taken, and advice that the editors of *Microwaves & RF* will certainly consider when developing articles for the remainder of 2017.

Jack Browne
Technical Contributor

News

Operators Push Hybrid Standard BEFORE 5G

Vodaphone, Ericsson, and Qualcomm are among the major wireless companies that support moving up the due date for a radio standard lying between 4G and 5G, with an eye toward testing primitive networks a full year before a final 5G standard is likely to be finished.

Some 20 companies are voting to complete an air interface that rides on existing 4G networks early enough so that firms can start testing and selling 5G technologies in 2019. That would give them around a year before the 3G Partnership Project is expected to lay out the final standard.

Though the Non-Standalone 5G would be layered on top of 4G networks, it would give a glimpse at how mobile devices will communicate with 5G cellular equipment. These systems are expected not only to enable faster downloads for streaming data to cars and virtual reality headsets, but also offer connectivity for billions of tiny sensor devices.

The call to finish the standard early reflects the impatience swirling around 5G. The revenues at telecommunications companies have been falling for years, while the number of consumers buying smartphones—and data plans for them—has been falling. Many operators have pushed ambitious plans for 5G—12 are already field testing, according to a report from Viavi Solutions—which could restart growth.

Verizon has vowed to open such networks in 2018, and South Korean operators are aiming to show off 5G services for the 2018 Winter Olympics in Seoul. Both Intel and Qualcomm have announced 5G modems would start sampling this year and be included in products in 2018.

Nokia, which did not join in the push for Non-Standalone 5G, announced what is called its 5G First platform, suited for homes, offices, sports venues, and industrial plants. Following pilots in 11 American cities with Verizon, Nokia said that it was aiming to open commercial networks later in 2017.

But progress on the standard that entire industry will agree upon has been mired in a web of partnerships between operators, equipment makers, chip suppliers, and test companies. Nowhere was that confusion more palpable than Mobile World Congress in Barcelona last month, where everyone agreed what 5G will do but not on how it will work.

Still, there has been some work on listing the features that every 5G network will be required to have. In February, the International Telecommunications Union released a draft report on 5G specifications, which include 20 gigabits per second downloads and the ability to support 1 million devices per square kilometer. The report underlined that a final standard will not be in place until 2020.

The members signed onto the proposal—NTT Docomo, SK Telecom, British Telecom, Telstra, Korea Telecom, Intel, LG, KDDI, LG Electronics, Telia, Swisscom, TIM, Etisalat, Huawei, Sprint, Vivo, ZTE, and Deutsche Telekom—believe that reaching the intermediary standard first would speed up the 5G standards process.

"Our focus is on prioritizing important specifications in the standards to bring 5G to market as quickly as possible. In the process of defining any standard, it is normal to make some decisions earlier than others," said Tom Keathley, senior vice president of wireless network architecture at AT&T, which also signed onto the proposal, in a statement. ■

GLOBALFOUNDRIES Adds an Advanced RF SOI Manufacturing Process

IN RECENT YEARS, silicon has proven as tough to live with as to live without. The material has trouble hitting the high-frequency bands increasingly used in wireless communications, but it is also vital for etching filters, switches, and amplifiers all on the same chips, which engineers covet for being small and energy efficient.

But in February, an update came for one of the most successful technologies to bridge that gap. GlobalFoundries, one of the world's largest chip manufacturers, began selling tools to help engineers make chips based on its latest manufacturing process—one that is optimized for millimeter waves, which are considered vital for 5G communications.

The technology is known as a silicon-on-insulator process, more commonly known as SOI. It involves wrapping two layers of silicon around an insulator material—using anything from silicon dioxide to sapphire—slashing power leakage and improving efficiency. It has been used in computer processors and in the development of silicon photonics.

In a configuration called RF SOI, the chips are designed specifically for radio components, ranging from switches to low-noise amplifiers. These are major parts of the front ends that decipher wireless signals flowing in and out of smartphones and communications satellites. For 5G, they will have to support high-frequency bands, which are sparsely used in modern cellular equipment or consumer devices.

The new manufacturing process, 45RFSOI, involves etching circuits only 45 nanometers long onto silicon wafers, almost four times longer than the most advanced computer chips under development by GlobalFoundries. But those microscopic circuits are enough to lift RF SOI into high frequency bands, from 24 to 100 GHz, where wireless carriers are likely going to move communications after 4G.

The updated process is also the latest example of how companies plan to give RF SOI an edge over the competition. Peregrine Semiconductor, a San Diego-based company that claims to have founded the RF SOI market, revealed the twelfth generation of its technology in January, with the highest linearity and lowest radio losses yet. It worked with GlobalFoundries to render it on 300 mm wafers.

But many companies view RF SOI as outdated technology unsuited for the shift toward 5G standards. Smartphone makers are increasingly using tiny mechanisms, grown on silicon wafers and known as RF MEMS, to tune antennas into different frequencies. More competition comes from gallium arsenide, a semiconductor material used in radio components for multiple industries, like test equipment and cellular infrastructure.

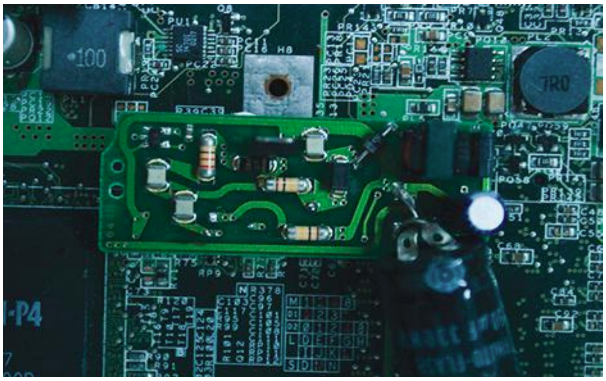

Pictured above is a silicon chip computer board. *(Courtesy of Thinkstock)*

"5G is expected to become the dominant worldwide mobile communications standard of the next decade and will usher in a new paradigm in mobility," said Bami Bastani, senior vice president of GlobalFoundries' RF business, in a statement. RF SOI "will help play a critical role in bringing 5G devices and networks to reality."

45RFSOI improves on earlier technology that had been developed for simpler communication systems. The passive devices built on the manufacturing process have high resistivity that maximizes quality factor—a measure of energy efficiency also known as the Q factor—and minimizes the disparity between phase and voltage.

One of the first chipmakers to sign on to the new process is Skyworks Solutions, a maker of wireless chips for smartphones and connected devices. The company has previously used RF SOI in its switching products, claiming that its efficiency and switching speed are better suited to operate over the growing number of spectrum bands used to send messages and stream video.

Peter Gammel, Skyworks' chief technology officer, said in a statement that the more advanced process will enable the company to further "advance the deployment of highly integrated RF front-ends for evolving mmWave applications," using an abbreviation for millimeter waves.

GlobalFoundries will produce the technology on 300 mm wafers at a factory in East Fishkill, N.Y., which was included in its acquisition of IBM's Microelectronics unit in 2015. Over 27 billion such chips have been shipped since the technology entered production in 2008, the company says. It also offers a process for making silicon-germanium chips favored for certain power amplifiers. ■

QUALCOMM PREPARES for a New Wi-Fi

FOR YEARS, CELLULAR technology that allows mobile phones to communicate has been Qualcomm's bread and butter. But now the world's largest maker of mobile chips has released two devices that support the latest version of Wi-Fi, one that borrows many features from cellular networks.

The first chip, the IPQ8074, is built using 14-nanometer technology for routers and access points, while the QCA6290 is designed for consumer gadgets ranging from smartphones to car dashboards. Both devices are capable of tapping into traditional Wi-Fi frequencies and newer ones that are catching the overspill.

The chips join a short list of other technologies that support the 802.11ax standard, which coordinates multiple antennas to beam multiple streams of data into devices. But it contrasts with earlier Wi-Fi technologies because it splits each stream again using the same self-organization and modulation methods as 4G networks.

The result is a more efficient network, lowering power consumption and increasing capacity up to four times over existing technology. That will make the biggest difference in Wi-Fi networks with lots of traffic or pushing up against other nearby networks in an apartment complex or office building.

"Capacity—not peak speed—has become the most important measure of a network's ability to handle the ever-increasing demands of today's diverse mix of application and services," said Rahul Patel, Qualcomm's senior vice president and general manager of connectivity, in a statement.

The new chips will exploit a technology called MU-MIMO, which stands for multi-user, multiple-input, multiple-output. It allows multiple devices to simultaneously absorb multiple streams of data, improving network capacity and download speeds. Both devices support 12 streams, with eight of those in the 5 GHz spectrum band and four in the traditional 2.4 GHz band.

For now, there is not much hardware to support the 802.11ax standard, which is not likely to be finalized before 2019. Quantenna appears to be the only other supplier to have released details of two new chips for routers and set-top boxes that comply with an early version of 802.11ax.

Quantenna has said that its two chips will start sampling early this year. For its part, Qualcomm expects to sample the IPQ8074 and QCA6290 in the first half of this year. ■

WINDING DOWN THE WOLFSPEED SAGA, an Executive Leaves and an Experiment Ends

NOW THAT CREE has scuttled the sale of Wolfspeed, the company is absorbing the brand into its main business and paring back the executive positions it created to run the power and radio frequency unit.

In a regulatory filing, the company said that Frank Plastina, Wolfspeed's chief executive and an executive vice president within Cree, has stepped down. Plastina, who had been tapped to run the business in late 2015, will leave Cree by July.

Plastina has served on Cree's board since 2007 and joined as the executive vice president of the power and radio frequency business, which is based in Research Triangle Park, N.C., in June 2015. Before that, he founded an angel investment firm called Arc & Company.

"Frank Plastina was brought into Wolfspeed as CEO to lead the separation of the business into an independent company. Now that Cree is reintegrating Wolfspeed as a division of Cree, this role is no longer required," a Cree spokesperson said. "We thank Frank for his effort and contributions."

It is not clear if other executives whose positions are being eliminated will leave the company. The spokesperson said that Cengiz Balkas, the chief operating officer of Wolfspeed, will take over leadership of the business as general manager.

The announcement is a subdued end for the Wolfspeed experiment. The initial plan was for Cree to spin off the unit into a separate company, with Cree's co-founder John Palmour as the chief technology officer and Plastina as the chief executive. Cree said that it wanted to give its main lighting business the breathing room it needed to thrive.

But at industry events, Wolfspeed representatives asked reporters if other companies were thinking about a possible acquisition. Last year, the German chip supplier Infineon threw its name out.

Infineon struck a deal to buy Wolfspeed for $850 million, bolstering its stable of advanced semiconductors used in power management and wireless equipment. The deal fit with the vision of chief executive Reinhard Ploss to expand in fields like electric cars and the infrastructure behind 5G communications.

But then in February, Cree reported that the deal was on the rocks. Top regulators in the United States withheld their blessing for the deal, likely because they were worried about losing Wolfspeed's expertise in gallium nitride, which is considered vital for new antiballistic missile radar. It has been at the center of other recently abandoned deals.

Wolfspeed is also a major manufacturer of gallium nitride for the Department of Defense, which orders chips for classified projects. Though it also sells chips based on silicon carbide, which is widely used in power electronics and lighting, Cree said it had been unable to work out a deal with Infineon to appease regulators.

The Wolfspeed business was a bright spot on Cree's troubled balance sheet, bringing in revenues of $173 million in 2015. Now that the deal has been canceled, Infineon is paying Cree $12.5 million in severance fees. The German chipmaker had planned to close the deal by the end of 2016.

"We are disappointed that the Wolfspeed sale to Infineon could not be completed," said Chuck Swoboda, Cree's chief executive, in a statement. "In light of this development, we are going to shift our focus back to growing the Wolfspeed business." ■

Inside TRACK with Klaus Werner

Executive Director, RF Energy Alliance

Interview by CHRIS DeMARTINO, Technology Editor

***DR. KLAUS WERNER** is the owner of kw tec b.v., a company active in the fields of metrology, automation, and consultancy. Currently, he focuses on RF energy market development as the RF Energy Alliance executive director. Werner previously served as solid-state RF energy markets business development manager at NXP Semiconductors. He studied physics at the RWTH Aachen University, Germany, and holds a Ph.D. in semiconductor device technology from Delft University of Technology, Netherlands. Werner started his professional career as a process engineer at Philips Semiconductors. Prior to his assignment in the RF power device business, he performed in several engineering and operational management roles.*

First, can you tell us a little about the RF Energy Alliance?

The RF Energy Alliance (RFEA) is a non-profit technical association comprised of companies dedicated to presenting solid-state RF energy's true potential as a clean, highly efficient, and controllable heat and power source. Members envision a fast-growing, innovative marketplace built around this sustainable technology, contributing to advances and paradigm shifts across many applications.

The RFEA is defining and standardizing several RF energy building blocks, their software and hardware interfaces, and their integration with power supplies and cooling systems. As such, the blocks will be "complete" and ready for use by application engineers. Ideally, this ease of use will give rise to the evolution of identified applications (i.e., microwave ovens) as well as the development of completely new applications (i.e., RF lighting, medical ablation devices, and RF plasma ignitions in automobiles).

By standardizing solid-state RF energy system components, modules, and application interfaces, the RFEA will:

- Reduce system cost
- Minimize design complexity
- Ease application integration
- Speed market adoption and enable growth
- Enhance user experiences

How do you see LDMOS and gallium-nitride (GaN) technology coexisting in terms of solid-state RF energy applications?

Currently, LDMOS is clearly the dominating technology for high-power RF applications. Based on silicon (Si), it enjoys the large economy of scale available in large wafer fabs and, hence, allows the "niche" LDMOS technology to benefit

> "When it comes to conceiving an RF energy system, a system architect must cover the usual suspects like power supplies, thermals, digital interfaces, microcontrollers, and firmware, as well as the intricacies around RF signal generation, amplification, and injection into the applicator."

from high-volume processing cost. From a semiconductor standpoint (silicon), the material parameters are far less attractive than those of GaN. The latter, being a high-bandgap, direct III/V semiconductor, offers increased efficiency, higher temperature operation, much higher breakdown voltages (ruggedness), and higher carrier mobilities, which makes this material the ideal semiconductor for high-power, high-frequency (RF energy) applications. Unfortunately, GaN at this point cannot be produced at a scale that would allow comparable cost levels as those of LDMOS.

To make a long story short, the above mentioned performance/cost differences will also determine the use of the materials in applications. The moment the application demands the best available efficiency or bandwidth, GaN will be the obvious choice. If it requires cost-effectiveness at decent performance, Si LDMOS will win.

This "separation" will stay unchanged until GaN can be processed at Si cost—recent advances in that respect (GaN-on-Si technology) may prove disruptive in the coming years, and could enable a whole new host of compact, efficient amplifiers driving new RF energy applications.

How can cooking appliances utilize solid-state RF energy? And what benefits can be achieved by using solid-state RF technology instead of traditional magnetrons in microwave ovens?

For cooking applications, such as the microwave oven, solid-state RF energy holds many advantages over traditional magnetrons. These benefits include:

- Exceptional control and feedback of RF signal frequency, phase, power, and energy levels
- Real-time adaptation to changing load conditions
- Higher energy efficiency and lower voltage
- Smaller form factor
- An "all-semiconductor" electronics footprint with associated integration possibilities and design flexibility

The traditional magnetron-based microwave creates hot spots and cold spots in the food, which is counterproductive and lowers the overall quality. The brick-shaped 3D standing wave patterns in the cavity of the traditional microwave causes these temperature differences, and is the reason a turntable must sweep the food through the RF field. Even with the turntable, residual temperature differences caused by the inhomogeneous fields are one of the reasons food instructions say "leave to stand for one minute after cooking."

With solid-state RF energy sources, the frequency can be shifted to move nodes and anti-nodes around the cavity, while the power can also be modulated quickly and with ease. Collectively, the technology's attributes yield an unprecedented process control range, even energy distribution, and rapid adjustment to changing load conditions. By using solid-state RF energy in microwaves, the overall quality and taste of the food we cook will improve.

Why has it taken so long to utilize solid-state RF technology in microwave ovens?

Solid-state RF energy for cooking applications is gaining industry momentum and a variety of solutions have recently hit the market.[1,2,3] However, challenges still remain for adoption in high-volume markets. The reasons often tie back to engineering complexity and system cost.

Solid-state RF energy system design requires engineering knowledge, which is not generally available due to RF (power) engineers being occupied with "linearized amplifier" systems for data-transmission purposes or concerned with magnetron sources for heating applications. There is a general lack of design knowledge with respect to applying solid-state RF generation to additional, less-focused-upon RF energy systems.

When it comes to conceiving an RF energy system, a system architect must cover the "usual suspects" like power supplies, thermals, digital interfaces, microcontrollers, and firmware, as well as the intricacies around RF signal generation, amplification, and "injection" into the applicator.

"Beyond residential cooking appliances, the RFEA is also targeting applications such as professional cooking appliances, industrial lighting, industrial heating, automotive ignition, plasma creation, and medical devices for imaging and treatment (MRI, ablation, hyperthermia, skin rejuvenation, etc.)."

Additionally, solid-state RF energy applications are still quite expensive due to the current volume supply base. The RFEA's efforts to develop specifications and roadmaps for solid-state RF energy will combat those obstacles—and we believe it will make solid-state RF mainstream. For example, the *"RF Power Amplifier (PA) Roadmap: Residential Appliances"* outlines multiple PA module scopes that feasibly reduce the system cost to be competitive with current magnetron-based solutions in the near future.

Do you expect magnetron-based microwave ovens to eventually be altogether replaced by solid-state ones?

Yes. Albeit that this will still be a couple of years out. The industry is actually moving ahead of the above mentioned roadmap; the implementation of the technology in consumer goods is just a year or two out. A lot of current investment goes into the integration of the new technology into appliances. But again, before the entire microwave oven market is converted, it will take couple of years—the magnetron is just too powerful and cheap to be that easily replaced.

What does solid-state RF energy mean for the industrial market?

The technology offers a number of advantages. First of all, the semiconductors are very reliable, can sweep frequency and power easily, and can be pulsed. The magnetron, on the other hand, is extremely powerful as a single source—the solid-state PAs need to be combined in relatively complex mechanical structures to achieve the same amount of output power as a single magnetron.

This may sound like a real disadvantage, and this may really be the case for some applications. But, overall, the smaller power chunks of the amplifiers also offers the opportunity to re-partition large industrial systems into smaller, independently controllable units, which then offer better process control and probably higher yields. Current industrial users still need to rethink their design flow to appreciate the benefits that a more granular, agile technology can bring to their systems.

Lastly, what other markets are being targeted?

Beyond residential cooking appliances, the RFEA is also targeting applications such as professional cooking appliances, industrial lighting, industrial heating, automotive ignition, plasma creation, and medical devices for imaging and treatment (MRI, ablation, hyperthermia, skin rejuvenation, etc.). mw

REFERENCES
1. http://www.popularmechanics.com/technology/infrastructure/a21030/solid-state-microwaves/
2. http://www.ampleon.com/news/news-articles/ampleon-and-midea-collaboration-results-in-world-s-first-solid-state-oven.html
3. https://www.macom.com/about/news-and-events/press-release-archive/row-col1/news--event-archive/macom-achieves-breakthrough-for

MAPPING DIELECTRIC PROPERTIES for Body-Based Networks

MEDICAL ELECTRONIC DEVICES are expanding the capabilities for remote monitoring of a patient's health and vital signs. As the number of these devices are worn by and/or embedded into a patient, nanonetworks are formed in which inter-device communications—as well as communication to a remote location like a hospital or doctor's office—are made possible by means of wireless internet links. To better understand how such nanonetworks will perform when surrounded by the dielectric material known as human skin, a research team based in London and Qatar focused on the parameter extraction of skin material using terahertz-frequency time-domain spectroscopy (TDS) in the band from 0.1 to 2.5 THz.

The dielectric characteristics of skin and tissues are based largely on the high water content (water with a dielectric constant of about 80), and terahertz radiation has been shown to be very sensitive to changes in the water content of different materials, including skin and tissues. The terahertz spectroscopy was performed on human skin and tissue to develop better models for what will be wireless communications networks formed with the internet of nanothings for biomedical applications. The research team consisted of Nishtha Chopra, Ke Yang, Mike Philpott, and Akram Alomainy from the Queen Mary University of London, as well as Qammer Abbasi and Khalid Qaraqe from Texas A&M University at Qatar (Education City, Al-Rayyan, Qatar).

Considering the fact that human skin consists of three layers—the epidermis, dermis, and fat layers—the intent of using terahertz spectroscopy was to noninvasively study the dielectric characteristics of the dermis skin layer and its many complex structures (e.g., blood vessels, sweat ducts, and capillaries). The TDS system relies on coherent detection of pulsed terahertz waves mixed with sampling optical pulses in a detector. The terahertz spectral waveforms provide information about both phase and amplitude. Optical beams are split into two parts, so that not only the absorption of a sample can be obtained, but also the dispersion by analyzing the Fourier transform of the detected waveforms. The terahertz TDS system at Queen Mary University of London, which has a typical frequency range of 0.1 to 4.0 THz, was used in the analysis.

Insight into the dielectric properties of human skin was gained by studying dehydrated skin samples. This also reinforced the fact that the dielectric impact of water in human bodies must be modeled and accounted for when optimizing future in-body nanonetworks, such as those using medical sensors for analysis and study of tumors and cancers.

See: "THz Time-Domain Spectroscopy of Human Skin Tissue for In-Body Nanonetworks," *IEEE Transactions on Terahertz Science and Technology*, Vol. 6, No. 6, November 2016, p. 803.

SYSTEM COMBINES Optical and Terahertz Signals at 400 GHz

DATA-HUNGRY APPLICATIONS are steadily consuming wireless bandwidth, to the point where network managers are eying available bandwidth at millimeter-wave and even terahertz frequencies. To that end, researchers based in Lyngby, Denmark and Cambridge, England have surveyed efforts at developing terahertz wireless-communications systems and evaluated various methods of designing terahertz-frequency communications links for high-data-rate applications.

The team learned that links can be assembled completely from electrical components using electromagnetic (EM) energy or from a combination of electrical and optoelectronic technologies. Since higher data rates have been achieved with the latter approach, the researchers propose an optoelectronics terahertz wireless communications system operating in the 400-GHz band; it uses optical signals in a 12.5-GHz ultradense wavelength division multiplexing (UD-WDM) grid.

The research and system development were performed by Xianbin Yu from Zhejiang University (Hangzhou, China) and DTU Fotonik (Department of Photonics Engineering, Technical University of Denmark), along with Rameez Asif of the University of Cambridge and a team consisting of Molly Piels, Darko Zibar, Michael Galili, Toshio Morioka, Peter Jepsen, and Leif Oxenlowe (also from DTU Fotonik). The terahertz carriers are generated by heterodyne photomixing of free-running optical sources—in this case, a 100-kHz continuous-wave (CW) laser array with frequency stability of ±12.5 GHz and power stability of ±0.003 dB over 24 h.

This generation of millimeter-wave and terahertz signals is transparent to modulation sources already being used in WDM optical communications systems. The researchers demonstrated the compatibility of their system with optical networks by using spectrally efficient optical Nyquist channels with a quadrature-phase-shift-keying (QPSK) modulation format, as used for commercial 100 Gigabit Ethernet applications.

For testing, a wireless propagation distance was fixed at 50 cm, with path loss of less than 2 dB achieved under optimum conditions. Downconversion was to intermediate-frequency (IF) channels in the 20-GHz band. The researchers achieved aggregated data rates to 60 Gb/s with their system, and showed the potential for a terahertz-frequency communications link that combines optical and EM signals.

See: "400-GHz Wireless Transmission of 60-Gb/s Nyquist-QPSK Signals Using UTC-PD and Heterodyne Mixer," *IEEE Transactions on Terahertz Science and Technology,* Vol. 6, No. 6, November 2016, p. 765.

GVA AMPLIFIERS

NOW DC* to 12 GHz   up to 1W Output Power   from 94¢ ea. (qty.1000)

GVA amplifiers now offer more options and more capabilities to support your needs. The new **GVA-123+** provides ultra-wideband performance with flat gain from 0.01 to 12 GHz, and new model **GVA-91+** delivers output power up to 1W with power added efficiency up to 47%! These new MMIC amplifiers are perfect solutions for many applications from cellular to satellite and more! The GVA series now covers bands from DC to 12 GHz with various combinations of gain, P1dB, IP3, and noise figure to fit your application. Based on high-performance InGaP HBT technology, these amplifiers are unconditionally stable and designed for a single 5V supply in tiny SOT-89 packages. All models are in stock for immediate delivery! Visit minicircuits.com for detailed specs, performance data, export info, **free X-parameters**, and everything you need to choose your GVA today!

US patent 6,943,629

**Low frequency cut-off determined by coupling cap.*
For GVA-60+, GVA-62+, GVA-63+, and GVA-123+ low cut off at 10 MHz.
For GVA-91+, low cut off at 869 MHz.

NOTE: GVA-62+ may be used as a replacement for RFMD SBB-4089Z
GVA-63+ may be used as a replacement for RFMD SBB-5089Z
See model datasheets for details

FREE X-Parameters-Based
Non-Linear Simulation Models for ADS   Modelithics®
http://www.modelithics.com/mvp/Mini-Circuits.asp

Mini-Circuits®

www.minicircuits.com   P.O. Box 350166, Brooklyn, NY 11235-0003   (718) 934-4500   sales@minicircuits.com   458 rev P

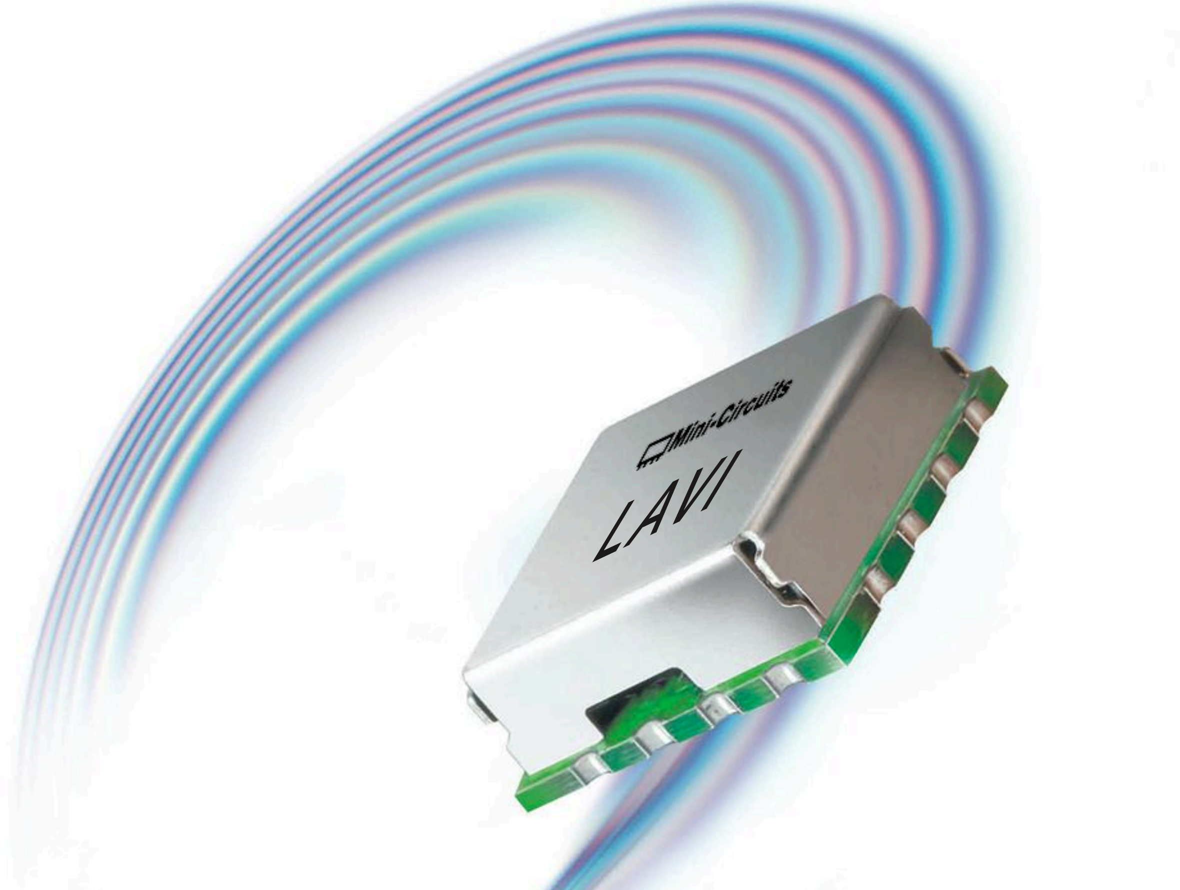
Mini-Circuits
LAVI

CEES LINKS | General Manager of the Wireless Connectivity Business Unit, Qorvo
www.qorvo.com

How Smart Homes Can Deliver Sustainability as a Service

Smart-home services have the potential to impact households in a profound way.

WITHIN JUST THREE years, it's estimated that as many as five billion people and 50 billion devices could be connected. While those numbers alone are impressive, it's the potential of that connectivity to improve many aspects of our lives (including the health of our planet) that's truly eye-opening.

Many discussions surrounding the smart home focus on benefits that can be realized by the people living in them. But a truly smart, connected home—one that can independently assess and respond to real-time requirements for power, water, heating, and similar resources—is able to promote sustainability. In addition, it can avoid serious damage to the home by independently identifying waste and avoiding spillage.

The introduction of highly power-efficient chips that support multiple communications protocols—e.g., IEEE 802.15.4, ZigBee 3.0, Thread, and Bluetooth Low Energy (BLE)—is rapidly driving advances in smart-home networking.

1. These are the types of events and behavior patterns that a smart home will track and learn from to recognize what is going on in the home.

But in order to realize the environmental benefits of smart-home technology, we must first understand what a smart home really is (not just a collection of connected devices) and have insight into what consumers want from a smart home (services).

WHAT IS A SMART HOME?

Too often, the words "smart" and "connected" are used interchangeably when discussing the devices that power the Internet of Things (IoT). But they are not the same. Many of today's devices are essentially internet-enabled remote controls that require human action to be turned on and off.

The term "smart" implies intelligence with decision-making capabilities. A smart device and application can analyze incoming data and make a decision to control or activate a device without human intervention.

In the context of the home, "smart" refers to a network of sensors in the house that measures and monitors the environment. The network senses who is in the home, where they are in the home, and what the "normal" activity is in the home at that particular day and time.

By using intelligence and information that the system has learned about the residents, it makes decisions about whether to lock doors and windows; turn on or off the heater, air conditioner, lights or entertainment systems; activate the security system; and more *(Fig. 1)*.

For example, if a family was streaming a movie on a hot summer night, a smart-home system would turn off the lights and turn down the A/C in the empty parts of the home. In addition, if power-consuming devices are on but not in use, such as a computer or gaming console, the system turns those off as well.

After the family goes to bed, the system can then turn off the A/C or heating in the unused areas and keep it on only in the areas where people are sleeping. Since many people prefer cooler temperatures for sleeping, the system could be smart enough to slowly reduce the temperature at night and then raise it again in the morning. It could further reduce energy consumption by anticipating the falling outside temperature during the night.

The network learns from the people who live in the home to make predictions about future behaviors. It knows the number of household members, how rooms are used and when, bedtimes, who works from home and where, who gets up early, etc. Patterns are absorbed by the system and used to enhance comfort and convenience settings. These settings are also cost-saving and have the potential to significantly reduce energy consumption.

This type of sophisticated smart-home network requires specific capabilities:

1. It must connect to and communicate with other smart or connected devices in the home.
2. It must be intelligent, recognize what goes on in the home, and learn what is normal.
3. Residents must be able to manage functions with a single integrated application on a smartphone or other web-connected device.

Smart devices are essential to what consumers really want—namely, services. A 2016 study showed that consumers are not interested in simply having a bunch of connected devices that remotely control various things in the home. They desire services, and having these services without the hassle of investigating, purchasing, installing, and maintaining a system of disparate connected devices. In short, consumers want a smart home as a service.

WHAT IS SHaaS?

Smart Home as a Service (SHaaS) is a collection of services that analyzes input from the smart home's sensors, learns how the family lives and how the home is used, and can make intelligent decisions to make homes more comfortable, safe, and energy-efficient *(Fig. 2)*.

Instead of a consumer having to decide which hardware and software options or which wireless technology to implement in their home, they can simply leave it up to the providers of services they already use (e.g., internet access, security, and entertainment).

By opting for SHaaS, consumers don't have to be technologically savvy or care about the underlying wireless technology. Having one provider responsible for installation, setup, and management of the network makes it much faster to implement services, add new services, and ensure that controls and user interfaces are unified.

This is how the four basic components of a SHaaS work together:

1. A network of sensors in the home provides a general indication of when and where movement occurs in the home and whether the home is secure, what the environmental conditions are, and whether there are any issues (a leak, for example).
2. The information derived from these sensors is wirelessly collected by a local hub (gateway, set-top box, etc.) and securely transmitted to an intelligent cloud service that collects and analyzes the data, and sends alerts to family members when it detects changes.
3. A central management app enables the consumer to manage the network via a smartphone or any web-connected device in a single user interface.
4. The service provider is able to easily handle customer support, billing, and subscriber management, as well as software and service upgrades and changes.

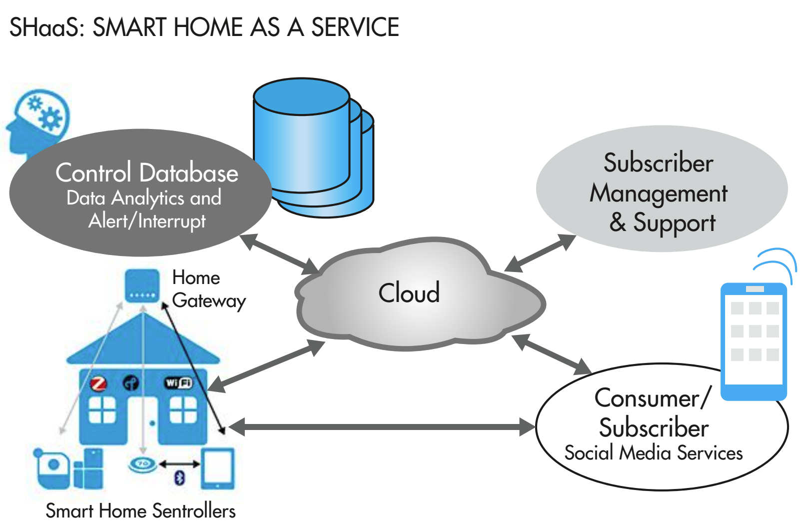

2. A Smart Home as a Service (SHaaS) system consists of multiple services that leverage input from sensors.

HOW CAN THE SHaaS REDUCE ENVIRONMENTAL IMPACTS?

It's easy to see how a SHaaS can increase efficiency, safety, and comfort within the home and help its occupants better manage and live their lives. But SHaaS benefits reach well beyond the walls of the home, helping to reduce the use of our planet's natural resources and our carbon footprint *(Fig. 3)*.

3. The SHaaS acts as a butler in the home, using a network of sentrollers and cloud intelligence to create an environment that benefits those who live in it—and also helps to support the health of our planet.

Water. Water conservation is one such example. Most everyone has experienced a leaking water heater. If the leak is not immediately detected, the water heater continues to run, inefficiently heating and wasting water, causing costly damage in the home, and resulting in high energy and water bills.

One fix is to install a leak detector that sends an alarm when the tank fails. But by taking that a step further and connecting that leak detector sensor to a smart-home network—one that includes actuators and controls on the power and water sources—the smart home can alert the home owner and control the power and water systems that feed it.

This same scenario applies to frozen water pipes. If the network notices that water is moving in the pipes with no one home, it can send a notice to the homeowner and turn off the water at the main valve. In daily applications, the smart home would recognize that water is flowing when no one is home, talk to the water meter, and turn off the flow.

Power. Power use is another area where the SHaaS delivers environmental benefits. A green smart home would monitor how and when power is consumed and manage power in the home based on that data. For example, the home would make sure A/C and heating systems are not in use until someone is home, and would automatically open and close window shades or curtains to adjust for the sun and the season.

The home's power-storage system can be charged during the day via solar panels on the roof, or at night when power is less expensive. That way, the home's power-hungry appliances can use "cheap" stored electricity instead of drawing from the grid during expensive rate times. These systems are already in use in industrial applications and will soon be moving to home use.

The smart-home power system can learn which devices are the worst power consumers when not in use and simply disconnect them. If the home network recognizes that the family is away on vacation, it can disconnect all devices that consume standby power.

People. A smart home can have environmental benefits in subtle ways, as well. Families with an older parent who lives alone can use the smart-home network to maintain awareness of their daily well-being without having to drive or take the bus across town, reducing CO_2 emissions.

An effective smart home makes its people smarter, too. When people are educated about how much appliances are actually costing in power, they are more likely to turn off the appliances when not in use and to be more conscientious in their use of energy.

HOME SENSORS AND ANALYTICS SUPPORT SUSTAINABILITY

On April 22, countries around the world will mark Earth Day. Our ideas about the role of home connectivity in environmental stewardship have been transformed since the first celebration of this event in 1970.

New technology, composed of sensors and analytics, is empowering smart-home solutions that learn from the people who live there. These systems use this knowledge to make predictions about future behaviors and take actions that enhance comfort and convenience, save money, and reduce environmental impacts. Smart Home as a Service enables consumers to practice sustainability and help ensure a cleaner future simply by exerting greater control over the way resources are used in their homes. mw

Check this out ...

RF Signal Generators

just became affordable!

- *2 GHz, 4 GHz & 6 GHz models*
- *Excellent phase noise*
- *AM, FM, ΦM, PM & sweeps*
- *Square wave clock outputs*
- *Ethernet, GPIB & RS-232*

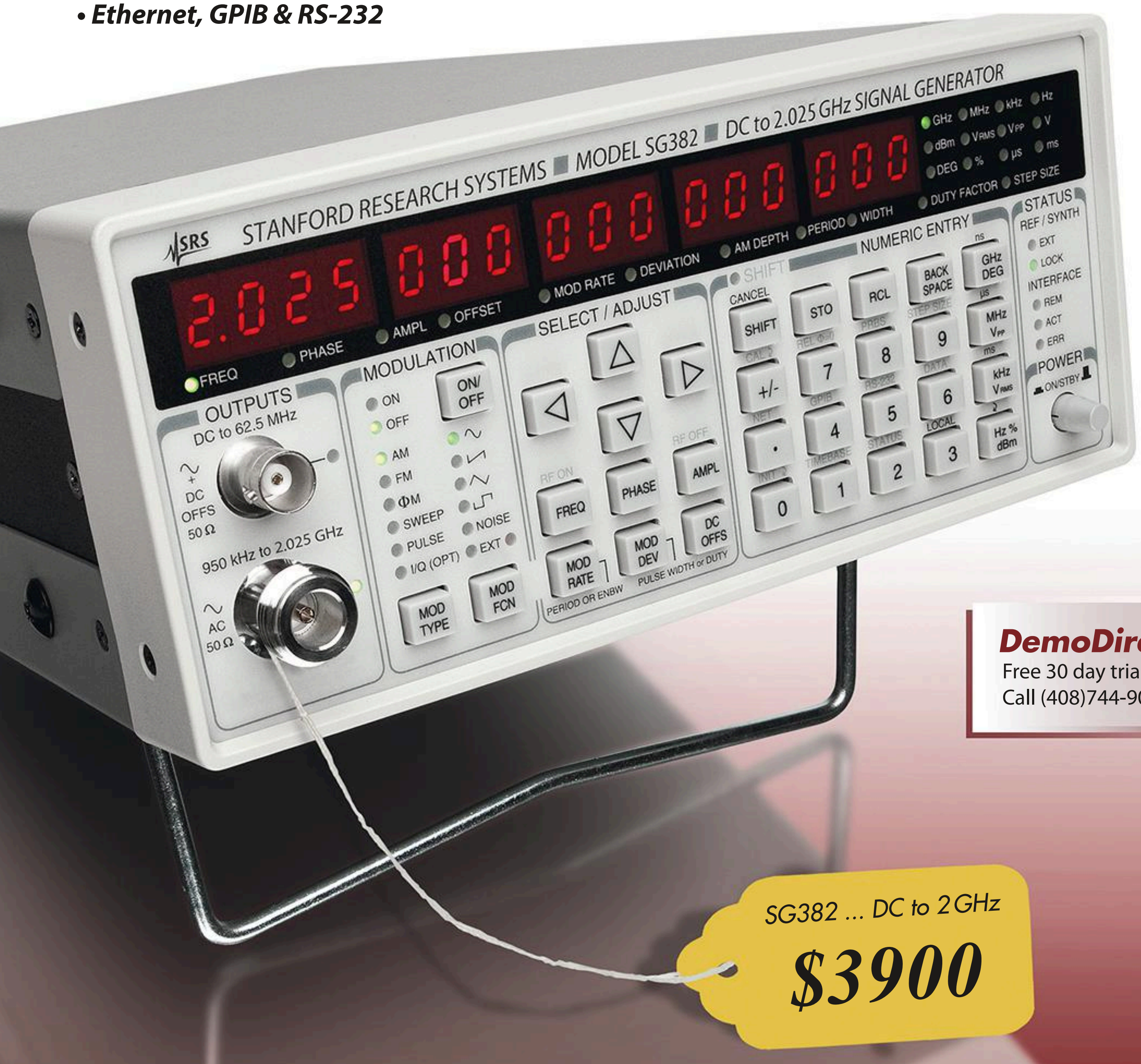

DemoDirect
Free 30 day trial
Call (408)744-9040

SRS Stanford Research Systems **Tel: (408)744-9040 • www.thinkSRS.com**

JACK BROWNE | Technical Contributor

Managing Modulation and Demodulation

Digital modulation/demodulation formats provide options in terms of bandwidth efficiency, power efficiency, and complexity/cost when meeting a modern communications system's data-transfer needs.

MODULATION AND DEMODULATION provide the means to transfer information over great distances. As noted in the first part of this article *(see "Basics of Modulation and Demodulation" on mwrf.com)*, analog forms of modulation and demodulation have been around since the early days of radio. Analog approaches directly encode information from changes in a transmitted signal's amplitude, phase, or frequency. Digital modulation and demodulation methods, on the other hand, use the changes in amplitude, phase, and frequency to convey digital bits representing the information to be communicated.

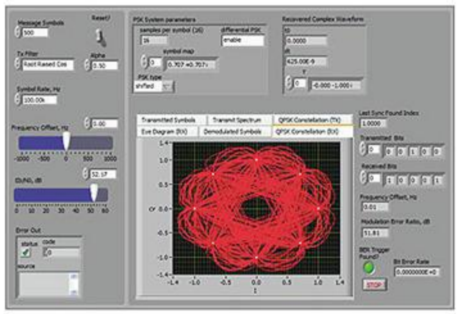

1. The Modulation Toolkit of LabVIEW simulation software allows users to predict performance of different modulation formats under changing conditions. *(Courtesy of National Instruments)*

With growing demands for voice, video, and data over communications networks of all kinds, digital modulation and demodulation have recently replaced analog modulation and demodulation methods in wireless networks to make the most efficient use of a limited resource: bandwidth. In this second part, we explore how some higher-order modulation and demodulation formats are created, and how software and test equipment can help to keep different forms of modulation and demodulation working as planned.

ENHANCING EFFICIENCY

Efficiency is a common goal of all modulation/demodulation methods, whether they involve conserving bandwidth, power, or cost. Digital modulation/demodulation formats, in particular, have been found able to transfer large amounts of information with minimal bandwidth and power. While increased data capacity tends toward increased complexity in digital modulation/demodulation, high levels of integration in modern ICs have made possible communications systems capable of reliable, cost-effective operation with even the most advanced digital modulation/demodulation formats.

Reasonable bandwidth efficiency is possible with standard digital modulation formats, such as amplitude-shift keying (ASK), frequency-shift keying (FSK), and phase-shift keying (PSK). By executing additional variations, more complex digital modulation formats can be created with improved data capacity and bandwidth efficiency, as measured in the number of digital bits that can be transferred in a given amount of time per unit amount of bandwidth (b/s/Hz).

For example, with minimum-shift keying (MSK), essentially a form of FSK, peak-to-peak frequency deviation is equal to one-half the bit rate. A further variation of MSK is Gaussian MSK (GMSK), in which the modulated signal passes through a Gaussian filter to minimize instantaneous frequency variations over time and reduce the amount of bandwidth occupied by the transmitted waveforms. GMSK maintains a constant envelope and provides good bit-error-rate (BER) performance in addition to its good spectral efficiency.

By applying some small changes, it is also possible to improve power efficiency. Quadrature PSK (QPSK) is basically a four-state variation of simple PSK. It can be modified in different ways—e.g., offset QPSK (OQPSK)—to boost efficiency. In QPSK, the in-phase (I) and quadrature (Q) bit streams are switched at the same time, using synchronized digital signal clocks for precise timing. A given amount of power is required to maintain the timing alignment.

In OQPSK, the I and Q bit streams are offset by one bit period. Unlike QPSK, only one of the two bit streams can change value at any one time in OQPSK, which also provides benefits in terms of power consumption during the bit switching process. The spectral efficiency, using two bit streams, is the same as in standard QPSK, but power efficiency is enhanced due to reduced amplitude variations (by not having the amplitudes of both bit streams passing at the same time). OQPSK does not have the same stringent demands for linear amplification as QPSK, and can be transmitted with a less-linear, more-power-efficient amplifier than required for QPSK.

THE ROLE OF FILTERING

The bandwidth efficiency of a modulation/demodulation format can be improved by means of filtering, removing signal artifacts that can cause interference with other communications systems. Various types of filters are used to improve the spectral efficiency of different modulation formats, including Gaussian filters (with perfect symmetry of the rolloff around the center frequency); Chebyshev equiripple, finite-impulse-response (FIR) filters; and lowpass Nyquist filters (also known as raised-cosine filters, since they pass nonzero bits through the frequency spectrum as basic cosine functions).

The goal of filtering is to improve spectral efficiency and reduce interference with other systems, but without degrading modulation waveform quality. Excessive filtering can result in increased BER due to a blurring of transmitted symbols that comprise the data stream of a digital modulation format. Known as intersymbol interference (ISI), this loss in integrity of the symbol states (phase, amplitude, frequency) make it difficult to decode the symbols at the demodulator and receiver in a digitally modulated communications system.

An ideal filter is often referred to as a "brickwall" filter due to its instant changeover from a passband to a stopband. In reality, filters do not provide an ideal reduction in signal bandwidth due to the need for some amount of transition between a filter passband and its stopband; longer transitions require more bandwidth.

Filters for digital modulation/demodulation applications are regularly characterized by a parameter known as "alpha," which provides a measure of the amount of occupied bandwidth by a filter. For example, a "brickwall" filter, with instant transition from stopband to passband, would have an alpha value of zero. Filters with longer transitions will maintain larger values of alpha. Smaller values of filter alpha result in increased ISI, because more symbols can contribute to the interference.

MODELING AND MEASURING

A wide range of suppliers offer modulators and demodulators in various formats, from highly integrated ICs to discrete components. A number of those highly integrated transceiver ICs can be used for both functions—as transmitters/modulators and receivers/demodulators. Some are even based on software-defined-radio (SDR) architectures with sufficient bandwidths to serve multiple wireless communications standards and modulation/demodulation requirements.

Modeling software helps simplify the determination of requirements for a communications system's modulation/demodulation scheme. Some software programs provide general-purpose modulation/demodulation analysis capabilities, allowing users to predict the results of using different analog and digital modulation schemes. For example, the Modulation Toolkit *(Fig. 1)* from National Instruments *(www.ni.com)* works with the firm's popular LabVIEW design software to simulate communications systems based on different analog and digital modulation/demodulation formats. The software makes it possible to experiment with different variables, such as carrier frequency, signal strength, and interference; and predict different performance parameters, such as BER, bandwidth efficiency, and power efficiency, under different operating conditions.

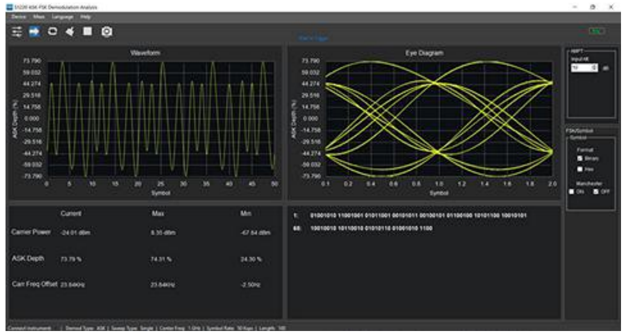

2. S1220 software, when used with a series of commercial spectrum analyzers, is aimed at optimizing ASK and FSK demodulation in IoT applications. *(Courtesy of RIGOL Technologies USA)*

In contrast, S1220 software from RIGOL Technologies USA *(www.rigol.com)* simulates ASK and FSK demodulation, in particular for Internet of Things (IoT) applications *(Fig. 2)*. The software teams with the company's spectrum analyzers to study modulation/demodulation over a carrier frequency range of 9 kHz to 3.2 GHz (and to 7.5 GHz with options). It provides an ASK symbol rate measurement range of 1 to 100 kHz and FSK deviation measurement range of 1 to 400 kHz.

Test instruments are an important part of achieving good modulation/demodulation performance. Numerous test-equipment suppliers offer programmable signal generators, such as arbitrary waveform generators, that can create different modulation formats to be used with or without a carrier signal generator for emulating modulated test signals. Spectrum analyzers provide windows to the modulation characteristics of waveforms within their frequency ranges. And some specialized measurement instruments have been developed for the purpose of testing modulation and demodulation and associated components, such as modulation domain analyzers (MDAs).

A number of different display formats provide ways to visualize modulated signals—with both signal analyzers and software—including constellation diagrams, eye diagrams, polar diagrams, and trellis diagrams (for trellis modulation). For example, separate eye diagrams can be used to show the magnitude versus time characteristics of two separate I and Q data channels, with I and Q transitions appearing as "eyes" on a computer or instrument display screen. Different modulation formats will show as different types of displays; for instance, QPSK will appear as four distinct I/Q states, one in each quadrant of the display screen. A high-quality signal creates eyes that are open at each symbol. mw

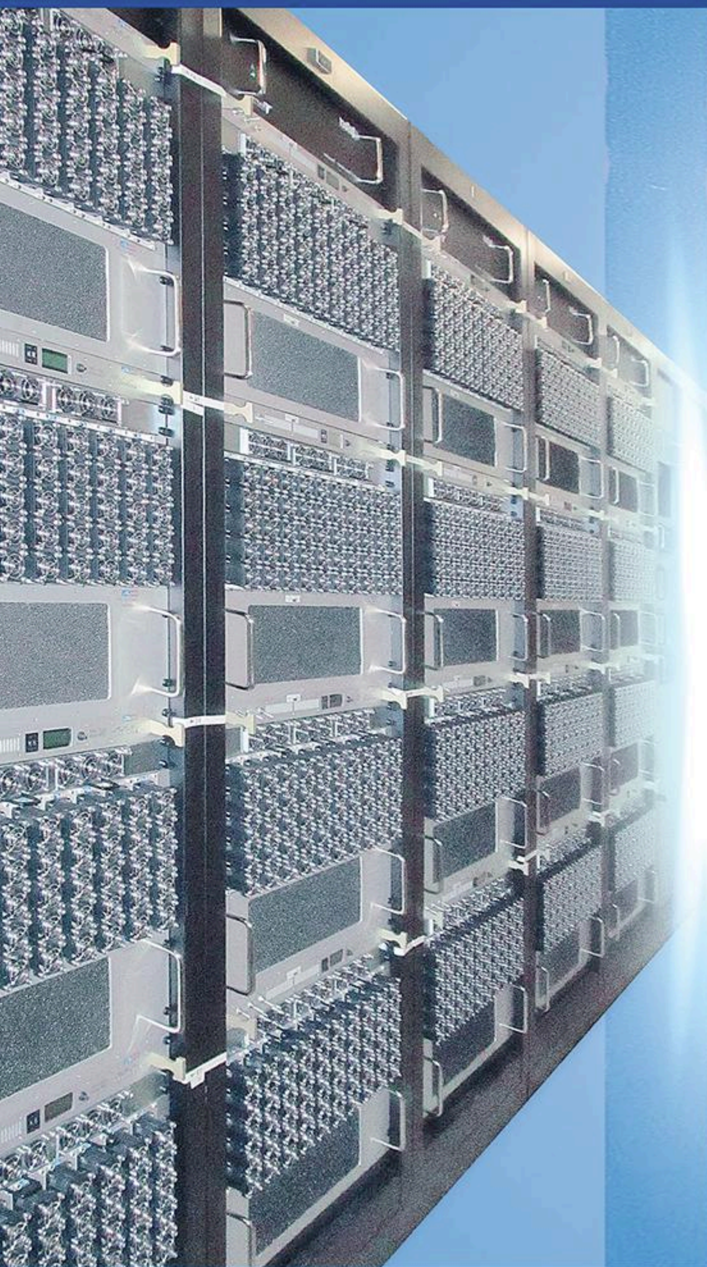

GRAHAM FREELAND | Consultant Software Engineer, MathWorks
MARC BARBERIS | Principal Application Engineer, MathWorks
www.mathworks.com

Device-to-Device Communication Aids Public Safety

LTE technology is enabling the next wave of public safety communication networks.

RELEASE 12 OF THE 3rd Generation Partnership Project (3GPP) LTE standard introduced a device-to-device (D2D) interface aimed primarily at allowing LTE to support public safety communication systems. A key driver for this LTE feature is the First Responder Network Authority (FirstNet), established by the U.S. government. This organization is tasked with creating and maintaining a single high-speed nationwide wireless broadband network dedicated to public safety.

It was decided that this public safety network would be based on LTE technology. As a result of this decision, a number of U.S. organizations engaged with 3GPP and its members with a view to extend the LTE standard to support features required for public safety. One such feature, for example, is in regard to communication within out-of-coverage scenarios.

The first results of this work are standardized as the Proximity Services (ProSe) features in LTE Release 12. This work continues to evolve in Release 13 and beyond. There is now worldwide backing, from the likes of the TETRA and Critical Communications Association (TCCA), for the use of LTE in next-generation critical communication systems as a replacement for TETRA and P25.

ProSe introduced sidelink connectivity, a new interface with a set of transport and physical channels with associated physical signal. Resource pools define physical resources in time and frequency that carry D2D control and traffic data. These resource pools, which are a new concept in the LTE standard, are key to understanding how ProSe traffic can coexist with legacy LTE traffic.

In this article, we discuss some of the main features of D2D in LTE Release 12 and focus on the concept of resource pools and sidelink transmission. The MathWorks LTE System Toolbox is utilized to present ProSe performance results.

DIRECT DISCOVERY VS. DIRECT COMMUNICATION

D2D communication offers a number of advantages over network-based communication. These advantages include shorter latency, decreased network traffic, power savings, and a fallback system in the case of network failure.

Two features are specified as part of ProSe in Release 12:

- **Direct discovery:** This is used in commercial applications like targeted advertising. Direct discovery enables UEs to advertise and discover content of interest in their immediate surroundings (up to a few hundred meters), or transfer data between LTE-enabled devices.
- **Direct communication:** This is currently reserved for public safety usage.

This article focuses exclusively on direct communication as defined for public safety usage.

Several scenarios are defined for coverage *(Figure 1)*:

- UE in coverage
- UE in partial coverage
- UE out of coverage

When at least one of the UEs is either in coverage or in partial coverage, the LTE network may play a part in coordinating transmission between nearby UEs. On the other hand, one new aspect of direct communication allows LTE devices to communicate without the assistance of the network, as in the out-of-coverage scenario.

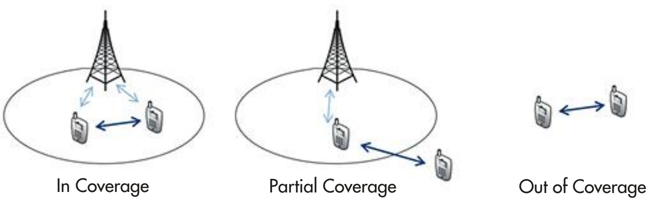

1. This figure illustrates three different coverage scenarios.

SIDELINK CONNECTIVITY

One of the first decisions the LTE standards body had to make was whether to reuse some of the same physical resources as the downlink or uplink. It was decided that the UE shall transmit on uplink LTE frequencies, using single-carrier frequency division multiple access (SC-FDMA) modulation and resources from the uplink. To explain how the eNodeB or UE selects those uplink resources, however, we first need to introduce resource pools and some of the sidelink channels.

Release 12 of the LTE standard defines sidelink as a new interface with a set of transport and physical channels, with associated physical signals to support deployment of the D2D direct communication and direct discovery features.

Some of the sidelink physical channels include:

- **Physical Sidelink Shared Channel (PSSCH):** This channel carries sidelink data. Sidelink transmission is defined as a one-to-many scheme, meaning that the data is to be received by multiple UEs that belong to a group.
- **Physical Sidelink Control Channel (PSCCH):** This channel is analogous to the traditional Physical Downlink Control Channel (PDCCH) in that it carries the sidelink control information (SCI) message, which contains information about the resource allocation of the physical sidelink shared channel.

The following sidelink physical signals are also defined:

- **Demodulation reference signals:** These symbols are used for channel estimation.
- **Primary and Secondary Sidelink Synchronization Signals (PSSS and SSSS):** These synchronization signals are needed to synchronize UEs that are out of coverage and therefore cannot use the primary and secondary synchronization signals emitted by the eNodeB.

RESOURCE POOLS

A resource pool is a set of resources defined by a subset of subframes and resource blocks available within these subframes. The block of resources is repeated with a period, known as the PSCCH period, which can range from 40 to 320 ms. A resource pool is designed to set aside physical resources for transmission of sidelink data (including associated control).

3GPP TS 36.101 defines examples of resource pool settings. We consider the PSCCH period defined in Annex A.7.2 Table 7.2.1-1 for 5-MHz bandwidth.

LTE System Toolbox lets users model and visualize this setting with just three lines of code:

- *params = PSCCHPeriod.defaultConfig(1,'5MHz');*
- *period = PSCCHPeriod(params);*
- *displayPeriod(period);*

Figure 2 shows a PSCCH period for the default 5-MHz setting.

TRANSMISSION AND MODULATION

Both PSCCH and PSSCH use resources selected from the resource pools. The PSCCH is transmitted using quadrature phase-shift-keying (QPSK) modulation and a very low coding rate. It is sent twice in two different subframes in order to further increase the signal-to-noise ratio (SNR) and, thereby, the probability of correct demodulation.

The PSSCH is transmitted using either QPSK or 16-state quadrature amplitude modulation (16-QAM), and one of the allowed coding rates. This modulation and coding scheme (MCS) is included in the sidelink control information carried by the PSCCH.

Each transport block is sent four times with a fixed redundancy version sequence in order to let the receiver(s) use soft combining. Note that PSSCH carries data meant to be received by a group of UEs, as opposed to a single UE. Therefore, there cannot be a closed-loop HARQ scheme. Rather, all transmissions are always repeated four times, although any individual UE may successfully decode a transport block in fewer than four transmissions.

The PSCCH and PSSCH are mapped to physical resources included in the resource pools described earlier, using one of

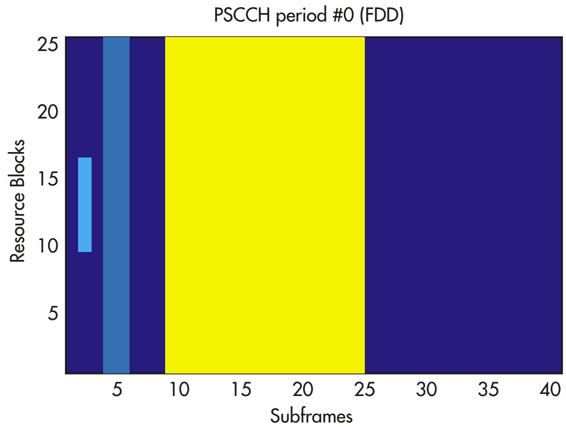

2. This is an example of a full-band resource pool. Shown are synchronization transmission (light blue), control resource pool (dark blue), and shared resource pool (yellow). Resource blocks are numbered from 1 to 25, corresponding to indices 0 through 24.

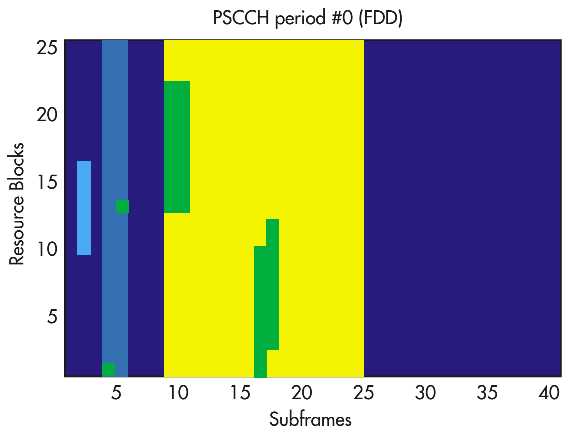

3. This is an example of PSCCH and PSSCH allocation within a resource pool. Resource blocks are indexed starting with 1.

two strategies that correspond to the two transmission modes defined in LTE Release 12:

- **Transmission mode 1 (network-directed):** When the UE is in coverage, the eNodeB can dynamically assign resources to the UE for D2D transmission. In this transmission mode, the eNodeB can guarantee no collision between any sidelink transmission and any uplink transmission, or between sidelink transmissions.

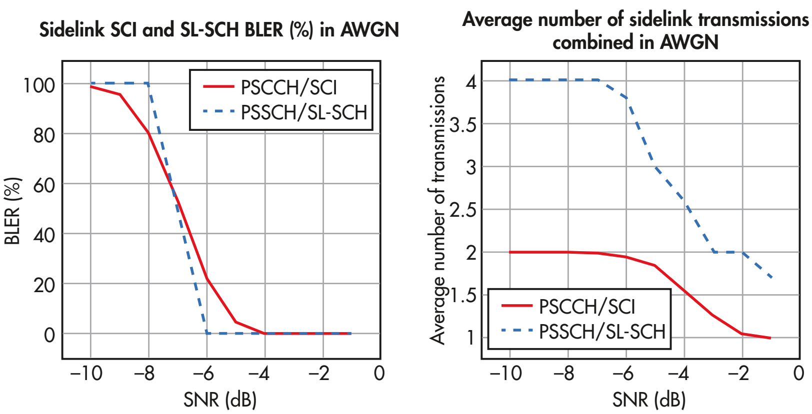

4. These plots show the BLER and average number of transmissions combined for sidelink SCI and SL-SCH over 1000 periods.

- **Transmission mode 2 (UE-selected):** The UE selects which resources to use for transmission. Transmission mode 2 is applicable to all scenarios, in coverage and out of coverage. The resources are selected at random to minimize the collision risk.

SIDELINK PERFORMANCE

We now want to illustrate a concrete example of a resource pool configuration and how to determine the performance of sidelink control and data channels using LTE System Toolbox.

Here, we assume transmission mode 2, meaning that the transmitting UE must randomly select suitable resources from a predefined resource pool. Note that the UE could be in coverage or out of coverage.

The main steps are:

- Set up a resource pool according to predefined parameters.
- Create an SCI message. This message carries all necessary pieces of information, including resource allocation for the PSSCH and modulation and coding scheme.
- Create a PSSCH transport block.

- Transmit the SCFDMA modulated signal over a channel.
- Demodulate the signal.
- Blindly detect the SCI by trying out all possible PSCCH resources.
- Once the SCI is decoded, extract the relevant resource blocks where PSSCH is located.
- Decode the PSSCH over up to four retransmissions (open-loop HARQ).

The simulation determines the error rate on PSCCH and PSSCH decoding. Here, we chose an MCS value of 11, which corresponds to 16-QAM.

Figure 3 shows which resources were actually picked by the UE for a particular subframe for PSCCH and PSSCH. They are highlighted in green.

Observe the two PSCCH and four PSSCH transmissions in different subframes that belong to their respective resource pools. The PSCCH transmissions occupy one physical resource block each (1 and 13) in the first and second subframes of the PSCCH resource pool (dark blue). PSSCH transmission occupies contiguous physical resource blocks in two groups of two consecutive subframes within the (yellow) PSSCH resource pool: PRBs 13 through 22, 13 through 22, 1 through 10, and 3 through 12.

Finally, the block error rate (BLER) for both PSCCH and PSSCH are shown as a function of the SNR, as well as the number of retransmissions that were combined *(Fig. 4)*. Combining stops when the channel is successfully decoded or the maximum number of transmissions is reached (2 for PSCCH, 4 for PSSCH).

For low SNRs, the receiver always needs both PSCCH and all four PSSCH transmissions. For -10 dB, we can see that the BLER is 100%. Thus, even with all retransmissions, the receiver cannot correctly decode either channel with this weak signal. Conversely, at -1 dB, the BLER is always 0, meaning that both the SCI and Sidelink Shared Channel (SL-SCH) are correctly decoded, after an average of 1 and 1.7 transmissions, respectively.

CONCLUSION

The LTE standard is constantly evolving and introducing new capabilities supported by new features. Proximity services are one of the main recent additions to the LTE standard, with applications in both public safety and commercial deployments. Furthermore, LTE Release 14 may add a vehicle-to-vehicle (V2V) and vehicle-to-everything (V2X) capability based on the sidelink with suitable modifications to accommodate specific requirements, such as low latency and high reliability. mw

MARK SCOTT LOGUE | Engineer

Low-Noise Amplifier Spans DC to 17 GHz

This novel pHEMT LNA design combines low-frequency and high-frequency circuit techniques to achieve extremely low noise levels over a wide frequency range.

Low-noise amplifiers (LNAs) are essential for receiving low-level communications signals, although such amplifiers are typically not broadband in their frequency coverage. However, an innovative LNA design approach blends low- and high-frequency circuit design techniques to achieve low noise from dc to 17 GHz. The amplifier, based on enhancement-mode, pseudomorphic high-electron-mobility-transistor (E-pHEMT) semiconductor technology, achieves low 1/f noise with low harmonic distortion and relatively flat gain across its wide frequency range.

The novel amplifier design (*Fig. 1*) features a cascode configuration with an op-amp-based error amplifier, transconductance (g_m) current driver, lowpass filter (LPF), and active current source to supply a dc offset current to the error amplifier. The amplifier design also includes a 50-Ω resistive divider that serves as an input for the differential amplifier. The LPF isolates the transconductance driver from the cascode at high frequencies and provides a 100-Ω high-frequency termination.

The LNA circuit cascode is formed by the E-pHEMTs J27 and J31. Amplifier gain is set by resistor R126 in the source of transistor J31 and load resistor RL in the drain of device J27. For modeling purposes, source resistor RS is used to connect to the gate of transistor J31. The signal at the source of J31 consists of an attenuated version of VIN plus random noise and harmonic distortion.

Resistors R129 and R139 form a broadband 50-Ω voltage divider, with the output of R129/(R129 + R139) = $1/g_m$ + R126, where g_m is the transconductance of J31. The output of the voltage divider is connected to resistor R135, one of the input resistors at the positive input port of the error amplifier. This amplifier, X38, is a high-speed op amp with ultralow 1/f noise. It has gain of 6, which is set by the ratio of resistor R136 to R134 and the ratio of resistor R137 to R135.

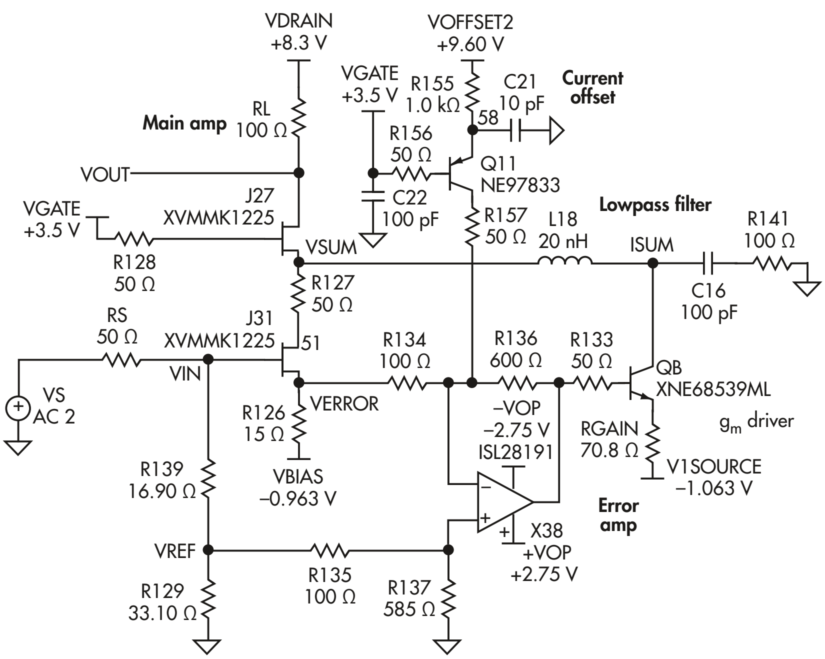

1. This schematic diagram shows the architecture of the broadband, low-noise amplifier.

TRANSCONDUCTANCE

Bipolar transistor Q8 forms a low-noise transconductance amplifier that drives the source of the common gate of transistor J27 in the cascode. The voltage of the differential error amplifier is applied to the transconductance amplifier to develop an error current that is summed at the source of transistor J27. Passive components L18, C16, and R141 provide isolation for the transconductance amplifier from the cascode, as well as produce a 100-Ω termination at high frequencies for the error amplifier. The transconductance of the error amplifier is set to a first-order value of 14.12 mmho, or 1/70.8 Ω. This is referred to as RGAIN. Inductor L18 has a very high resonant frequency, in the gigahertz range, and provides isolation between the cascode and error amplifier.

In the LNA, Q11 is a bipolar transistor current source that provides an offset dc current to the summing node of the error amplifier, with the offset current set by resistor R155 and a dc supply of +9.5 V dc, VOFFSET2. Capacitor C21 provides a high-frequency ac ground to the emitter of Q11, and resistor R156 provides a high-frequency 50-Ω termination to the base of Q11.

Node VREF contains an attenuated signal, VIN, at the gate of J31, which serves as the reference signal for the error amplifier. The second

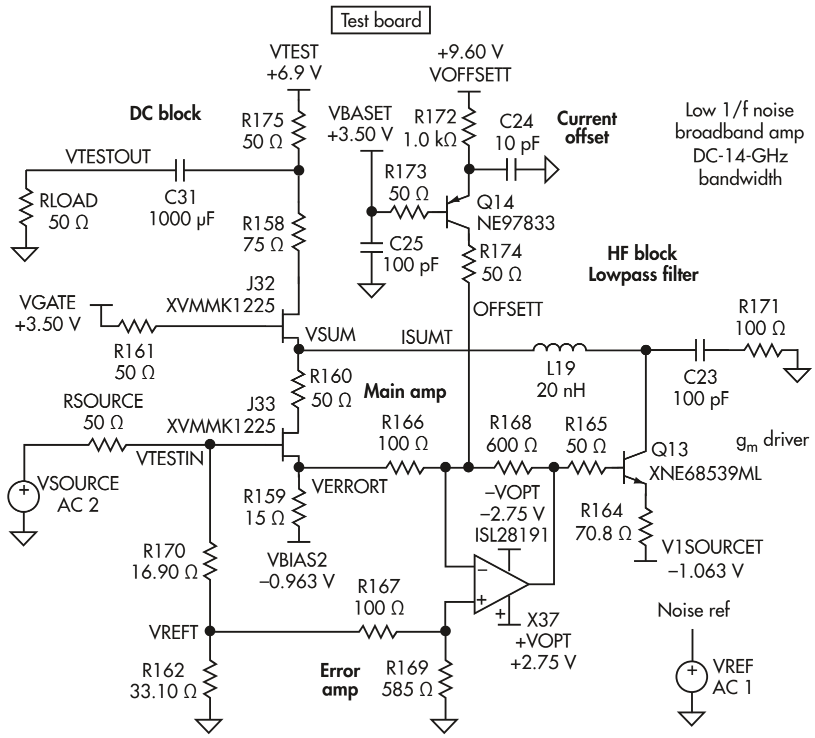

2. The test fixture for evaluating the low-noise amplifier is represented in this schematic diagram.

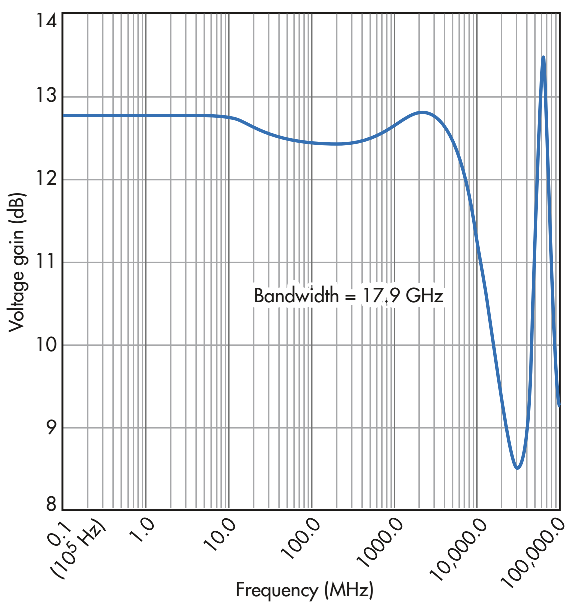

3. The amplifier offers consistent, linear response at high frequencies.

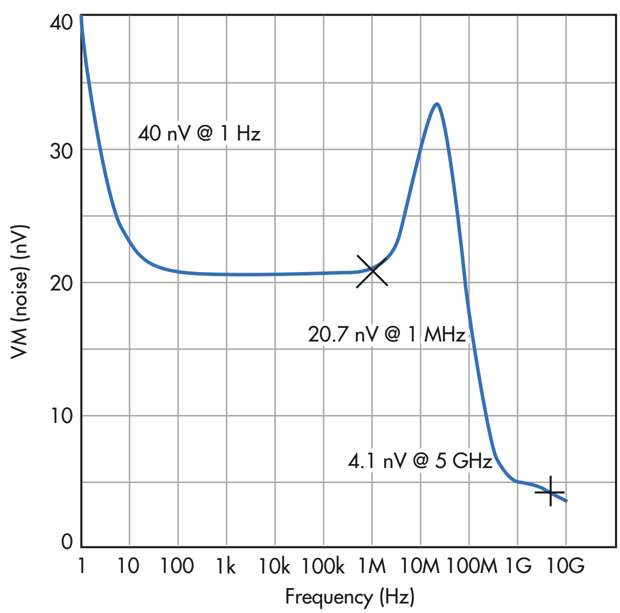

4. This plot shows the output RMS noise voltage versus frequency.

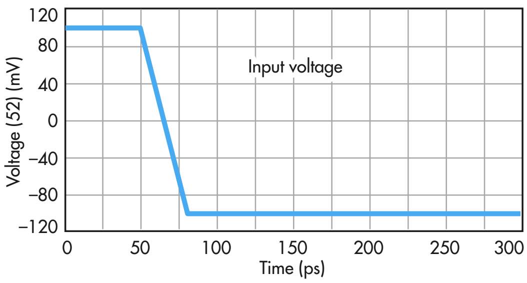

5. This is a plot of the input voltage supplied to the amplifier.

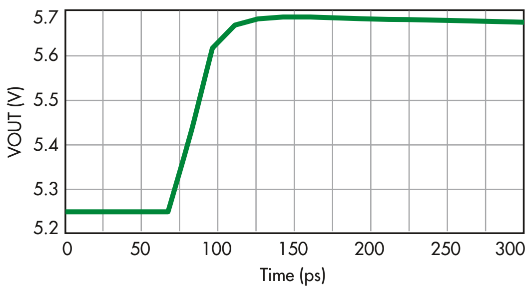

6. Here, the trace indicates output voltage from the broadband amplifier.

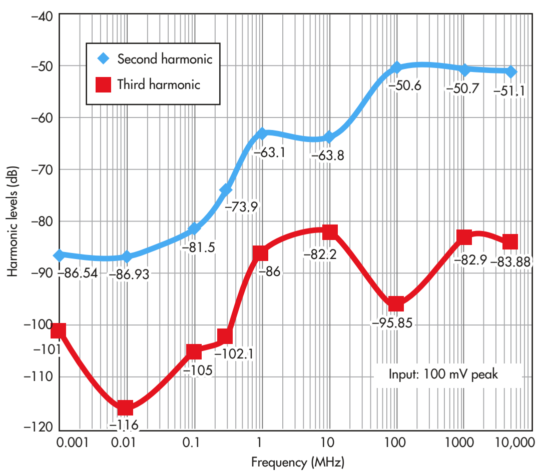

7. Using a peak input of 100 mV, these are the calculated second- and third-order harmonic responses of the broadband, low-noise amplifier.

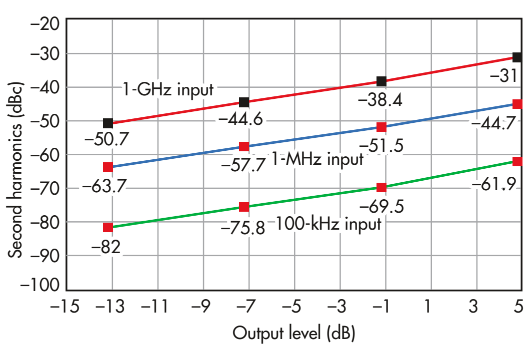

8. These second-harmonic responses were calculated for different output voltages at frequencies of 100 kHz, 1 MHz, and 1 GHz.

input signal to the error amplifier is from the emitter of J31, which contains an attenuated version of VIN plus an error signal. The error term consists of harmonic distortion plus random noise.

The output of the error amplifier is the error term multiplied by the amplifier's gain of 6. This output is then passed through a transconductance amplifier with gain of 14.2 mmho, which converts the signal to an error signal current that is summed into the source of transistor J27.

TESTING THE PROTOTYPE

A test board fixture was assembled (*Fig. 2*) to evaluate the prototype LNA circuit. The load resistor for the cascode was split into two resistors, providing a pickoff of the signal output of the cascode. A number of different measurements were performed to characterize the amplifier for its wideband performance. For example, *Fig. 3* shows voltage gain as a function of frequency, with the marker indicating a usable bandwidth of 17.9 GHz.

Figure 4 plots the output noise of the LNA from 1 Hz to 10 GHz. The peak 1/f noise of 40 nV RMS occurs at the lowest frequency, 1 Hz. The output noise drops to 22 nV RMS at 10 Hz with the noise remaining flat to 1 MHz. A second peak in the output noise level, at about 33 nV RMS, occurs at 30 MHz. Output noise drops to 4.1 nV RMS at 5 GHz.

Figure 5 illustrates a plot of the input voltage step at node 52, with impressive 90%-to-10% fall time of 22 ps. *Figure 6* is a plot of the output voltage at node VOUT. The step appears to be a dominant pole response, with an output step of less than 30 ps. The output has no ringing and no aberrations appearing 50 ps after the step.

Figure 7 shows second- and third-harmonic distortion as a function of frequency for a peak input of 100 mV. Second-harmonic distortion is –86.54 dBc at 1 kHz, remaining flat to about 10 kHz. The first peak in the second-harmonic distortion curve occurs at –63.1 dBc, remaining flat to about 10 MHz. The second peak in the second-harmonic distortion curve occurs at about –50.6 dBc at 100 MHz, with second-harmonic distortion remaining at about that level to about 8 GHz. Third-harmonic distortion is below –82.2 dBc from 1 kHz to 8 GHz.

Figure 8 plots second-harmonic distortion in dB as a function of LNA output-power level, for input signals of 100 kHz, 1 MHz, and 1 GHz. For an output level of –13 dB, for example, the second-harmonic distortion is about –82.0 dB at 100 kHz, –63.7 dB at 1 MHz, and –50.7 dB at 1 GHz. For an output level of +5 dB, the second-harmonic distortion increases to –61.9 dB at 100 kHz, –44.7 dB at 1 MHz, and –31.0 dB at 1 GHz.

The novel amplifier delivers impressive noise performance over an extremely wide bandwidth, making it suitable for receivers and other applications from audio through microwave frequencies. The integral error amplifier helps minimize noise, and E-pHEMT active devices enable consistent gain to beyond 17 GHz. The patented design is usable down to dc with stable and consistent gain and noise performance. mw

UP TO **100 Watt**

AMPLIFIERS

NOW! **100 kHz to 26.5 GHz**

from **$995** ea. qty. (1-9)

High-powered performance across wide frequency ranges. Mini-Circuits' class A/AB linear amplifiers have set a standard for wideband high-power performance throughout the RF and microwave industry. Rugged and reliable, they feature over-voltage and over-temperature protections and can withstand opens and shorts at the output! Available with or without heat sinks, they're perfect for demanding test lab environments and for integrating directly into customer assemblies. With standard models covering frequencies from 100 kHz up to 26.5 GHz, chances are we have a solution for your needs in stock. Place your order on minicircuits.com today for delivery as soon as tomorrow! Need a custom model? Give us a call and talk to our engineers about your special requirements!

Model	Frequency (MHz)	Gain (dB)	Pout@ Comp. 1 dB (W)	Pout@ Comp. 3 dB (W)	$ Price* (Qty. 1-9)
ZVM-273HP+	13000-26500	14.5	0.5	0.5	2195
ZVE-3W-83+	2000-8000	35	2	3	1424.95
ZVE-3W-183+	5900-18000	35	2	3	1424.95
ZHL-4W-422+	500-4200	25	3	4	1160
ZHL-5W-422+	500-4200	25	3	5	1670
ZHL-5W-2G+	800-2000	45	5	5	995
ZHL-10W-2G+	800-2000	43	10	12	1395
• ZHL-16W-43+	1800-4000	45	12	16	1595
• ZHL-20W-13+	20-1000	50	13	20	1470
• ZHL-20W-13SW+	20-1000	50	13	20	1595
LZY-22+	0.1-200	43	16	30	1595
ZHL-30W-262+	2300-2550	50	20	32	1995
ZHL-30W-252+	700-2500	50	25	40	2995
LZY-2+	500-1000	47	32	38	2195
LZY-1+	20-512	42	50	50	1995
• ZHL-50W-52+	50-500	50	63	63	1395
• ZHL-100W-52+	50-500	50	63	79	1995
• ZHL-100W-GAN+	20-500	42	79	100	2845
NEW! ZHL-100W-272+	700-2700	48	79	100	7995
ZHL-100W-13+	800-1000	50	79	100	2395
ZHL-100W-352+	3000-3500	50	100	100	3595
ZHL-100W-43+	3500-4000	50	100	100	3595

Listed performance data typical, see minicircuits.com for more details.

• Protected under U.S. Patent 7,348,854

**Price Includes Heatsink*

Mini-Circuits®

www.minicircuits.com P.O. Box 350166, Brooklyn, NY 11235-0003 (718) 934-4500 sales@minicircuits.com

416 rev AK

KIMBERLY RENEE ALVAREZ | Consultant; www.microwaveandrfconsulting.com

Designing a Step-Recovery-Diode-Based Comb Generator

By leveraging advanced software, accurate results were obtained in the design and testing of a comb generator.

The task of designing frequency multipliers and comb generators has traditionally been plagued by challenges such as low output power, unexpected parasitic frequencies, and oscillations. Computer-aided-design (CAD) software can overcome these problems, though. The purpose of this work is to predict the behavior of a nonlinear step-recovery diode (SRD) in a harmonic-generator circuit. By doing so, one can achieve high correlation between simulation results and measured data.

A post-processing display of the harmonically rich output frequency spectrum was produced with Microwave Office software. Output harmonics and their respective magnitudes were graphically displayed for a given single input frequency. Furthermore, the output waveform on a time scale was closely examined.

CIRCUIT DESIGN

Microwave Office software was used to design a complete comb circuit and fabricate several circuits. The test results fully agree with the computer-predicted output spectrum. The output power of each harmonic was measured, demonstrating agreement with the simulated results. The output spectrum displays 12 harmonics with no spurious frequencies or oscillations.

The SRD was selected for this design due to its nonlinear properties and ability to attain good higher-order frequency multiplication and fast pulse generation. It takes advantage of its diffusion capacitance for charge storage, resulting in a fast snap time. This design employs an input lowpass filter to provide an impedance match to the diode.

While most multipliers utilize an output "ringer" bandpass filter to suppress the undesired harmonics, this design exploits all of the generated harmonics—a wide range is required. This simplifies the design considerably, making it low cost and easy to manufacture.

The nonlinear behavior is described in the diode model provided by the Microwave Office component models list. The model properties are manually set to the appropriate values consistent with the published Metelics (now MACOM) diode that was selected for this design.

DIODE PROPERTIES

Multiplier (and comb generator) circuits are reactively terminated at the higher-order harmonics at the output port. Consequently, the power is partially reflected and recombined to produce stronger harmonics. The damping factor of the SRD is one of the primary drivers in frequency-multiplier or comb-generator design. It is defined as follows:

$$\varsigma = (1/2R_L)(L/C_d)^{1/2}$$

where L is the diode's inductance, C_d is the diode's reverse capacitance, and R_L is the load resistance.

A good practical range for the damping factor (ς) is between 0.4 and 0.5. If damping is too low, stability problems can arise. If it is too high, the output pulse will become too long.

(Continued on page 70)

HIGH POWER

5 - 500 WATTS PRODUCTS

POWER DIVIDERS RoHS

Model #	Frequency (MHz)	Insertion Loss (dB) [Typ./Max.] ◊	Amplitude Unbalance (dB) [Typ./Max.]	Phase Unbalance (Deg.) [Typ./Max.]	Isolation (dB) [Typ./Min.]	VSWR (Typ.)	Input Power (Watts) [Max.] ◦	Package
2-WAY								
CSBK260S	20 - 600	0.28 / 0.4	0.05 / 0.4	0.8 / 3.0	25 / 20	1.15:1	50	377
DSK-729S	800 - 2200	0.5 / 0.8	0.05 / 0.4	1 / 2	25 / 20	1.3:1	10	215
DSK-H3N	800 - 2400	0.5 / 0.8	0.25 / 0.5	1 / 4	23 / 18	1.5:1	30	220
P2D100800	1000 - 8000	0.6 / 1.1	0.05 / 0.2	1 / 2	28 / 22	1.2:1	2	329
DSK100800	1000 - 8000	0.6 / 1.1	0.05 / 0.2	1 / 2	28 / 22	1.2:1	20	330
DHK-H1N	1700 - 2200	0.3 / 0.4	0.1 / 0.3	1 / 3	20 / 18	1.3:1	100	220
P2D180900L	1800 - 9000	0.4 / 0.8	0.05 / 0.2	1 / 2	27 / 23	1.2:1	2	331
DSK180900	1800 - 9000	0.4 / 0.8	0.05 / 0.2	1 / 2	27 / 23	1.2:1	20	330
3-WAY								
S3D1723	1700 - 2300	0.2 / 0.35	0.3 / 0.6	2 / 3	22 / 16	1.3:1	5	316
4-WAY								
CSDK3100S	30 - 1000	0.7 / 1.1	0.05 / 0.2	0.3 / 2.0	28 / 20	1.15:1	5	169S

◦ With matched operating conditions

HYBRIDS RoHS

Model #	Frequency (MHz)	Insertion Loss (dB) [Typ./Max.] ◊	Amplitude Unbalance (dB) [Typ./Max.]	Phase Unbalance (Deg.) [Typ./Max.]	Isolation (dB) [Typ./Min.]	VSWR (Typ.)	Input Power (Watts) [Max.]	Package
90º								
DQS-30-90	30 - 90	0.3 / 0.6	0.8 / 1.2	1 / 3	23 / 18	1.35:1	25	102SLF
DQS-3-11-10	30 - 110	0.5 / 0.8	0.6 / 0.9	1 / 3	30 / 20	1.30:1	10	102SLF
DQS-30-450	30 - 450	1.2 / 1.7	1 / 1.5	4 / 6	23 / 18	1.40:1	5	102SLF
DQS-118-174	118 - 174	0.3 / 0.6	0.4 / 1	1 / 3	23 / 18	1.35:1	25	102SLF
DQK80300	800 - 3000	0.2 / 0.4	0.5 / 0.8	2 / 5	20 / 18	1.30:1	40	113LF
MSQ80300	800 - 3000	0.2 / 0.4	0.5 / 0.8	2 / 5	20 / 18	1.30:1	40	325
DQK100800	1000 - 8000	0.8 / 1.6	1 / 1.6	1 / 4	22 / 20	1.20:1	40	326
MSQ100800	1000 - 8000	0.8 / 1.6	1 / 1.6	1 / 4	22 / 20	1.20:1	40	346
MSQ-8012	800 - 1200	0.2 / 0.3	0.2 / 0.4	2 / 3	22 / 18	1.20:1	50	226
180º (4-PORTS)								
DJS-345	30 - 450	0.75 / 1.2	0.3 / 0.8	2.5 / 4	23 / 18	1.25:1	5	301LF-1

◊ In excess of theoretical coupling loss of 3.0 dB

COUPLERS RoHS

Model #	Frequency (MHz)	Coupling (dB) [Nom]	Coupling Flatness (dB)	Mainline Loss (dB) [Typ./Max.]	Directivity (dB) [Typ./Min.]	Input Power (Watts) [Max.] ◦	Package
KFK-10-1200	10 - 1200	40 ±1.0	±1.5	0.4 / 0.5	22 / 14	150	376
KDS-30-30	30 - 512	27.5 ±0.8	±0.75	0.2 / 0.28	23 / 15	50	255 *
KBS-10-225	225 - 400	10.5 ±1.0	±0.5	0.6 / 0.7	25 / 18	50	255 *
KDS-20-225	225 - 400	20 ±1.0	±0.5	0.2 / 0.4	25 / 18	50	255 *
KBK-10-225N	225 - 400	10.5 ±1.0	±0.5	0.6 / 0.7	25 / 18	50	110N *
KDK-20-225N	225 - 400	20 ±1.0	±0.5	0.2 / 0.4	25 / 18	50	110N *
KEK-704H	850 - 960	30 ±0.75	±0.25	0.08 / 0.2	38 / 30	500	207
SCS100800-10	1000 - 8000	10.5 ±1.5	±2.0	1.2 / 1.8	8 / 5	25	361
KBK100800-10	1000 - 8000	10.5 ±1.5	±2.0	1.2 / 1.8	8 / 5	25	322
SCS100800-16	1000 - 7800	16.8 ±1.5	±2.8	0.7 / 1.0	14 / 5	25	321
KDK100800-16	1000 - 7800	16.8 ±1.5	±2.8	0.7 / 1.0	14 / 5	25	322
SCS100800-20	1000 - 7800	20.5 ±2.0	±2.0	0.45 / 0.75	12 / 5	25	321
KDK100800-20	1000 - 7800	20.5 ±2.0	±2.0	0.45 / 0.75	14 / 5	25	322
KEK-1317	13000 - 17000	30 ±1.0	±0.5	0.4 / 0.6	30 / 15	30	387

* Add suffix - LF to the part number for RoHS compliant version.

◦ With matched operating conditions

Unless noted, products are RoHS compliant.

SYNERGY®
MICROWAVE CORPORATION

Phone: (973) 881-8800 | Fax: (973) 881-8361
E-mail: sales@synergymwave.com
Web: WWW.SYNERGYMWAVE.COM
Mail: 201 McLean Boulevard, Paterson, NJ 07504

MAHMOUD A. ABDALLA | Professor, Electronic Engineering Department, Military Technical College (MTC)
Cairo, Egypt; +2 01118750114, e-mail: maaabdalla@ieee.org, *www.mtc.edu.eg*

AHMED A. IBRAHIM | Professor, Faculty of Engineering, Minia University, El-Minia, Egypt
e-mail: ahmedabdel_monem@mu.edu.eg, *www.minia.edu.eg*

Metamaterials Sculpt UWB Bandpass Filter

By combining left- and right-handed transmission lines with conventional microstrip circuitry, it is possible to achieve a wide passband for an UWB bandpass filter.

Modern communications rely on many separate frequency bands, but can also be conducted at low power levels across the single ultrawideband (UWB) range of frequencies from 3.1 to 10.6 GHz. To serve those applications, an UWB bandpass filter (BPF) was designed using metamaterials and composite-right-left-handed (CRLH) transmission lines.

The UWB filter, with a passband from 3.1 to 10.6 GHz, is based on a modified microstrip stepped-impedance-resonator (SIR) filter. Metamaterial transmission lines replace the microstrip SIR, with the metamaterial section designed with one CRLH unit cell. The filter design is only 23.4 × 20 mm^2. Using this approach increases the possible number of transmission poles from three in a conventional microstrip design to six in this CRLH design.

The U.S. Federal Communications Commission (FCC) approved the use of 3.1 to 10.6 GHz and fractional bandwidths for indoor/outdoor data communications systems, according to certain provisions.[1] One of the key components for these systems is a BPF with extremely wide passband.[2-4]

A variety of approaches were attempted to cover the necessary bandwidth, including cascading bandpass and bandstop filters.[5,6] This was accomplished by cascading ring resonators and short-circuit stubs, although the result is physically large. UWB filters have also been designed by combining BPFs and lowpass filters (LPFs) in a single design to save space.[7] The tradeoff is that these filter types lack sharp bandstop attenuation.

Hybrid designs with transitions between different transmission lines, such as microstrip and coplanar waveguide (CPW), have also been tried, although they can be difficult to fabricate.[8,9] Use of short-circuited stubs has been suggested for UWB filters as a way to achieve high selectivity.[10,11]

Multimode resonators (MMRs) also were employed in UWB filter designs.[12-15] The approach is based on generating

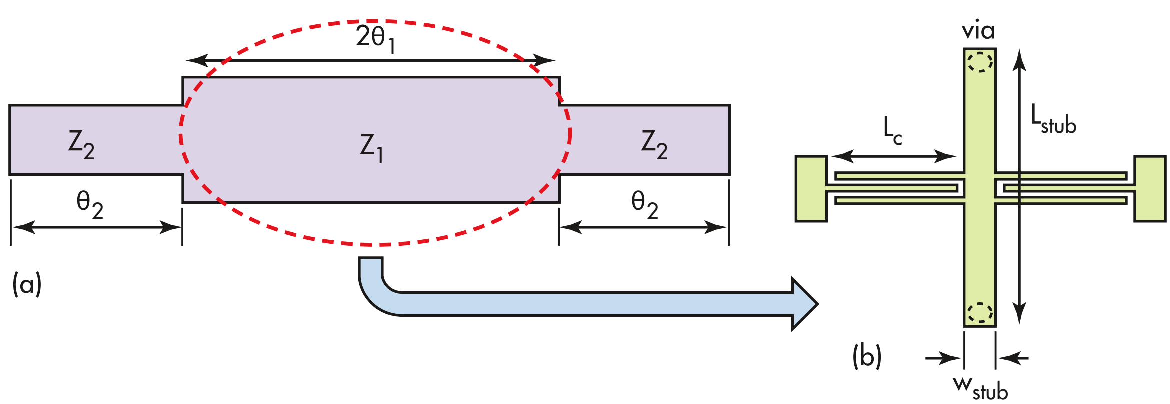

1. The layout for a two-section SIR filter (a) is shown alongside the layout for a CRLH unit cell (b), with L_{stub} = 10 mm, L_c = 4 mm, and W_{stub} = 1 mm.

multiple resonant modes (transmission poles) with the UWB passband. To reduce filter size, a stub-loaded MMR design technique was suggested.[15-17] Tight coupling can be used at the input and output ports of an UWB filter to generate additional transmission poles.[18-23] The tradeoff in all designs is good selectivity for small size, with selectivity sacrificed to achieve miniaturization. For smaller filters, SIRs have been used to design UWB circuits.[24-26]

WHAT'S THE LINE ON CRLH?

CRLH metamaterial transmission lines are characterized by nonlinear phase shifts, which can be leveraged to reduce the size of many microwave circuits, including filters.[27] A CRLH transmission line has a nonlinear, positive/negative frequency-dependent phase response, which has been employed in a number of different compact BPF designs.[28-33] The CRLH approach has led to a number of highly selective, while still compact, UWB filters.[34-40]

Increasing the number of transmission poles through the use of a CRLH unit cell made it possible to design an UWB BPF with good selectivity and relatively small size. The filter design is performed in two steps. The first step involves the design of a conventional, two-stage SIR BPF (*Fig. 1a*), and the second step is modifying the filter by adding a CRLH unit cell (*Fig. 1b*).

In the first step, the conventional two-stage SIT BPF circuitry is implemented on RT/duroid 6010 circuit material from Rogers Corp. (*www.rogerscorp.com*). The circuit laminate is a ceramic/PTFE composite material with a high dielectric constant (Dk) of 10.2 for miniaturization of transmission lines and circuit dimensions for a given characteristic impedance. The filter was fabricated on material with thickness, h, of 0.625 mm.

The SIR BPF was realized using two cascaded transmission lines having different impedances, Z_1 and Z_2, and different electrical lengths, θ_1 and θ_2, respectively. The characteristic impedances of the transmission lines are $Z_1 = 20\ \Omega$ and $Z_2 = 32\ \Omega$. The length, L, of each section is identical, at 3.8 mm. The input impedance of the SIR filter, Y_i, can be expressed by means of Equation 1 in terms of the ratio of the two impedances, $k = Z_2/Z_1$ with electrical length, $\theta = \theta_1 = \theta_2$:

$$Y_i = ({}_jY_2)[2(1+k)(k - \tan^2\theta)\tan\theta]/[(k-2)(1+k+k^2)(\tan\theta)] \quad (1)$$

The conventional SIR filter design achieves zero input admittance ($Y_i = 0$) at 4.5 GHz, 7 GHz, 9.25 GHz, and 13.4 GHz. These frequencies were selected to be at the start, center, and stop of the UWB bandwidth. Hence, the filter structure has corresponding resonances at $\theta_0 = 52$ deg.; $\theta_{s1} =$ deg.; $\theta_{s2} = 127$ deg.; and $\theta_{s3} = 180$ deg. at 4.5 GHz, 7 GHz, 9.25 GHz, and 13.4 GHz, respectively.

Computer simulations were performed on circuit models of the two-stage SIR filter using commercial electromagnetic (EM) simulation software. *Figure 2* shows scattering (S) parameters of magnitude from those simulations. The computations reveal a bandpass response within the frequency range from 3.1 to 10.6 GHz, but the filter also has poor attenuation rolloff at the lower and upper cutoff frequencies. It can be seen that the two-stage SIR filter has three transmission poles in the passband, at 4.5, 7.0, and 9.25 GHz.

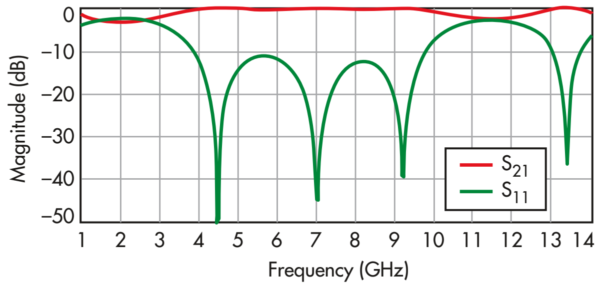

2. The plots trace simulated S-parameters for the magnitude responses of a conventional two-section SIR UWB filter.

The second step in the filter design involves replacing the 20-Ω transmission line with a 20-Ω CRLH metamaterial unit cell (*Fig. 1b*). The unit cell contains a left-handed (LH) section that is designed with two series interdigital capacitors and two shunt stub inductors. A small section of a right-handed (RH) microstrip transmission line with 20-Ω impedance is placed next to the LH section.

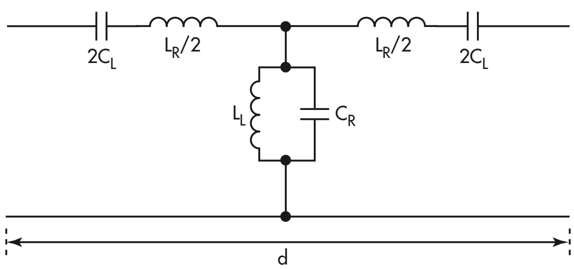

3. This equivalent circuit represents the experimental CRLH transmission line.

Figure 3 illustrates an equivalent circuit of the CRLH transmission line. The values for the optimized interdigital capacitor and stub inductor are as shown in *Fig. 1b*. The CRLH transmission line was designed as a balanced configuration, with LH and RH sections maintaining identical characteristic impedances. The characteristic impedance (Z_{CRLH}) and the transmission phase shift (ϕ_{CRLH}) of this balanced CRLH transmission line are expressed by Equations 2 and 3 (ref. 9):

$$Z_{CRLH} = Z_{RH} = (L_R/C_R)^{0.5} = Z_{LH} = (L_L/C_L)^{0.5} \quad (2)$$

$$\phi_{CRLH} = 1/\omega(C_L L_L)0.5 - \omega(C_R L_R)^{0.5} \quad (3)$$

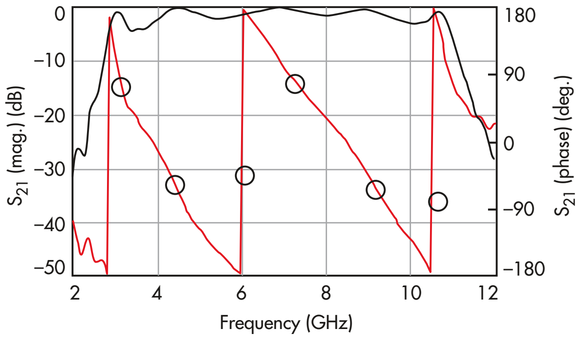

4. These plots show the simulated transmission magnitude and phase coefficients of the CRLH transmission line.

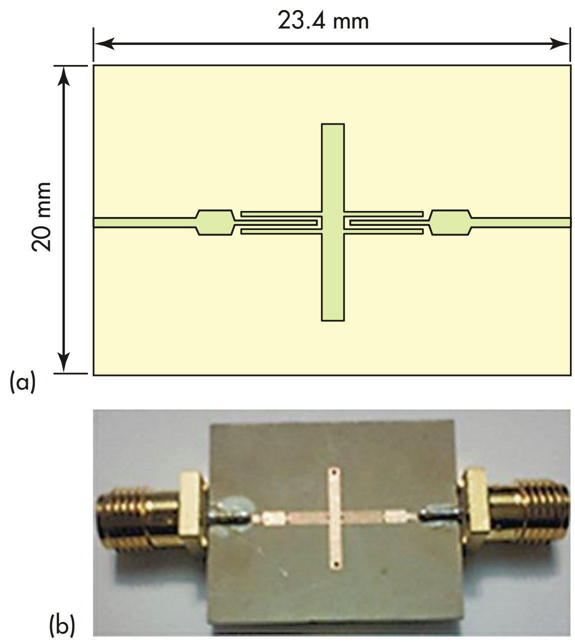

5. Shown are a two-dimensional layout of the UWB BPF (a) and a photograph of the fabricated CRLH SIR UWB filter (b).

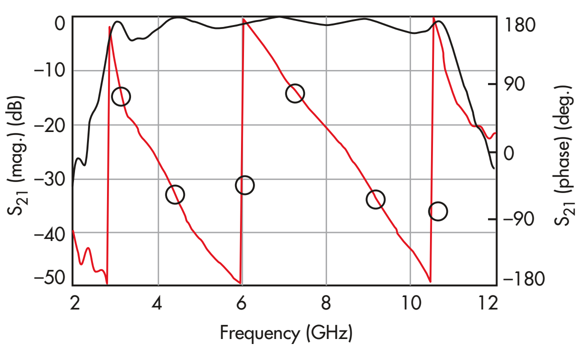

6. These plots compare S-parameter magnitudes of simulated and measured responses for the CRLH UWB SIR filter.

REALIZING DESIGN GOALS

The first design objective of the CRLH transmission-line section is to achieve a balanced 20-Ω line for all desired frequency bands. A second objective was the optimization of the LH and RH phases to satisfy the resonant conditions and create more poles within the UWB frequency range. Essentially, this means meeting the following conditions within the filter's passband: at $\theta_0 = 52$ deg.; θ_{s1}=90 deg.; θ_{s2}=127 deg.; and θ_{s3}=180 deg. By controlling the nonlinear phase shift in the LH passband, more than three frequencies would satisfy these phases within the UWB passband.

To meet these design goals, the 20-Ω CRLH transmission line was designed such that the LH lower cutoff frequency was 3 GHz, the RH upper cutoff frequency was 11 GHz, and the transition point between the LH and RH passbands is at 8 GHz. The transition frequency was selected to help in controlling a nonlinear slow phase shift in the LH passband and to achieve better resonant conditions.

Following an optimization process, the magnitude (insertion loss) and phase of the UWB BPF were simulated with commercial EM software (*Fig. 4*). Due to the phase behavior of the CRLH transmission line, it can be seen that a phase condition of 90 deg. was satisfied twice within the UWB passband at two resonant frequencies: 3.1 and 7.0 GHz. A phase of –52 deg. was also repeated twice at two resonant frequencies within the passband, at 4.5 and 9.2 GHz. A phase of 180 deg. was repeated within the passband at 6.0 and 10.3 GHz. From these phase values, it can be claimed from the LH phase of this CRLH transmission-line section that integrating a conventional SIR filter circuit will increase the number of transmission poles.

The final UWB filter was fabricated on 0.625-mm-thick RT duroid circuit material with 50-Ω microstrip feed line. *Fig. 5a* shows the filter layout, with the fabricated filter shown in *Fig. 5b*. The fabricated filter measures 23.4 × 20 mm^2. Some optimization was performed when cascading the CRLH transmission line with the 30-Ω transmission line in the SIR filter circuit, with the final optimized length of line segment L_c being 4.2 mm.

Figure 6 shows the measured and simulated S-parameters for the filter. Good agreement was found between the simulated and measured insertion loss, around 0.5 to 1.0 dB within the frequency range from 4.2 to 10.6 GHz. At lower passband frequencies, however, the insertion loss was only about 4 dB from 3.1 to 4.2 GHz. This is due to the difficulty in meeting the CRLH transmission-line impedance criteria for the six phase requirements of the full UWB bandwidth.

The filter design is intended to have six poles from 3.1 to 10.6 GHz, and the simulations indicate that transmission poles can be found at resonant frequencies of 3.1, 4.5, 6.5, 9.2, 10.2, and 10.5 GHz. The measured return loss shows only five transmission poles, but those results are slightly shifted due to the challenges of the circuit fabrication process.

(Continued on page 62)


HAWAI`I 5G
Visit us at
IMS2017!
Booth 640
... ALSO INTRODUCING THE NEW
SAGE STOCKROOM
IN STOCK
WG to Coax Adapters
Balanced Mixers
Orthomode Transducers
Bulkhead Adapters
Sector Antennas
Faraday Isolators
Harmonic Mixers
Power Dividers
Horn Antennas
Magic Tees
Omni Directional Antennas
Waveguide Terminations
Directional Couplers
Full-Band Attenuators
Taper Transitions
visit us
online
for more!
WWW.SAGEMILLIMETER.COM/STOCKROOM
Over 1,000 millimeterwave
components off-the-shelf,
in stock, and ready to ship
guaranteed in only 1-3 days.
SAGE
STOCKROOM

The overall technique of using CRLH metamaterials and substituting LH and RH transmission lines for conventional microstrip transmission lines shows great promise in this UWB filter design.

(Continued from page 58)

Figure 7 shows the simulated and measured group delay of the UWB filter. The simulated results demonstrate that the filter has almost constant group delay of 0.35 ns, with maximum variation of less than 0.1 ns within the passband. However, the group-delay variations increase from that 0.1-ns value, from 3.1 to 4.5 GHz and from 10.0 to 10.6 GHz. The measured results reveal that the group-delay variations are 0.2 ns from 4.5 to 10.0 GHz, and increased to about 0.5 ns from 3.0 to 4.5 GHz.

The overall technique of using CRLH metamaterials and substituting LH and RH transmission lines for conventional microstrip transmission lines shows great promise in this UWB filter design. However, fabrication and manufacturing processes must be refined to gain the full benefits of the design approach. Still, the fairly close agreement between computer simulations and measurements reveals the potential of applying this transmission-line technique to other circuit designs that require extremely broadband impedance matching. mw

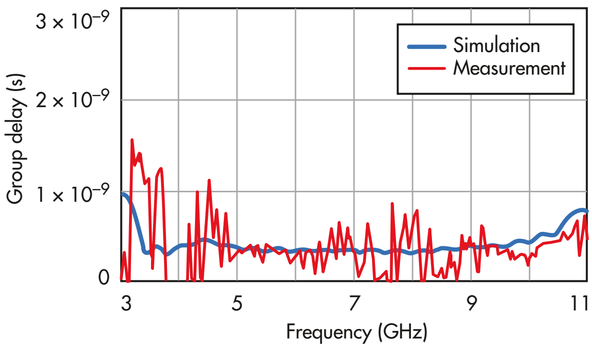

7. This plot traces the group delay of CRLH UWB SIR filter.

REFERENCES

1. United States Federal Communications Commission (FCC), "Revision of part 15 of the commission's rules regarding ultra-wideband transmission system," Federal Communications Commission, Washington, D.C., Technical Report ET-Docket
98-153, FCC02-48, April 2002.
2. Zhang-Cheng Hao and Jia-Sheng Hong, "Ultrawideband filter technologies," *IEEE Microwave Magazine*, Vol. 11, No. 4, 2010, pp. 56-68.
3. Wenjie Feng, Wenquan Che, and Quan Xue, "Transversal Signal Interaction: Overview of High-Performance Wideband Bandpass Filters," *IEEE Microwave Magazine*, Vol. 15, No. 2, 2014, pp. 84-96.
4. Vicente E. Boria, Pablo Soto, and Santiago Cogollos, "Distributed Models for Filter Synthesis," *IEEE Microwave Magazine*, Vol. 12, No. 6, 2011, pp. 87-100.
5. C.W. Tang and M.G. Chen, "A Microstrip Ultra-Wideband Band-pass Filter with Cascaded Broadband Bandpass and Bandstop Filters," *IEEE Transactions on Microwave Theory & Techniques*, Vol. 55, No. 11, 2007, pp. 2412-2418.
6. Y. Liu, C.H. Liang, and Y.J. Wang, "Ultra-Wideband Bandpass Filter Using Hybrid Quasi-Lumped Elements and Defected Ground Structure," *IET Electronics Letters*, Vol. 5, No. 17, 2009, pp. 899-900.
7. J.L. Lee and Y.S. Kim, "Ultra-Wideband Band-pass Filter with Improved Upper Stopband Performance Using Defected Ground Structure," *IEEE Microwave and Wireless Components Letters*, Vol. 20, No. 6, 2010, pp: 316-318.
8. Xiaofeng Sun and Eng Leong Tan, "Novel Ultra-Wideband Filter Using Coplanar Waveguide To Microstrip Transition and Stubs," *Microwave and Optical Technology Letters*, Vol. 55, No. 10, 2013, pp. 2269-2271.
9. Sangyeol Oh, Beomsoo Shin, Jaehyuk Lim, Jongwon Choi, Seungjin Lee, and Jaehoon Lee, "UWB bandpass filter with dual notched bands based on microstrip to CPW transition," in IEEE 16th Annual Wireless and Microwave Technology Conference (WAMICON), 2015, pp. 1-4.
10. H. Shaman and J.-S. Hong, "A novel ultra-wideband (UWB) bandpass filter (BPF) with pairs of transmission zeroes," *IEEE Microwave and Wireless Components Letters*, Vol. 17, No. 2, 2007, pp. 121–123.
11. Xiuping Li and Xiang Ji, "Novel compact UWB bandpass filters design with cross-coupling between $\lambda/4$ short-circuited stubs," *IEEE Microwave and Wireless Components Letters*, Vol. 24, No. 1, 2014, pp. 23-25.
12. L. Zhu, S. Sun, and W. Menzel, "Ultra-wideband (UWB) bandpass filter using multiple-mode resonator," *IEEE Microwave Wireless Components Letters*, Vol. 15, No. 11, November 2005, pp. 796-798.
13. S.W. Wong and L. Zhu, "Quadruple-mode UWB Bandpass filter with improved out-of-band rejection," *IEEE Microwave and Wireless Components Letters*, Vol. 19, No. 3, March 2009, pp. 152-154.
14. Xilong Lu, Bin Wei, Zhan Xu, Bisong Cao, Xubo Guo, Xiaoping Zhang, Ruixia Wang, and Fei Song, "Superconducting Ultra-Wideband (UWB) Bandpass Filter Design Based on Quintuple/Quadruple/ Triple-Mode Resonator," *IEEE Transactions on Microwave Theory & Techniques*, Vol. 63, No. 4, 2015, pp. 1,281-1,293.
15. H.W. Deng, Y.J. Zhao, L. Zhang, X.S. Zhang, and S.P. Gao "Compact quintuple-mode stub-loaded resonator and UWB filter," *IEEE Microwave and Wireless Components Letters*, Vol. 20, No. 8, August 2010, pp. 438-440.
16. Q.-X. Chu, X.-H. Wu, and X.-K. Tian, "Novel UWB Bandpass filter Using stub-loaded multiple-mode resonator," *IEEE Microwave and Wireless Components Letters*, Vol. 21, No. 8, August 2011, pp. 403-405.
17. Y.X. Zhou, D.X. Qu, X.J. Zhong, J.D. Ye, and K. Li, "A novel compact ultra-wideband bandpass filter using microstrip stub-loaded triple-mode resonator doublets," 2015 IEEE International Wireless Symposium (IWS), 2015, pp. 1-4.
18. Amin M. Abbosh, "Design method for ultra-wideband bandpass filter with wide stopband using parallel-coupled microstrip lines," *IEEE Transactions on Microwave Theory & Techniques*, Vol. 60, No. 1, 2012, pp. 31-38.
19. Amin M. Abbosh, "Ultrawideband balanced bandpass filter," *IEEE Microwave and Wireless Components Letters*, Vol. 21, No. 9, 2011, pp. 480-482.
20. H. Wang, Y.Y. Zheng, W. Kang, C. Miao, and W. Wu, "UWB bandpass filter with novel structure and super compact size," *Electronics Letters*, Vol. 48, No. 17, 2012, pp. 1,068-1,069.
21. Huanting Chen, "Compact UWB BPF using coupled-line triple-mode resonator," *Electronics Letters*, Vol. 49, No. 24, 2013, pp. 1,541-1,542.

22. Ting Zhang, Fei Xiao, Jingfu Bao, and Xiaohong Tang, "Compact ultra-wideband bandpass filter with good selectivity," *Electronics Letters*, Vol. 52, No. 3, 2016, pp. 210-212.
23. Q.X. Chu and X.K. Tian, "Design of UWB bandpass filter using stepped-impedance stub-loaded resonator," *IEEE Microwave and Wireless Components Letters*, Vol. 20, No. 9, 2010, pp. 501-503.
24. Feng Wei, Wen Tao Li, Xiao Wei Shi, and Qiu Lin Huang, "Compact UWB Bandpass Filter With Triple-Notched Bands Using Triple mode Stepped Impedance Resonator," *IEEE Microwave and Wireless Components Letters*, Vol. 22, No. 10, 2012, pp. 512-514.
25. Mahmoud. A. Abdalla, Mohamed A. Fouad, Ali M. Rayad, and Aser M. Medhat, "A compact ultrawide BPF for high speed communications," 2nd MeCAP Conference, December 2012, Cairo, Egypt, pp. 1-4.
26. Zhaojiang Shang, Xubo Guo, Bisong Cao, Bin Wei, Xiaoping Zhang, Yong Heng, Guannan Suo, and Xiaoke Song, "Design of a superconducting ultra-wideband (UWB) bandpass filter with sharp rejection skirts and miniaturized size," *IEEE Microwave and Wireless Components Letters*, Vol. 23, No. 2, 2013, pp. 72-74.
27. C. Caloz and T. Itoh, *Electromagnetic Metamaterials Transmission Line Theory and Microwave Applications*, Wiley, New York, 2006.
28. Mahmoud Abdalla, A.Y. Hassan, A.M. Galal Eldin, "A Compact High Selective Coupled Gap CRLH TL Based Bandpass Filter," 9th International Congress on Advanced Electromagnetic Material in Microwave and Optics, United Kingdom, September 7-12, 2015, pp. 237-239.
29. Mohammed. A. Fouad and Mahmoud A Abdalla, "Ultra Compact CPW Dual Band Filter Based on ∏-Generalized Metamaterial NRI Transmission Line," *Journal of Electromagnetic Waves and Applications*, Vol. 9, No. 8, 2015, pp. 1093-1103.
30. Ahmed Ibrahim, Adel Abdel-Rahman, and Mahmoud Abdalla, "Design of Third Order Band Pass Filter Using Coupled Meta-material Resonators," 2014 IEEE APS International Antenna and Propagation Symposium Digest, Memphis, TN, July 6-11, 2014, pp. 1702-1703.
31. Mohammed. A. Fouad and Mahmoud A Abdalla, "A New π-T Generalized Metamaterial NRI Transmission Line for a Compact CPW Triple BPF Applications," *IET Microwave, Antennas and Propagation*, Vol. 8, No. 9, June 2014, pp. 1097-1104.
32. Ahmed A. Ibrahim, Adel B. Abdel-Rahman, Mahmoud A. Abdalla, and Hesham F. A. Hamed, "Compact Size Microstrip Coupled Resonator Band Pass Filter Loaded with Lumped Capacitors," International JEC-ECC, Cairo, Egypt, 2013, pp. 1-4.
33. M. A. Abdalla, M. A. Fouad, H. A. Elregeily, and A. A. Mitkees, "Wideband Negative Permittivity Metamaterial for size reduction of stopband filter in Antenna Applications," *Progress in Electromagnetics Research C*, Vol. 25, 2012, pp. 55-66.
34. Ahmed Kafil Uddin and Bal S. Virdee, "Ultra-wideband bandpass filter based on composite right/left handed transmission-line unit-cell," *IEEE Transactions on Microwave Theory & Techniques*, Vol. 61, No. 2, 2013, pp. 782-788.
35. Abdullah Alburaikan, Mohammed Aqeeli, Xianjun Huang, and Zhirun Hu, "Miniaturized Ultra-Wideband Bandpass Filter Based on CRLH-TL Unit Cell," 44th European Microwave Conference (EuMC), 2014, pp. 540-543.
36. Ali Abid and Zhirun Hu, "Metamaterial Resonator Based Wave Propagation Notch for Ultra-wideband Filter Applications," *IEEE Antennas and Wireless Propagation Letters*, Vol. 7, 2008, pp. 210 - 212.
37. Young-Chun Yun, Seung-Hun Oh, Jeong-Hyeok Lee, Kyung Choi, Tae-Kyung Chung, and Hyeong-Seok Kim, "Optimal Design of a Compact Filter for UWB Applications Using an Improved Particle Swarm Optimization," *IEEE Transactions on Magnetics*, Vol. 52, No. 3, 2016, pp. 1-4.
38. Xiuping Li and Xiang Ji. "Novel compact UWB bandpass filters design with cross-coupling between short-circuited stubs," *IEEE Microwave and Wireless Components Letters*, Vol. 24, No. 1, 2014, pp. 23-25.
39. He Zhu and Qing-Xin Chu, "Compact ultra-wideband (UWB) bandpass filter using dual-stub-loaded resonator (DSLR)," *IEEE Microwave and Wireless Components Letters*, Vol. 23, No. 10, 2013, pp. 527-529.
40. Xiao-Hu Wu, Qing-Xin Chu, Xu-Kun Tian, and Xiao Ouyang. "Quintuple-mode UWB bandpass filter with sharp roll-off and super-wide upper stopband," *IEEE Microwave and Wireless Components Letters*, Vol. 21, No. 12 , 2011, pp. 661-663.

JACK BROWNE | Technical Contributor

What's the Difference Between Optical and Wireless Communications?

Wireless and optical communications technologies are often found on the same cellular communications tower, supporting modern communications using different wavelengths.

Communications have relied on signals propagating through the air from the earliest drumbeats. Wireless communications technologies make effective use of that signal transport medium even as the appetite for more and faster voice, video, and data grows. Still, light has been another long-time form of communications, literally "as far as the eye could see," and optical communications has advanced at a pace equal to or exceeding the evolution of wireless communications. The technologies are much different, but each has its place, its strengths, and its weaknesses.

Wireless communications relies on the transmission and reception of RF/microwave signals modulated with the information to be carried while optical communications uses modulated light beamed through fiber-optic cables. For a fair comparison of the technologies, fixed wireless systems will be compared to optical communications systems because of the lack of mobility for optical links.

In the case of fixed wireless communications, the infrastructure is installed in discrete locations, with line-of-sight (LOS) paths between the locations so that radio waves can propagate through the atmosphere without obstructions. A typical example is the collection of cellular communications antennas and their towers found on hills or high points in the terrain, often along roadways. Signals from multiple individual fixed wireless links are routed through relay stations that join multiple connected wireless links for nearly instantaneous wireless communications across long distances.

LAYING FIBER

The infrastructure of an optical communications system, on the other hand, is distributed from one communications location to another. Fiber-optic cables must be installed from one point to the next to enable optical communications. The quality of those cables is important to the performance of an optical communications system, as is the integrity of the splices between sections of optical cable. Whereas a fixed microwave link sends information through the air between two points, a fiber-optic link depends upon these cables, which must be installed with care and then maintained over time, since they can deteriorate and wear out. Business models for laying fiber-optic cables typically assume a 50-year lifespan for the capital investment of installing the optical network equipment, which may also include links to individual subscribers, known as fiber-to-the-hole (FTTH) optical communications.

1. Wireless communications systems are clearly visible by their tower-mounted antennas pointed in the direction of a wireless link's other terminal. *(Courtesy of Stephouse Networks)*

Although the speed of light through a vacuum is well known (186,000 miles/s), light slows down when it is not in a vacuum (such as outer space). It can slow down significantly when it travels through a medium such as the glass or plastic fibers used in optical cables. While fixed wireless systems are designed for LOS links between transmitter and receiver, optical communications systems typically do not have the luxury of a straight

2. These fiber-optic cables include members of a high-performance ARINC 801 fiber-optic connector series capable of data transmission speeds of 10 Gb/s and higher. *(Courtesy of ITT Cannon)*

path and must often wind around corners through a city or in an office building for their signal paths. As with light reflecting off walls around a corner, every bend in the cable decreases the speed of the light propagating through that cable.

As a result, in terms of pure communications speed, fixed wireless links typically provide faster connections than optical links. The connection speed is usually measured in terms of a system's latency, which is essentially the time required to receive and respond to a signal. The latency of a fiber-optic system is typically longer than that of a fixed wireless link for the same distance, and increases significantly with increases in link distance compared to a fixed wireless link.

BRING THE BANDWIDTH

Perhaps the key differentiator between fixed wireless links and optical communications systems is in bandwidth. Fiber-optic cables are capable of supporting almost unlimited bandwidth, which translates to Gb/s data rates. Fixed wireless links (and all wireless systems), since they are sending signals through free space rather than through an optical fiber or other confined medium, operate within fixed segments of frequency spectrum that must be licensed for different applications to avoid interference from too many signals within the same frequency range in the same location.

The bandwidth of an optical fiber is potentially as wide as the optical portion of the electromagnetic (EM) spectrum, or about 10 THz or more. Of course, to take advantage of such bandwidth, a transmitter and receiver are needed at both ends of a link. While the components for an optical transmitter, such as a light-emitting diode (LED) or laser transmitter, and a photodiode-based receiver are fairly common and low in cost, the data speeds of systems using these components is still limited to the low Gb/s range rather than the Tb/s range.

Because of the enormous bandwidth available using fiber-optic cables, they are often used to route signals from fixed and mobile wireless base stations to their carrier's signal switching stations for making interconnections to customers. Fiber-optic cables have replaced metal cables in many fixed communications installations, such as in warehouses and office buildings, and serve as communications backbones in many types of wireless communications systems, including in base stations for the latest 4G LTE mobile wireless communications systems. Likely, optical communications links will serve similar functions in emerging 5G mobile wireless communications systems.

Similar to the way that frequency bandwidths are divided in wireless systems using frequency division multiplex (FDM), optical communications systems use forms of wavelength division multiplexing (WDM) to increase capacity over optical fiber lines by using different wavelengths through the cable for different carriers. The two chief WDM methods currently in use in optical communications systems are dense WDM (DWDM) and coarse WDM (CWDM), which has less wavelength channels with wider spacing than DWDM. The result is lower data rates, but CWDM systems can be implemented with lower-cost components without the need for the stability and precision required by the closely spaced carriers in DWDM optical communications systems.

Because they send signals through free space rather than through a "captive" propagation medium such as an optical cable, wireless communications systems are licensed for their use of frequency bandwidth to avoid congestion within one band. As it is, some bands become overcrowded, such as 2.45 GHz, because of the low cost of implementing hardware at that frequency compared to higher frequencies. Licensing of frequency spectra by different agencies, such as the FCC, is meant to organize different wireless applications, including communications systems, into different bands.

Just as some optical energy is lost as a function of distance through an optical cable, some EM energy is lost by microwave signals propagating through the atmosphere, with loss increasing as a function of distance and increasing frequency. As a result, while bandwidth is available for wireless communications at millimeter-wave frequencies and even as high as THz frequencies, the practical range of any wireless communications system based on such high frequencies will be limited, with THz communications limited to the near fields of the antennas, essentially within the same room.

As for in-building use, most office buildings function by means of Wi-Fi wireless communications, although fiber-optic networks have a place because of a key advantage over wireless communications technology: they are immune to the effects of electromagnetic interference (EMI). For that reason, and because of the difficulty of "eavesdropping" on a fiber-optic network, optical communications systems are often used as the communications backbone for surveillance systems in buildings. For the difficulty of installing a fiber-optic network, it has its rewards of amazing bandwidth and robustness. mw

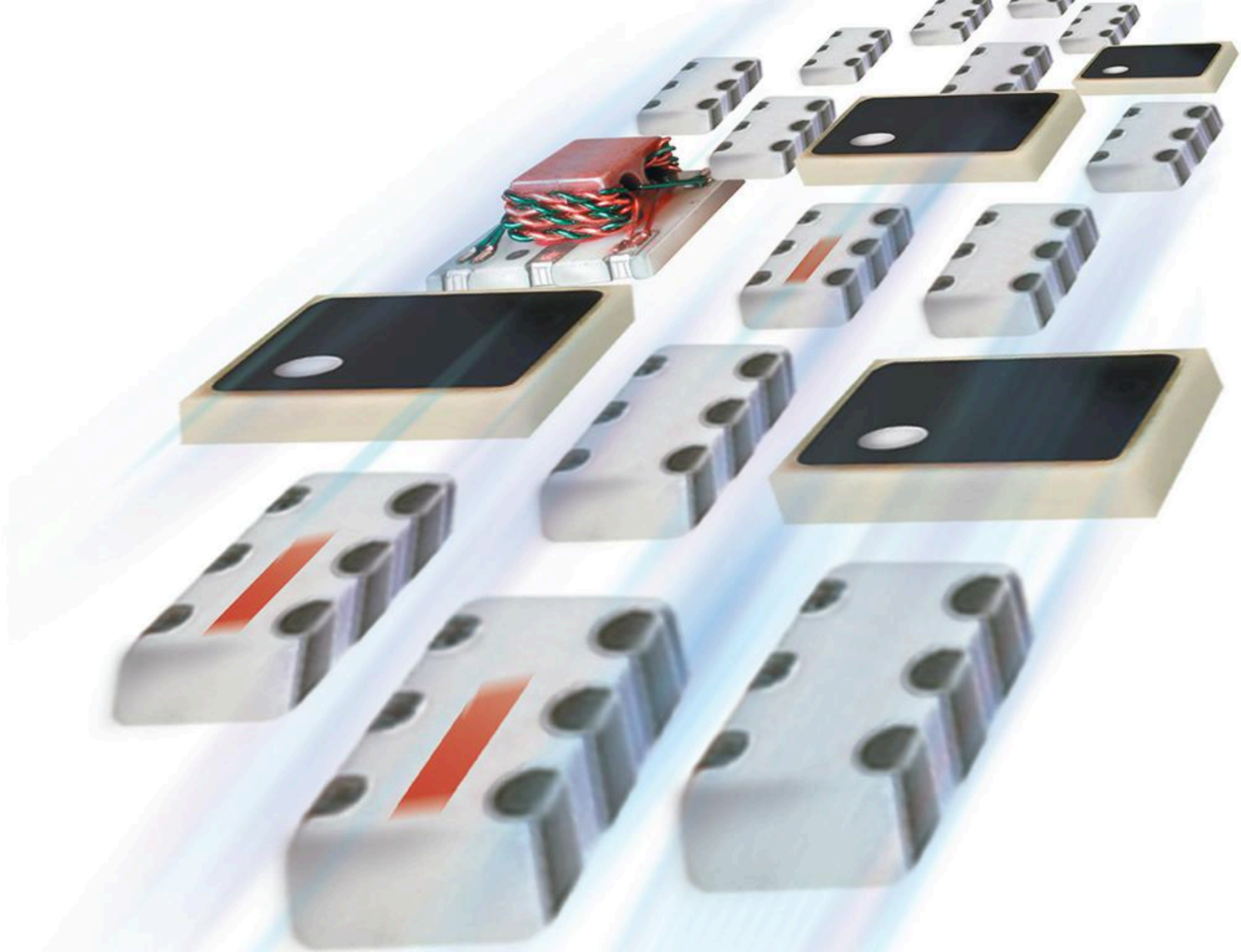

CHRIS DeMARTINO | Technical Writer

The Differences Between Transmitter Types, Part 1

Whether coming from your pocket or from up in the stratosphere, massive amounts of data are on the move at all times, and the ubiquitous transmitter makes it all happen.

A TRANSMITTER IS NO DOUBT a critical part of any communications system. Simply put, the purpose of a transmitter is to transmit signals that contain some form of information. The explosion of mobile communications means that many people actually have a transmitter right in their pocket. In addition, many people today still listen to AM and FM radio stations, which obviously require transmitters in order to broadcast programs. Moreover, aircraft, radar systems, and a host of other applications depend on transmitters to enable communication.

This article, Part 1 of a two-part series, provides a general overview of transmitters, including discussion of classical AM and FM transmitters. Part 2, which will appear in the April issue of *Microwaves & RF*, will focus on additional transmitter implementations, as well as delve into modern digital techniques.

As its name implies, the general purpose of a transmitter is to transmit signals. These signals contain information, which can be audio, video, or data. In essence, a transmitter launches signals into the air via a transmitting antenna. After traveling some distance, the transmitted signal eventually reaches the receiving antenna of a receiver. The receiver then deciphers and processes the information contained in the transmitted signal.

A transmitter's functionality is achieved through a series of steps. First, a carrier signal must be generated. The actual information signal then modulates this carrier signal. Thus, the information signal is often referred to as the modulating signal (it is also occasionally called the message signal). The carrier signal essentially "carries" the modulation information.

Once the carrier signal is modulated, it is amplified to a level sufficient to allow for transmission over the required distance. The final amplification stage is realized by a power amplifier (PA), an important component in any transmitter. Once the PA amplifies the signal, it is fed to the transmitter's antenna and subsequently launched.

The PA's performance depends on the requirements of the specific application. Thus, any transmitter has its own specific power requirements. For example, base-station power requirements have been increasing in recent years, with power levels expected to be as high as 100 W in the future. For AM radio broadcasting, power levels of transmitted signals reach the kilowatt range.

Of course, many transmitter implementations are possible. Take, for instance, the large number of modulation techniques currently being employed. However, the process described here can be considered a very general overview of a transmitter's functionality.

As mentioned, AM and FM broadcasting have been exploited for many years. AM and FM modulation are both forms of analog modulation. Nonetheless, much of today's wireless communication takes advantage of digital modulation techniques. This will be discussed in greater detail in Part 2.

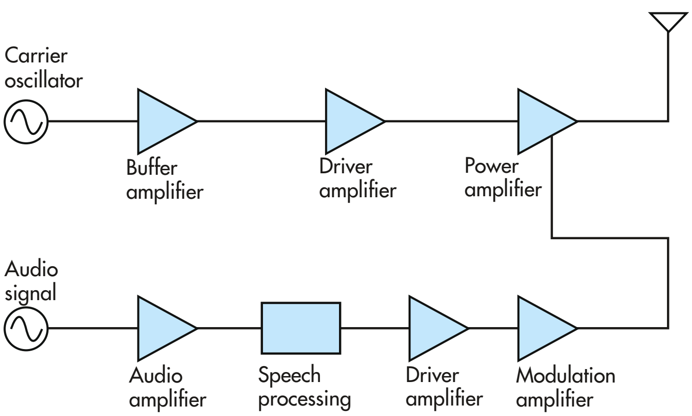

1. This is a block diagram of a high-level AM transmitter.

In the U.S., AM radio broadcasting utilizes carrier frequencies ranging from 540 to 1,700 kHz at 10-kHz intervals. AM extends beyond radio broadcasting—for example, aircraft communication also uses AM.

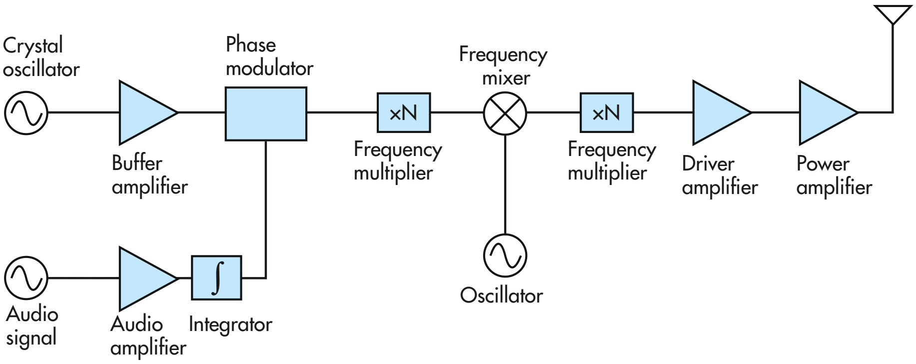

2. The indirect method is applied in this FM transmitter configuration.

AM TRANSMITTERS

AM broadcasting dates back to the early part of the 20th Century. In the U.S., AM radio broadcasting utilizes carrier frequencies ranging from 540 to 1,700 kHz at 10-kHz intervals. AM extends beyond radio broadcasting—for example, aircraft communication also uses AM.

With AM modulation, the modulating, or audio, signal varies the instantaneous amplitude of the carrier signal. In effect, the instantaneous value of the carrier signal's amplitude is determined by the instantaneous amplitude of the modulating signal.

Figure 1 shows a block diagram of an AM transmitter implementation.[1] This configuration is known as a high-level AM transmitter. An oscillator generates the carrier signal, which is amplified by a buffer amplifier and then again by a driver amplifier. The driver amplifier must raise the signal's power level to an amount that is sufficient enough to drive the final-stage PA.

Meanwhile, an audio signal is generated and then amplified. Once amplified, the audio signal is fed to a speech-processing circuit to ensure that only the desired frequencies are passed. Next, a driver amplifier boosts the signal's power level in order to drive the high-power modulation amplifier.

The high-power modulation amplifier's output signal then modulates the final-stage PA. Now, the presence of this audio signal, as well as the carrier signal driving the input of the PA, results in a high-power, AM modulated signal at the PA's output. This AM signal is then fed to an antenna and launched. Eventually, an AM receiver receives the signal, and in turn recovers the audio information.

FM TRANSMITTERS

Like AM, FM radio broadcasting has been in play for many years. In the U.S., FM radio broadcasting operates in the 88- to 108-MHz frequency band. With FM modulation, the carrier frequency varies in proportion with the amplitude of the modulating signal. The amount that the frequency varies is known as the frequency deviation. For FM radio broadcasting in the U.S., maximum frequency deviation is ±75 kHz.

Figure 2 shows a block diagram of one possible FM transmitter implementation. This particular transmitter takes advantage of what is known as the indirect method. A crystal oscillator generates the carrier signal, which is then amplified by a buffer amplifier before reaching a phase modulator.

Meanwhile, an audio signal is generated and amplified, and subsequently arrives at the phase modulator. The presence of both the audio and carrier signals now results in an FM signal at the output of the phase modulator.

In the transmitter shown, the crystal oscillator generates the carrier signal at a frequency lower than the final output frequency. Hence, the FM signal must pass through a frequency multiplier followed by a mixer and then another frequency multiplier. This process takes place so that the signal converts to the desired final output frequency while also attaining the required frequency deviation. That FM signal is amplified by a driver amplifier and then again by the PA before being fed to the antenna for transmission. The transmitted signal eventually reaches an FM receiver, which recovers the information.

Part 2 of this series will discuss other transmitter varieties, such as single-sideband (SSB) transmitters. It will also delve into the digital techniques used to enable modern wireless technology. Unlike AM and FM radio transmitters, a number of today's transmitters actually transmit digitally modulated signals. mw

REFERENCE:

1. Frenzel, Louis E., Principles of Electronic Communication Systems, Fourth Edition, McGraw Hill, 2016.

(Continued from page 54)

Other parameters important in diode selection are reverse breakdown voltage (V_b), reverse capacitance (C_d), minority carrier lifetime (τ_n), and transition time (T_t).

In a good multiplier or comb-generator design, T_t should always be less than the output pulse length (T_p), defined as:

$$T_p = \pi/\omega_n$$

where ω_n is the input frequency.

The carrier lifetime must be sufficiently large to allow for recombination while the diode is charging. A practical guideline is:

$$\tau_n > 10/F_{in}$$

where F_{in} is the input frequency.

The carrier lifetime should also be long enough for the reverse current to accumulate a high charge level. Then, when forward-biased, an extremely fast "snap" into its high impedance state creates the harmonically rich output.

The diode thermal resistance θ_{jc} value is required in order to determine the operating diode temperature. The temperature rise above the baseplate temperature is:

$$\Delta T = (\theta_{jc})(P_{in})$$

DIODE SELECTION

The MMD 840-C11 diode was selected for this design. Its published parameters are:

- Breakdown voltage: 15 V
- Diode capacitance: 0.2 to 0.4 pF
- Carrier lifetime: 15 ns
- Transition time: 35 ps
- Thermal resistance: 60°C/W

A good compromise is achieved among the diode's parameters, making it a good candidate for this application. The vendor supplied the detailed Spice property values that were entered into the library model.

COMB-GENERATOR CIRCUIT DESIGN

The schematic and circuit layout are shown in *Figures 1 and 2*, respectively. All of the circuit elements used in the optimization of this design can be seen in the schematic. All connecting wires, ground via holes, circuit layout details, and material properties were included in the circuit model. The inductor manufacturer supplied the Spice parameters used for the spiral inductors. The circuit was tuned and optimized

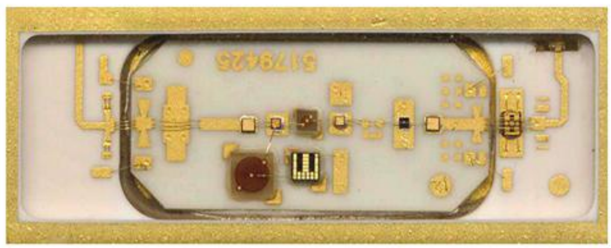

2. This is a photo of the assembled comb generator.

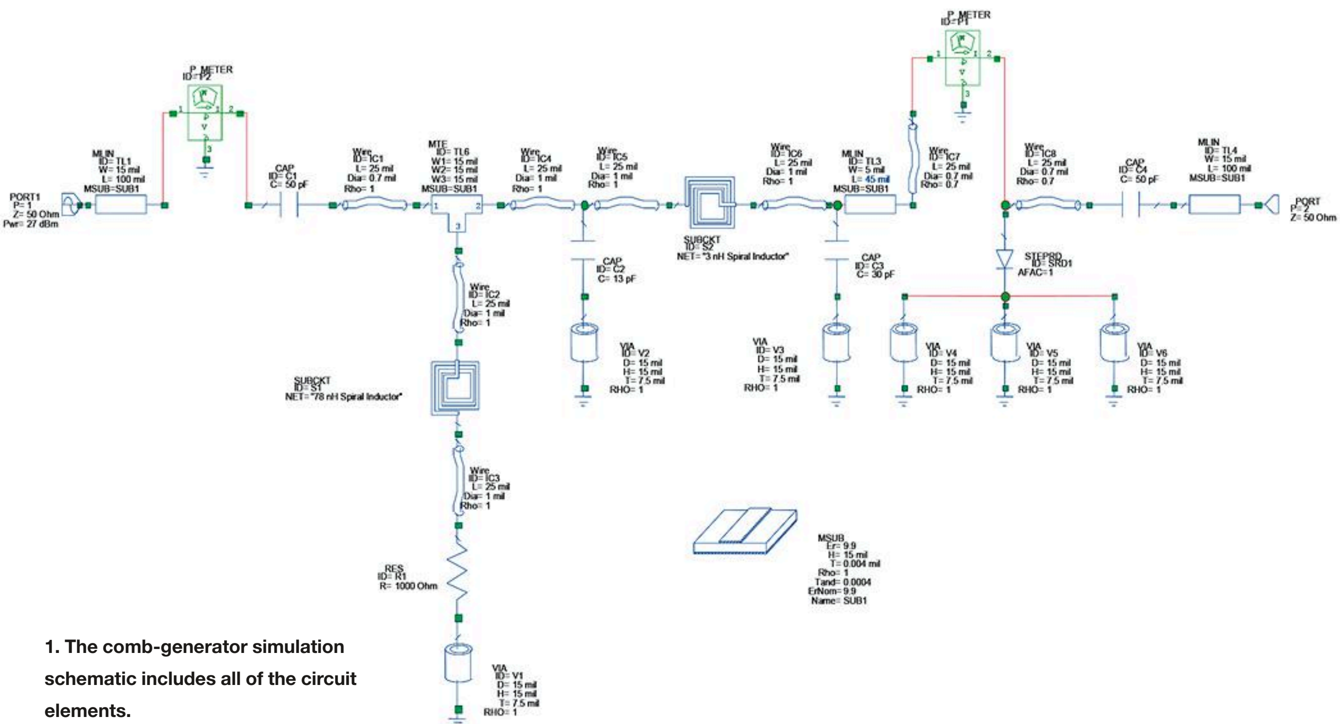

1. The comb-generator simulation schematic includes all of the circuit elements.

so that all harmonic signals up to the 12th harmonic are strong. The circuit was constructed on a 15-mil-thick alumina substrate with a dielectric constant of 9.9.

In terms of simulation, *Figure 3* shows the computer-predicted harmonic signal levels. *Figure 4* presents the output waveform that displays the "snap" action.

from +19 to +28 dBm. Ambient temperature testing was performed on the remaining eight circuits.

The circuits were then transitioned into production. The test data of all circuits is consistent with the data presented in this article. *Figure 5* presents graphical data of the measured comb-generator circuit (serial number 04).

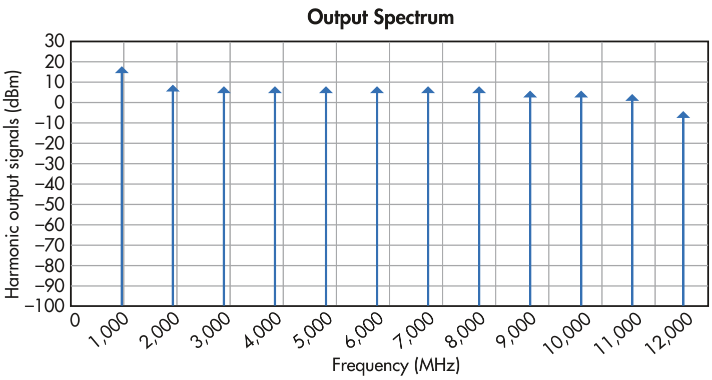

3. Shown are the harmonic levels predicted by the simulation software.

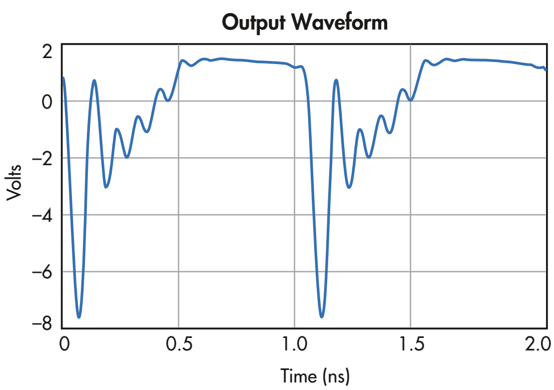

4. The "snap" action can be seen in the output waveform predicted by the software.

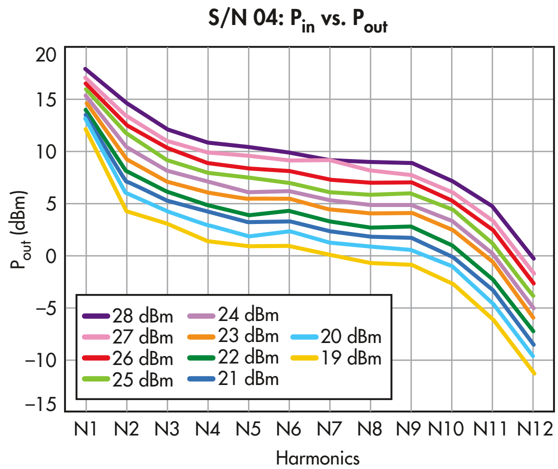

5. These plots illustrate the measured harmonic levels of the comb generator.

TESTING

Ten circuits were constructed and measured. The data is consistent with the predicted harmonic levels. All of the circuits functioned immediately upon first-time power "turn-on." This was gratifying and is a tribute to the Microwave Office software. No time was spent troubleshooting the circuits for unexpected problems like instability, i.e., output breakups into triangular "Christmas tree" spectrums. Circuit performance was stable and tested predictably over a temperature range of –40 to +85°C.

Extensive testing and characterization were performed on two circuits, serial numbers 03 and 04. These were both measured over a wide range of temperatures: –40, +5, +25, +50, and +85°C. In addition, the input power levels ranged

CONCLUSION

A comb generator was successfully created using nonlinear simulation techniques. The implemented topology supported the creation of multiple harmonics from a single diode. The measured results are in close correlation with the simulated values. Several comb generator circuits were fabricated during the design phase.

Consistency among each of the circuits valid=ated the design's robustness. Thus, the usage of the Microwave Office nonlinear simulation software resulted in a comb-generator circuit design that accurately predicted 12 harmonics. mw

ACKNOWLEDGEMENT

I would like to thank Joe Wong and Chung Ly for their prior work and insights on comb generators. Joe Wong did the very early designs, and Chung Ly worked with me in accomplishing this work.

REFERENCES

Wayne Thomas, R. Clayton Smith, and Kipp Schoen, "Comb Generator with excellent harmonic flatness to 40 GHz," Picosecond Pulse Labs, Boulder, Colo., 80301.

"Pulse and waveform generation with step recovery diodes," Agilent application note 918.

"Harmonic Generation using step recovery diodes and SRD modules," Agilent application note 920.

George H. Stauffer Jr., "Spice up the development of a step recovery diode frequency multiplier," *RF Design*, June 1999.

DEREK S. LINDEN | Director of Technology, AWR Group, NI
JENNIFER RAYNO | Senior Development Engineer, AWR Group, NI
www.awrcorp.com

Create Robust UHF RFID Tag Antennas on Dielectric Substrates

The latest synthesis and optimization tools offer dynamic, less complex approaches to designing RFID tag antennas.

Ultra-high-frequency (UHF) radio-frequency identification (RFID) tag antennas, commonly used for inventory and tracking, need to be inexpensive, compact, and robust for the environment in which they will be installed. New antenna synthesis tools have proven very effective in the design of antennas for a wide variety of applications. Now these tools are being applied to overcome the challenges of designing RFID tag antennas.

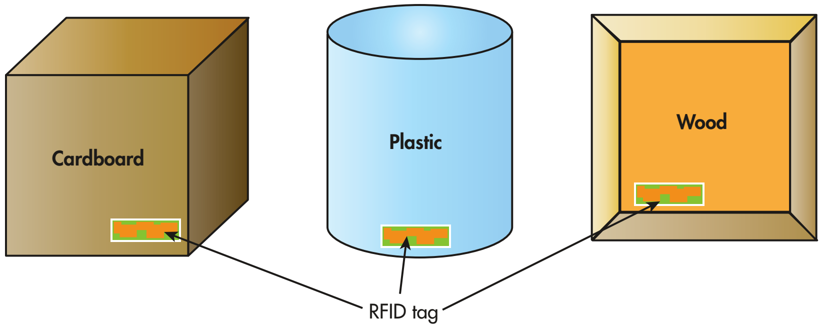

1. A UHF RFID tag can be applied to a variety of materials, which emphasizes the need for a robust design.

This article describes how the AntSyn antenna synthesis and optimization tool, along with the NI AWR Design Environment, are employed to combat these challenges. It also presents an example RFID tag antenna that was created with this technology.

RFID TAG ANTENNA DESIGN ISSUES

The design and integration of RFID tag antennas in the real world can be difficult when trying to make them environmentally immune to the mounting platform. This is especially the case when installing them over a dielectric, as the underlying dielectric properties are likely to be highly variable. A single tag design may be used, for instance, on cardboard, drywall, plastic, fiberglass, wood, or other dielectrics[1] *(Fig. 1)*.

Designing a broadband response is a common approach to ensuring that antenna performance is maintained over a variety of dielectric substrates, each of which will shift the resonant frequency.[2-4] However, to support integration on a wide variety of objects while reducing costs, RFID tag antennas also need to be compact. Unfortunately, when an antenna is made smaller compared to wavelength, the bandwidth narrows,[5] and thus becomes much more sensitive and difficult to design.

In addition, while antennas are usually designed to match a real (typically 50 Ω) standard line impedance, the RFID chips themselves are generally not 50-Ω devices and have reactive impedances. A typical value for a chip impedance might be 16 – j148 Ω.[2]

To minimize reflection losses, it is desirable to directly design the antenna impedance to be a conjugate match of the RFID chip's complex impedance. Therefore, a matching network will not be necessary. Direct antenna-to-chip matching will significantly decrease the cost and complexity, as well as improve the overall reliability. However, this non-standard impedance matching makes the design challenge even more complex.

The various approaches[2-4] used in prior research to meet the challenges associated with designing RFID tag antennas have employed human-in-the-loop engineering methods. Designing and optimizing such antennas by hand is a time-consuming and difficult process, and electromagnetic (EM) tools generally offer limited ability to explore the design space beyond modest tweaking of the antenna's geometry through parameterization. Furthermore, limited design space optimization is particularly restrictive when making an environmentally robust antenna.

AntSyn antenna synthesis software, on the other hand, has proven its effectiveness at efficiently creating many different types of antennas,[6,7] and is now being used to overcome RFID tag antenna design issues. It supports the simultaneous optimization of RFID antennas directly to chip impedance on an array of user-specified dielectric substrates.

AUTOMATED SYNTHESIS DESIGN APPROACH

AntSyn software uses evolutionary algorithms (EAs), a programmatic method that leverages EM simulations to efficiently explore the design space and automatically locate high-performance design options. Users are able to enter RF and form-factor specifications such as bands, patterns, efficiency, geometry constraints, and more. It maintains a library of design templates and takes advantage of a full-wave 3D EM simulation[8] solution to obtain performance information on candidate designs. Advanced algorithms are employed to select and create antennas that are optimized to meet user requirements.

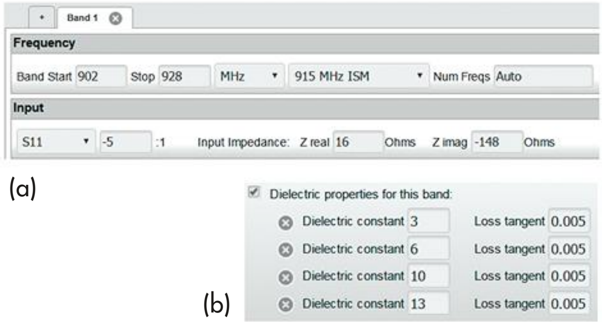

2. Users can specify complex port impedance (a) and dielectric properties for the desired frequency band (b).

The AntSyn band control option enables the user to select many different performance criteria generally related to frequency bands, such as start and stop frequencies, pattern requirements, polarization, and cross-polarization levels. AntSyn also makes it possible to specify a complex input impedance and multiple dielectric properties to be simultaneously optimized for the specified frequency band *(Fig. 2)*. During optimization, antenna performance is evaluated on each of the specified dielectrics.

Another antenna type in the AntSyn library enables environmentally immune design, using a generic XY-mesh type antenna. The antenna is a single-layer, connected XY-mesh design on a dielectric substrate. Since the substrate is utilized to simulate the surface on which the RFID antenna will be installed, it provides fixed user-specified dimensions relative to the antenna rather than being optimized as part of the antenna. Antenna dimensions are limited by the user-specified geometry control.

RFID APPLICATION EXAMPLE

AntSyn was used to synthesize an RFID tag antenna matched to four dielectric substrates and a complex chip impedance. The specifications shown in Fig. 2 were applied, in addition to the following "box" geometry limits: X = 4 in., Y = 1 in., and Z = 0.25 in. A 2-mm

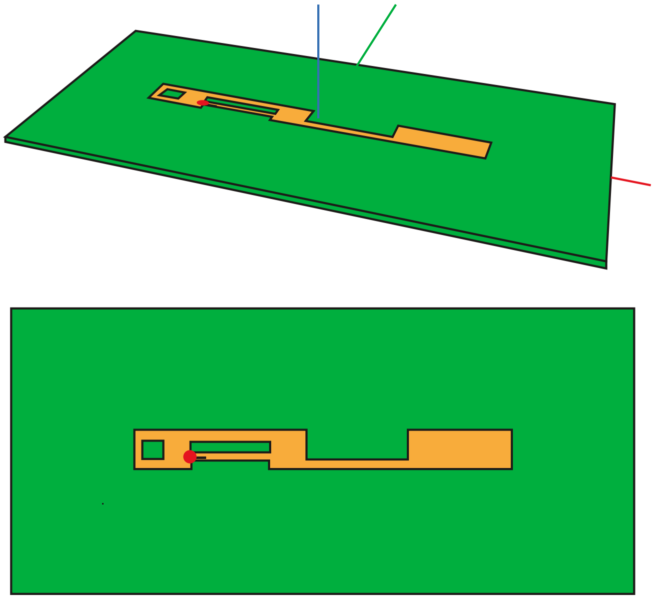

3. These images represent the RFID tag antenna design, which features a single gold layer on a dielectric.

substrate thickness was used, as in Ref. 2. It took only a few minutes to set up the specifications, and then the run was executed. Edging of the mesh was used to increase the accuracy of the simulation at the expense of a longer simulation run time.

The resulting antenna design features a single metallic layer (gold) on a dielectric (green) *(Fig. 3)*. The red dot indicates the chip position. The antenna dimensions are 100.5 × 9.6 mm (3.96 × 0.38 in.), while the overall substrate measures 167.1 × 76.1 × 2 mm.

The input impedance and return loss (matching of the conjugate antenna impedance to the chip impedance) for this antenna are shown in *Figure 4*. According to Ref. 2, a coupling of –2 dB appears to be acceptable; the synthesized antenna is well below this specification over the desired frequency band of 902 to 928 MHz.

CONCLUSION

Thanks to new capabilities in antenna synthesis tools, such as AntSyn, antenna designers can successfully and efficiently overcome challenges in designing RFID tag antennas and meet requirements for low cost, small footprint, and robustness to the installation environment.

The example provided in this article illustrates that it is possible to automatically synthesize a compact antenna that works on multiple substrates and directly matches chip impedance. These new tools can be used for many other applications

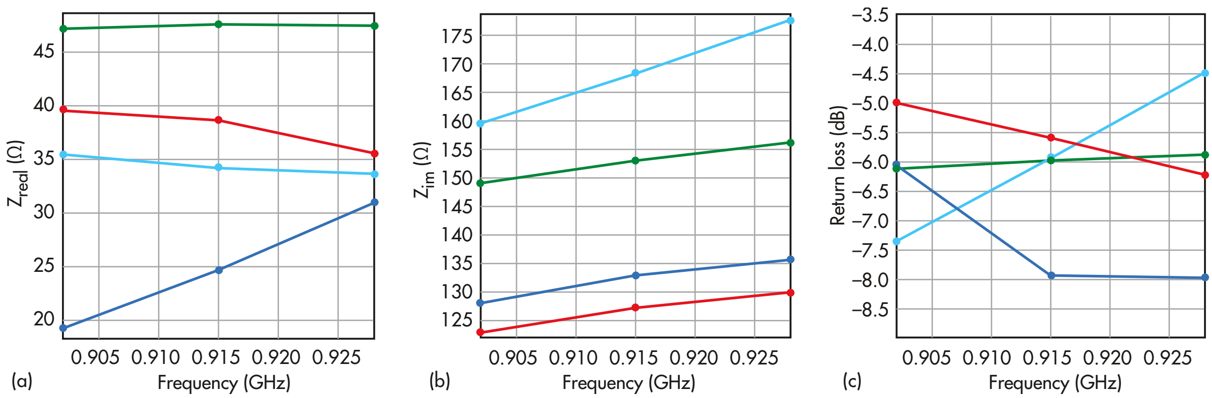

4. These plots show the real Z_{in} (a), imaginary Z_{in} (b), and return loss (c) of the design example.

beyond RFID antenna design, such as to increase yield for antennas that are sensitive to dielectrics or for body-worn or body-internal antenna design. mw

REFERENCES

1. Gaetano Marrocco, "The Art of UHF RFID Antenna Design: Impedance-Matching and Size-Reduction Techniques," IEEE Antennas and Propagation Magazine, Vol. 50, No. 1, February 2008, pp.66-79.
2. Shuai Shao, Robert J. Burkholder, and John L. Volakis, "Design Approach for Robust UHF RFID Tag Antennas Mounted on a Plurality of Dielectric Surfaces," IEEE Antennas and Propagation Magazine, Vol. 56, No. 5, October 2014, pp 158-166.
3. T. DeJeruyelle, P. Pannier, M. EgeJs, and E. Bergeret, "An RFID Tag Antenna Tolerant to Mounting on Materials," IEEE Antennas and Propagation Magazine, Vol. 52, No. 4, pp 14-19, August 2010.
4. Jun Zhang and Yunliang Long, "A Dual-Layer Broadband Compact UHF RFID Tag Antenna for Platform Tolerant Application," IEEE Transactions on Antennas and Propagation, Vol. 61, No. 9, pp. 4447-4455, September 2013.
5. R. F. Harrington (1960). "Effects of antenna size on gain, bandwidth, and efficiency." Jour. Nat'l Bureau of Standards. Washington D.C., USA: US National Bureau of Standards. 64–D: 1–12.
6. Jason D. Lohn, Derek S. Linden, Bruce Blevins, Thomas Greenling, and Mark R. Allard, "Automated Synthesis of a Lunar Satellite Antenna System," IEEE Transactions on Antennas and Propagation, vol 63, no 4, pp.1436-1444, April 2015.
7. http://hothardware.com/news/3d-systems-3d-printing-with-conductive-ink-for-project-ara-antennas
8. WIPL-D Pro v11.0, Software and User's Manual, WIPL-D d.o.o., Belgrade, 2014.

IEEE

MTT-S®

WAMICON

IEEE Wireless and Microwave Technology Conference

WAMICON 2017

Hilton Cocoa Beach Oceanfront

Cocoa Beach, Florida

April 24-25, 2017

JOIN US

The 18th annual IEEE Wireless and Microwave Technology Conference (WAMICON 2017) will be held in Cocoa Beach, Florida on April 24-25, 2017. The conference will address up-to-date multidisciplinary research needs and interdisciplinary aspects of wireless and RF technology. The program includes both oral and poster presentations as well as tutorials and special sessions. The conference also features an active vendor exhibition area and an array of networking opportunities.

Conference Highlights

- **Keynote Speaker:**

Paul Colestock, Founder and Head of the Exploratory Design Group
Global Foundries
"The impact of Silicon as an emerging technology for 5G Circuits and System Solutions"

Registration includes:

- Access to all technical sessions and keynotes
- Breakfast and lunch both days. Morning and afternoon beverage/snack breaks
- Monday evening awards banquet

Visit ***www.wamicon.org*** for complete details.

Exhibit & Sponsorship Opportunities Available!
Email: jassurian@reactel.com • dzavac@tte.com


TELEDYNE
MICROWAVE SOLUTI
Everywhereyoulook™
A Proud 50 Year Heritage
Supporting Critical
EW Programs
AN/ALR-20
USAF, B-52, C-130
AN/ALR-59 – USAF, F-15, F-16, C130J
AN/ALR-69 – USAF, A-10, B-52, C-130, F-16
AN/ALQ-99 – USN/ USMC, EA-18G/EA-6B
AN/ALQ-126
USMC, AV-8B
AN/ALQ-131
USAF POD, F-16
AN/ALQ-135
USAF/FMS, F-15
AN/ALQ-136
USA, AH-1F
AN/ALQ-161
USAF, B-1B
AN/ALQ-164
USMC POD, AV-8B
AN/ALQ-165
USAF, FA-18
AN/ALQ-172
USAF, B-52
AN/ALQ-184
USAF POD, F-16
AN/ALQ-187
USAF, F-16
AN/ALQ-196
USAF, C-130
AN/ALQ-211 – USA, AH-64D, CH-47, CV-22
AN/ALQ-211(V9)
FMS, F-16
AN/ALQ-214
USN, FA-18
AN/ALQ-221
USAF, U-2
AN/APR-39
USA, USAF, USMC, USN rotary wing
AN/SLQ-32
USN, CVN-68, CG-47, DDG-51
teledynemicrowave.com | 1.800.832.6869 | microwavesolutions@teledyne.com
Radar Warning Receivers
EW TWTs
YIG Filters and Subassemblies
Switched Multiplexers
Integrated Microwave Assemblies
RF Channelizers
SDLVAs
Amplifier Products, SSPAs & Wideband GaN Amplifiers
Fast Tune Notch Filters
Tranceivers

defense electronics

A Special Section to PENTON'S DESIGN ENGINEERING & SOURCING GROUP MARCH 2017

Of Modeling and Materials p | 80

Sensor-Based System Detects Hidden Bombs and Weapons p | 82

Foundry Forms Semiconductors with GaN, GaAs, and InP p | 86

JACK BROWNE | Technical Contributor

SOFTWARE HELPS SPEED SiGe RECEIVER DESIGN

MILLIMETER-WAVE FREQUENCIES have long been essential to defense-related applications, well before designers starting applying them to automotive safety systems and future cellular network schemes. To develop a broadband receiver based on silicon-germanium (SiGe) semiconductor process technology, the Defense Science and Technology (DST) Group within Australia's Department of Defence depended on modern computer-aided-engineering (CAE) design and simulation software to help realize a complex circuit and layout (*see figure*). Specifically, the DST Group used the Analog Office RFIC design software within the National Instruments (NI) Applied Wave Research (AWR) Design Environment.

The SiGe receiver was designed for use from 24 to 45 GHz, with specific performance requirements for noise figure, gain flatness, input third-order intercept point (IIP3), and image rejection across the wide frequency range. The software contains a comprehensive library of accurate device models for use in circuit designs. It also performs electromagnetic (EM) simulation and optimization to allow users to study the predicted results of different circuit components and configurations, even on relatively "exotic" substrate materials such as SiGe.

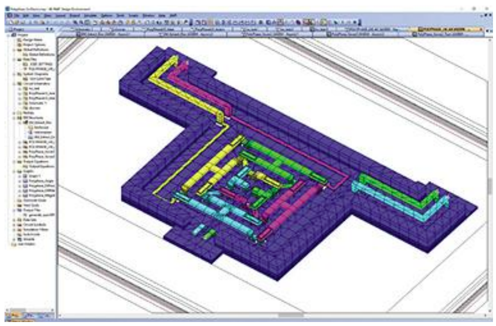

The NI AWR Design Environment provides three-dimensional (3D) representations of high-frequency transmission lines, active devices, and passive devices as part of providing EM simulations of integrated circuits (ICs). (*Courtesy of NI AWR*)

According to DST Group designer Leigh Milner, "Analog Office provided the design team with a significant advantage. The software's custom PCells boosted the capabilities of the foundry PDKs, simplifying the SiGe design flow by automating the process to layout complex structures over previous manual methods. In addition to saving engineering time, the new capability helped improve the accuracy of the layouts by eliminating potential data-entry errors." Semiconductor foundries rely on process design kits (PDKs) to model and simulate different conditions for a semiconductor process, including gate structures for active devices. de

USAF BUILDS on Human Interface R&D

RESEARCH ON human interface technology is leading to an improved understanding of human behavior, and developing methods for combatting such psychological problems as post-traumatic stress disorder (PTSD). In support of such research, the U.S. Air Force Research Laboratory (AFRL) recently awarded contract modifications to Ball Aerospace & Technologies Corp. (*www.ball.com*) and Infoscitex Corp. (*www.infoscitex.com*) worth a combined $75 million. The modifications apply to a previously awarded indefinite-delivery/indefinite-quantity (ID/IQ) contract for the Human Interface Research and Technology program.

The program is focused on research in the areas of human perception and cognitive technologies in attempts to improve a warfighter's situational-awareness and decision-making capabilities. The work by both companies will be performed at Wright-Patterson Air Force Base and the Biodynamics Laboratory (managed by Infoscitex for the AFRL) in Dayton, Ohio, through 2020. ■

Of Modeling and Materials

MATERIALS PLAY a large part in the future of electronic circuits and systems, but development of new electronic materials requires a number of orchestrated efforts. A new material must first be "discovered," typically by researchers who gain an understanding of a material's different properties. It must then be manufactured in sufficient quantities.

Users of III-V semiconductor materials, such as GaAs, know this to be a painfully slow process. It takes a long time before wafers of sufficiently large size can be produced with adequate device yields per wafer to drive down the cost of each device.

Once a material *can* be produced in practical quantities, it must then be put to use where its particular properties can provide benefits to an application. In the "good old days," this involved building a number of amplifier prototypes and then making measurements.

In high-power systems like radar transmitters, heat can stop a circuit or system dead in its tracks. Whether it is a circuit-board material, an adhesive, a solder, or a heatsink, thermal stability and predictability are essential to the long-term health of an electronic design. The complexity of measuring an electronic material's behavior under different power loads and changing thermal conditions can be extremely complex. This may explain the current trend of defense electronic-system designers reaching for simulation software.

Design engineers have long created mathematical models of circuits and their associated materials in attempts to better understand what will happen under different power levels and temperatures. Early simulation efforts involved "global" thermal models in which different operating temperatures were applied for the simulation of a design. But such models do not accurately predict the complex relationship of power and temperature for many designs.

In radar systems, power is not continuous; it occurs in pulses in very transient form. As a result, the heating effects occur for an extremely short time, followed by a short time of cooling, and then another burst of energy and heat. The short-term heating effects place tremendous thermal stresses on materials.

Ultimately, new materials may be the future of electronics designs, but they will go nowhere without the software. de

Jack Browne, Technical Contributor

ULTRA·REL™
CERAMIC MMIC AMPLIFIERS

10 MHz to 7 GHz

Low NF from 0.5 dB *High IP3 up to +42 dBm* *Low DC current 65 mA* *from* $7.45 *ea. (qty 20)*

When failure is not an option! Our CMA family of ceramic MMIC amplifiers is expanding to meet your needs for more critical applications. Designed into a nitrogen-filled, hermetic LTCC package just 0.045" high, these rugged models have been qualified and are capable of meeting MIL standards for a whole battery of harsh environmental conditions:

Qualified for: *(see website for complete list and details)*

Gross and Fine Leak	*HTOL (1700 hours @ +105°C)*
Mechanical Shock	*Steam Aging*
Vibration	*Solder Heat Resistance*
Acceleration	*Autoclave*
PIND	*And More!*

**Gross leak only*

Robust performance across wide bandwidths makes them ideal for military and defense applications, hi-rel instrumentation, and anywhere long-term reliability adds bottom-line value. Go to minicircuits.com for all the details today, and have them in your hands as soon as tomorrow!

Electrical Specifications *(-55 to +105°C)*

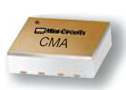

3 x 3 x 1.14 mm

Model	Freq. (GHz)	Gain (dB)	P_{OUT} (dBm)	IP3 (dBm)	NF (dB)	DC (V)	Price $ ea. (qty 20)
CMA-81+	DC-6	10	19.5	38	7.5	5	8.95
CMA-82+	DC-7	15	20	42	6.8	5	8.95
CMA-84+	DC-7	24	21	38	5.5	5	8.95
CMA-62+	0.01-6	15	19	33	5	5	7.45
CMA-63+	0.01-6	20	18	32	4	5	7.45
CMA-545+	0.05-6	15	20	37	1	3	7.45
CMA-5043+	0.05-4	18	20	33	0.8	5	7.45
CMA-545G1+	0.4-2.2	32	23	36	0.9	5	7.95
CMA-162LN+	0.7-1.6	23	19	30	0.5	4	7.45
CMA-252LN+	1.5-2.5	17	18	30	1	4	7.45

RoHS compliant

Mini-Circuits®

www.minicircuits.com P.O. Box 350166, Brooklyn, NY 11235-0003 (718) 934-4500 sales@minicircuits.com

Sensor-Based System
Detects Hidden Bombs and Weapons

SO-CALLED"SUICIDE BOMBERS," carrying or wearing hidden explosives or weapons as part of terrorist activities, have too often thwarted the best intentions of military and police forces to stop them. Fortunately, a weapon for battling such terrorist efforts has been developed by HSS Development (*www.scintel.com*): the latest upgrade of its RDS500 bomb-detection systems, the remote RDS500 Suicide Bomb Detector. This remote-controllable system can detect hidden "walk-by" bombs and weapons.

The sensor-based RDS500 system *(see photo)* is an effective tool for police, explosive-ordnance-disposal (EOD) teams, and counterterrorism units that must deal with attacks by terrorists or covert operatives. It can safely scan individuals within range for hidden body-warn explosives, covert weapons, or even embedded shrapnel.

The system employs various sensor technologies to detect metal objects worn under clothing or in backpacks, such as improvised explosive devices (IEDs). The RDS500 system can be covertly placed and controlled via its graphical user interface (GUI) on a remote PC by means of wired or wireless communications link, minimizing operator risk to threats from scanned individuals.

The RDS500 Suicide Bomb Detector is a remote-controllable system that can detect hidden explosives and weapons.

The RDS500 system can be contained in discrete enclosures—or even built into drywall or wall board in buildings—for ultimate concealment. It operates with ac power or a dc supply from a battery. The sensitivity can be user-adjusted to set the performance level as needed for a particular operating environment and application.

The RDS500 is the latest version of a system with well-established sensor technology that provides the performance and reliability to combat terrorist activities involving hidden bombs and weapons. The firm also supplies systems for detection of cellular radio signals and programmable bomb jammers, covering a total frequency range of 20 MHz to 6 GHz with different modules. ■

Lockheed Martin Seeks to Speed Satellite Operations

LOCKHEED MARTIN is seeking to increase the speed, control, and visibility of several government satellite programs being carried out at its Littleton, Colo. Space Systems facility. The company is looking to the FactoryLogix Manufacturing Execution Software (MES) from Philadelphia-based Aegis Software (*www.aiscorp.com*) for the solution.

The SBIRS GEO Flight 3 is an example of the satellites built by Lockheed Martin for government programs.
(Courtesy of Lockheed Martin)

The software is a good fit for manufacturers in aerospace and defense applications areas—in particular, for mission-critical applications where accessibility of real-time factory data can help find potential defects in a product and alert operators that changes must be made even as a design is on the production line. Lockheed Martin Space Systems *(www.lockheedmartin.com)* plans to use the software to access details on intelligent digital work instructions and advanced data analytics, so as to overcome any design issues and improve the efficiency of the production line by avoiding delays due to defects.

The facility is responsible for building satellites for a number of space missions and has a history of exploring advanced digital technologies throughout product design and manufacturing cycles to improve product quality and manufacturing efficiency *(see photo)*. The Digital Tapestry approach used by Lockheed Martin Space Systems helps identify nonconformance to production-line parameters and specifications, resulting in reduced time to market.

MES is an integrated suite of manufacturing software modules—such as NPI, Logistics, and Production—that can be used to adapt to different manufacturing environments. They can coordinate such functions as aerospace assembly validation, scheduling, warehouse maintenance, and even equipment wear prediction for efficient management of a production facility. ■

Test Systems Perform Munitions Measurements

The recently upgraded MTS-3060 SmartCan test system supports AIM-120 systems, including full functional testing of the AMRAAM's 1760 interface used on F-16, F-15, F-18, and other aircraft.

THE MTS-209 Common Armament and the MTS-3060 SmartCan | Universal O-Level Armament Test Sets from Marvin Test Solutions (MTS; *www.MarvinTest.com*) were both on display at the recent Aero India 2017 (Air Force Station Yelahanka, Bengaluru, India). The systems, which provide aircraft armament and munitions test capabilities for characterizing legacy and next-generation munitions systems, have wide application for global troops.

"Our test solutions are designed to provide commonality across aircraft platforms and serve at all maintenance levels, with the goal of making test easy for our customers," explained retired Major General Stephen T. Sargeant, USAF, the CEO of MTS and vice president of strategic development for The Marvin Group.

The test sets are designed for evaluating the performance of modern smart weapons systems meeting MIL-STD-1153 and MIL-STD-1760 requirements. As an example, the MTS-3060 SmartCan *(see photo)* has been recently upgraded to support AIM-120 systems, including full functional testing of the AMRAAM's 1760 interface used on F-16, F-15, F-18, and other aircraft. The test system has been deployed internationally on two F-16 Blocks (15 and 50) and was demonstrated on the F-15. ■

USAF Looks to UNM for Advanced R&D

THE U.S. Air Force has awarded a $7 million-plus contract to the University of New Mexico for advanced processing of electronics components R&D. The contract covers work on growing new defect-free semiconductor material systems using standard semiconductor growth techniques. Work will be performed in Albuquerque, and is expected to be completed by 2022. The award is part of a competitive acquisition process, with the University of New Mexico submitting one of four offers for the research contract. Kirtland Air Force Base, N.M., is the contracting activity (FA9453-17-C-0087). ■

Maritime Radar to Celebrate 70th Anniversary

THE FIRST TYPE 1 radar system was produced and installed on a fishing trawler in 1947. It would become the first type-approved radar of any kind, earning a type-approval certificate in August 1948. Kelvin Hughes (*www.kelvinhughes.com*), a company with a 250-year history, is proud of having produced that navigation radar system and achieving a milestone in maritime history. The firm has developed radar systems for commercial ships, fishing vessels, coast-guard patrol vessels, and warships.

One of the significant technology developments by Kelvin Hughes in the ensuing years was the launch of the SharpEye navigation radar in 2006, a fully solid-state electronic system that did away with the vacuum-tube magnetron as the microwave signal source. Although magnetrons had served well as high-power pulsed RF/microwave signal sources in a number of radar types since those early years, the use of solid-state oscillators and amplifiers brought a significant reduction in size, weight, and power consumption, along with a major improvement in reliability.

In 2010, the firm brought the SharpEye technology to Vessel Traffic Service (VTS) and coastal surveillance applications, the first time that solid-state technology had been available to these markets.

Most recently, in 2013, the company launched the first upmast multipurpose navigation radar located in a carbon composite housing with low radar cross-section (RCS) characteristics. That same year, the company also launched the SharpEye SxV system, which is a pulse Doppler radar system with full 360-deg. coverage of both ground surveillance and marine security applications.

Of course, these are just a handful of the technology advances that have occurred during the rich history of radar technology. Solid-state technology continues to advance, with semiconductor technologies such as gallium nitride (GaN) providing higher power levels from higher-frequency transistors and integrated circuits (ICs). In turn, system designers continue to look to improvements in antenna architectures and digital signal processing to learn how to make the best use of new RF/microwave capabilities. ■

LIFETIME PRODUCT SUPPORT!

State-of-the-Art Design Capability. Thousands of Models In Stock.

Looking for replacement solutions for competitor VCOs & Synthesizers? Whether you need a second source for end-of-life parts or you're working on a new design, Mini-Circuits is here to support you with thousands of models in stock and decades of design experience. Our VCOs and synthesizers don't just give you industry-leading performance, world-class quality, and fast, easy engineer-to-engineer application support whenever you need it. They also give you the peace of mind that comes with our promise of reliable product supply through the lifetime of your system.

Our engineers will work with you to find a solution from our extensive library of existing designs or develop a custom design to meet your exact requirements. Visit minicircuits.com to explore our catalog, or send your requirements to apps@minicircuits.com today!

- *VCOs from 3 to 7000 MHz*
- *Synthesizers from 56 to 7800 MHz*
- *Wide Variety of Coaxial and Surface Mount Packages*
- *Over 5300 Catalog Models and Engineering Designs*
- *Over 175,000 Units in Stock!*
- *Custom Designs in 3 to 4 Weeks*

Mini-Circuits®

www.minicircuits.com P.O. Box 350166, Brooklyn, NY 11235-0003 (718) 934-4500 sales@minicircuits.com

556 Rev Orig.

JACK BROWNE | Technical Contributor

Foundry Forms Semiconductors with GaN, GaAs, and InP

This versatile semiconductor foundry offers a choice of processes, technologies, and substrate materials, with capabilities in digital, power, and millimeter-wave devices and circuits.

ACTIVE DEVICES for many roads will literally depend on millimeter-wave signals for automotive safety. And if Fifth-Generation (5G) cellular wireless-communications networks use millimeter-wave backhaul links for high-data-rate signal transfers, high-frequency circuit designers will see an unprecedented demand for semiconductors capable of sending and receiving signals at 60 to 80 GHz and beyond.

Fortunately, at least one semiconductor foundry is already established as a logical starting place for the design and development of millimeter-wave discrete devices and integrated circuits (ICs)—Northrop Grumman's Microelectronic Products & Services' *(www.northropgrumman.com/mps)* foundry in Redondo Beach, Calif. While the prime contractor is associated with defense systems, the foundry is available to commercial and military customers through MPS.

The Northrop Grumman facility *(Fig. 1)* is a U.S. Department of Defense (DoD) trusted foundry, one that is well-equipped to fabricate a number of different high-frequency semiconductor technologies. These include devices and circuits on gallium-arsenide (GaAs), gallium-nitride (GaN), and indium-phosphide (InP) wafers. Three different processes are available on GaAs, based on pseudomorphic high-electron-mobility-transistor (pHEMT) active devices. One process is able to fabricate device gates with 0.15-μm gate lengths with maximum frequency for unity current gain (f_t) of 80 GHz and maximum frequency of oscillation (f_{max}) of 200 GHz.

The other processes (low noise and power) provide 0.10-μm gate features with f_t of 120 GHz and f_{max} of 250 GHz. The GaN HEMT process is capable of producing high-power devices with minimum feature size of 0.20 μm and maximum collector-emitter and drain-source voltage of 28 V.

The GaN HEMTs feature f_t of 60 GHz and f_{max} of 200 GHz. As noted in scores of articles, GaN HEMTs have become the active device of choice for high-power RF/microwave monolithic

1. The semiconductor foundry operated by Northrop Grumman Corp., and accessible through the Microelectronic Products & Services group, can fabricate devices in high volume through millimeter-wave frequencies on GaN, GaAs, and InP wafers.

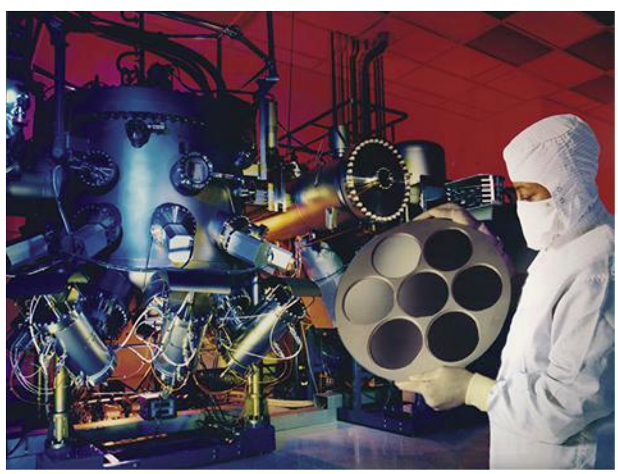

2. The Northrop Grumman semiconductor foundry employs multiple MBE reactors for fabrication of fine-featured devices and ICs on three different semiconductor substrate materials.

microwave integrated circuits (MMICs), notably for amplifiers and switches. The semiconductor material has the high electron velocity needed for high-speed, high-frequency circuits—but also much higher power density and breakdown voltage than other high-frequency materials, such as GaAs, for building high-power amplifiers that are small in size.

The GaN HEMT process technology provides two metal-interconnection layers, thin-film resistors, metal-insulator-metal (MIM) capacitors, air bridges, and backside vias for constructing high-power, high-frequency components and circuits. Amplifiers fabricated with the 0.2-μm GaN HEMT process have served such applications as military radar systems.

The diversified foundry offers four different InP processes: three based on heterojunction bipolar transistors (HBTs) and the fourth on pHEMTs. A 1-μm InP HBT process developed nominally for higher-power devices at high frequency has f_t of 80 GHz and f_{max} of 150 GHz. The other two InP HBT processes are nominally geared for high-speed digital circuits, such as analog-to-digital converters (ADCs) and digital-to-analog converters (DACs), with minimum feature sizes of 0.8 and 0.6 μm. The former has f_t of 160 GHz and f_{max} of 200 GHz, while the latter has f_t of 250 GHz and f_{max} of 300 GHz. The fourth InP process at Northrop Grumman's foundry, based on pHEMT active devices, realizes minimum feature size of 0.1 μm and achieves f_t of 180 GHz and f_{max} of 350 GHz.

The high performance of the processes is achieved with the aid of molecular-beam epitaxy (MBE) for deposition of single-crystal thin films on each wafer under high-vacuum conditions *(Fig. 2)*. Multiple-wafer MBE reactors enable the fabrication of high-purity device structures for excellent performance at millimeter-wave frequencies, while also achieving respectable device yields per wafer.

The foundry staff works closely with customers to meet the most challenging requirements, providing process design kits (PDKs) optimized for specific application areas. The PDKs are compatible with most commercial simulation software tools, including those from Cadence Design Systems *(www.cadence.com)*, Keysight Technologies *(www.keysight.com)*, and National Instruments/AWR *(www.ni.com)*. de

NORTHROP GRUMMAN CORP., Microelectronic Products & Services (MPS), One Space Park, Redondo Beach, CA 90278; (310) 814-5000, www.northropgrumman.com

JACK BROWNE | Technical Contributor

Pilfering Power on the Battlefield

Salvaging energy from electromagnetic sources—or even from soldiers' movements—can help extend the operating time from a battery in portable electronic gear.

PORTABLE RADIOS for tactical use have made tremendous strides in recent years. Borrowing from their commercial mobile wireless radio counterparts, they have added functionality while shrinking size and weight. But all of that communications capability can go to waste without power, and the last place to have a tactical radio's battery power run low is on the battlefield.

This may soon be avoidable, however, with the adoption of energy-scavenging technologies that can transform available RF/microwave energy in the operating environment to dc power. To give one example, with the technology developed by Radient micro-tech Corp. *(www.radientmicro.com)*, the surface of a mobile electronic device—such as a portable tactical radio—can be transformed into a second antenna for capturing "free" power in the environment.

Part of Radient's patented solution involves turning the surface of a cellular telephone or tactical radio into an energy-harvesting antenna. By doing so, the electromagnetic (EM) energy can be transformed into dc power and reused by the same or another electronic device *(see "Harvesting Energy from RF Sources" on mwrf.com)*. As much as 90% of the signal energy transmitted from a signal source, such as a cellular wireless base station, is dispersed into the environment and not used as part of the communications process.

The same is true for a tactical environment with wireless devices, such as tactical radios. If that energy can be captured, it can be reused to power multiple electronic devices. The Radient micro-tech technology allows users to charge the batteries of their mobile electronic devices from energy in the environment—or, in extreme cases, operate from that available energy and without a battery.

With the Radient approach, an electronic device equipped with an extra antenna can harvest its own transmitted RF/microwave power or the EM energy around it. The EM energy is converted to dc power, and then the electronic device's power-management circuitry makes best use of the scavenged power. For example, it could be used to power some of a radio's circuitry, saving its own battery power and extending operating time, or to charge the radio's battery for additional operating time.

The Energy Harvesting Assault Pack contains a generator and suspension systems that can convert a soldier's movements to electrical power. *(Courtesy of U.S. Army CERDEC)*

The RF-to-dc conversion circuitry is very low cost. The energy-scavenging solution, with its form-fitting antenna, can be added to a tactical radio or other electronic device without adding significantly to the cost of the device or its size and weight. In fact, with the additional power, the size of the battery (and thus, the radio) can even be reduced.

The concept of energy harvesting and reducing battery size for in-field electronic equipment has been of interest to researchers from the U.S. Army Material Command's Communications-Electronics Research, Development, and Engineering Center (CERDEC; *www.cerdec.army.mil*) for some time. Portable radios, GPS receivers, and night-vision goggles are just a few of the electronic devices carried by a modern soldier, all requiring batteries.

In seeking to reduce the weight of the batteries required for all of these electronic devices, CERDEC and its Command, Power, and Integration Directorate has developed the Energy Harvesting Assault Pack (EHAP; *see photo*). It is designed to convert the natural movements of soldiers into usable electrical power.

The CERDEC EHAP consists of a rack-and-pinion generator with spring-loaded, double-frame suspension systems attached to a rucksack. The rucksack moves up and down with each step taken by a soldier, moving the generator and producing electrical energy. CERDEC is studying the impact of soldiers carrying the added weight of the EHAP frame, hoping to create smaller, lighter versions with improved energy efficiency. Certainly, energy-harvesting methods such as the Radient micro-tech solution are also of interest.

JACK BROWNE | Technical Contributor

Diamond is Precious for Thermal Dissipation

Synthetic diamond heat spreaders have all of the properties needed to optimize thermal management for high-power-density circuits and semiconductor devices.

DIAMOND IS known to be an extremely hard material that's excellent for cutting tools. Less well known is the fact that it's also an excellent thermal conductor. In addition, it has mechanical and electrical properties that make it a strong candidate for heat spreaders for high-power, high-density circuits and devices.

Element Six *(www.e6.com)* has developed a process using chemical vapor deposition (CVD) by which thin diamond films can be synthesized under tightly controlled conditions *(see photo)*. This results in CVD polycrystalline diamond with high consistency and repeatability.

Diamond is a low-density material with high mechanical strength that has a low dielectric constant and is intrinsically a good electrical insulator. It is unparalleled as a thermal conductor, with the low thermal resistance and isotropic behavior that enables heat to flow freely through the material in all directions.

Element Six has engineered the material in many forms, in thicknesses from 100 to 2,000 μm and wafer diameters to 140 mm for mechanical and electrical products. In addition to its CVD growth process, the firm developed laser-cutting and polishing methods for achieving low surface roughness that have the high flatness required to achieve gap-free interfaces with semiconductor substrates and other packaging materials.

For heat-spreader applications, the company offers its Diafilm TM line of materials, which includes materials with four grades of thermal conductivity: Diafilm TM100, TM150, TM180, and TM200. As a heat spreader for high-power packages, all four grades offer considerably higher thermal conductivity than commonly used high-power package materials.

All four grades of heat-spreader CVD synthetic diamond materials have a Young's modulus between 1,000 to 1,100 GPa and density of 3.52×10^3 kg/m^3. The specific heat capacity for all four grades is 520 J/kg/K at 300 K. Diafilm TM100 materials have thermal conductivity of better than 1,000 W/m-K at 300 K and better than 900 W/m-K at 425 K. They exhibit a coefficient of thermal expansion (CTE) of 1.0 ± 0.1 ppm/K at 300 K and 4.4 ± 0.1 ppm/K at 1000 K. Thermal diffusivity is greater than 5.5 cm^2/s at 300 K.

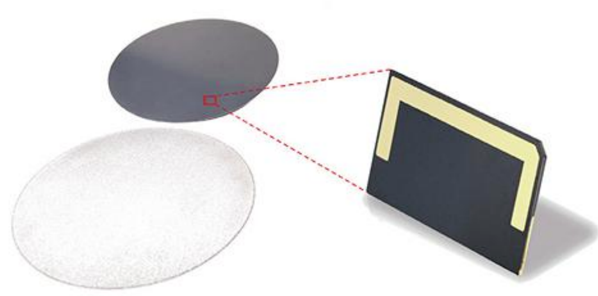

These are 120-to-140-mm-diameter CVD diamond wafers of different thermal grades, with a metallized head spreader (not to scale) shown at right.

The Diafilm TM150 synthetic diamond head-spreader materials offer higher thermal conductivity, with measured values of better than 1,500 W/m-K at 300 K and better than 1,400 W/m-K at 425 K. The CTE of this material is 1.0 ± 0.1 ppm/K at 300 K and 4.4 ± 0.1 ppm/K at 1000 K. Thermal diffusivity is greater than 8.3 cm^2/s at 300 K.

Going even higher, Diafilm TM180 materials have thermal conductivity of better than 1,800 W/m-K at 300 K and better than 1,500 W/m-K at 425 K, with CTE of 1.0 ± 0.1 ppm/K at 300 K and 4.4 ± 0.1 ppm/K at 1,000 K. Thermal diffusivity of this material is greater than 10.0 cm^2/s at 300 K. For the highest thermal conductivity, Diafilm TM200 diamond materials maintain thermal conductivity of better than 2,000 W/m-K at 300 K and better than 1,500 W/m-K at 425 K. They exhibit a CTE of 1.0 ± 0.1 ppm/K at 300 K and 4.4 ± 0.1 ppm/K at 1,000 K, with thermal diffusivity of greater than 11.1 cm^2/s at 300 K.

Element Six works closely with customers in terms of thickness, metallization, and soldering requirements to ensure that a heat-spreader solution based on CVD synthetic polycrystalline diamond achieves optimum results, enabling higher power levels in smaller size packages and circuits. de

ELEMENT SIX TECHNOLOGIES, 3901 Burton Dr., Santa Clara, CA 95054; (408) 986-2400, www.e6.com

JACK BROWNE | Technical Contributor

Spring-Loaded Probe Pins Cut Automated Testing Costs

These stamped, cost-effective, spring-loaded probe pins provide exemplary performance and long-term reliability for high-density automated testing and compression interconnections.

SPRING-LOADED PROBE pins have long been a part of electrical and environmental testing, even though they consist of three or four discrete parts and can be laborious (and costly) to assemble into probe assemblies. Also known as "pogo" spring probes, such spring-loaded probe pins provide the compliance to avoid damage to miniature circuits while still providing adequate contact force for sure electrical connections to packages and circuit probe points.

As discrete and integrated circuits (ICs) become more dense in attempts to design more functions into smaller packages, more probe pins are needed for a given probe area. Consequently, high-performance spring-loaded probe pins are often replaced with lower-cost (but lower-performance) stamped contacts.

However, thanks to the development of the H-Pin probe pin by Plastronics *(www.plastronics.com)*, the sacrifice of performance for cost is no longer necessary. The spring-loaded probe pins are suitable both for test applications and board-to-board (BTB) compression connectors.

The H-Pin is a cost-effective, stamped spring probe with outstanding mechanical, electrical, and thermal performance of a spring-loaded probe *(Fig. 1)*. It is a family of products that includes the HO33, HO38, HO57, and HO77 Series H-Pins, with different lengths and pitches to suit the needs of many applications. Models are available with 1-dB bandwidth of wider than 23 GHz.

All have nominal impedance of 50 Ω with low capacitance and self-inductance. They employ high-quality materials and trim manufacturing costs through the use of a high-volume beryllium-copper (BeCu) stamping process and high-speed assembly and inspection process.

Whether used as contacts for compression connectors or as test probe contacts, these probe pins represent impressive mechanical engineering and manufacturing, given the dimensions *(Fig. 2)*. They can be used in connectors and probes with pitches as fine as 0.2 mm. For example, the HO33 Series H-Pin products feature a minimum pitch of 0.4 mm and a working travel distance (for compression) of 0.4 mm.

Pin contacts in this series are available with lengths from 2.89 to 3.81 mm with a free-air current rating of 1.8 A. They feature 1-dB bandwidth of 10 GHz. The probe pins have less than 50 mΩ contact resistance, with capacitance of 0.067 pF and self-inductance of 0.75 nH. The HO33 Series H-Pins are rated for operating lifetimes of more than 50,000 contacting cycles.

1. The H-Pin spring-loaded probe pins are manufactured with a high-volume stamping process that helps to keep costs low in high volumes.

2. The H-Pin spring-loaded probe pins are available in different lengths and for pitch placement as fine as 0.2 mm.

At the high-frequency end of the product line, the HO77 Series H-Pins include probe pins with full lengths from 4.45 to 5.69 mm that can be positioned with minimum pitch of 1.0 mm. They have a working travel distance of 0.7 mm and are rated for mechanical life of better than 125,000 contact cycles. The HP77 probe pins feature contact resistance of less than 16 mΩ, capacitance of 0.19 pF, and self-inductance of 0.94 nH. They have usable 1-dB bandwidth of 23.3 GHz and offer current-handling capability of 4 A (in free air). de

PLASTRONICS, 2601 Texas Dr., Irving, TX 75062; (972) 258-2580, www.plastronics.com

GaN Amplifier Module Runs to 6 GHz

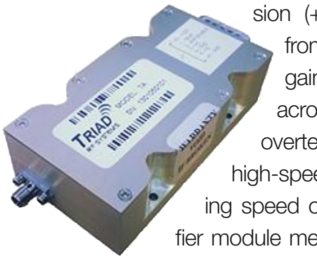

MODEL TA1049 is a Class AB GaN amplifier module capable of +37 dBm (5 W) typical output power at 1-dB compression (+38 dBm saturated output power) from 0.7 to 6.0 GHz. It provides 36-dB gain with better than ±2-dB gain flatness across the full frequency range. It features overtemperature shutdown protection and high-speed on/off control, with typical switching speed of 1 μs (maximum 2 μs). The amplifier module measures 3.75 × 2.00 × 1.063 in. and is available with an optional heatsink. It runs on a wide supply range of +9 to +36 V dc and draws 2 A typical current.

TRIAD RF SYSTEMS

11 Harts Ln., Ste. 1, E. Brunswick, NJ 08816; (855) 558-1001, www.triadrf.com

Digitizer Offers 14-b Resolution at 10 Gsamples/s

THE ADQ7DC is a high-speed digitizer designed for challenging measurement applications. It provides one or two analog input channels with a 5- to 10-Gsample/s sample rate per channel and 14-b vertical resolution. It is suitable for light detection and ranging (LIDAR), radar, and test applications, and is ac- and dc-coupled with 2.5-GHz analog bandwidth. The digitizer is Windows- and Linux-compatible, and contains 4-GB data memory. It includes PCIe, PXIe, USB 3.0, MTCA, and 10GbE data interfaces, and supports sustained data-transfer rates to 5 GB/s.

SIGNAL PROCESSING DEVICES SWEDEN AB (SP DEVICES)

Teknikringen 6, SE-583 30 Linkoping, Sweden; +46 (0) 13 4650600, www.spdevices.com

Linear Amplifier Powers 0.5 to 2.7 GHz

BROADBAND SOLID-STATE power amplifier model BME58278-100 provides 100 W output power at 3-dB compression from 0.5 to 2.7 GHz. The rugged Class AB linear amplifier boasts 52.5-dB gain with ±3.5-dB gain flatness. It has typical harmonic levels of –13 dBc and spurious levels of –60 dBc. The amplifier exhibits input VSWR of 2.0:1. The device operates on +18- to +36-V dc supply and features rapid enable time of less than 5 μs. It measures 8 × 6×1.8 in. and weighs 4 lb. The amplifier, which meets MIL-STD-810F requirements for shock and vibration, is designed for operating temperatures from –40 to +85°C.

COMTECH PST

105 Baylis Rd., Melville, NY 11747; (631) 777-8900, www.comtechpst.com

AC-DC Power Supplies Deliver 1 and 2 kW

THE RUGGEDIZED TWM Series of bulkhead ac-dc power supplies meet the needs of industrial and military applications. They convert ac voltage in the range of 100 to 260 V ac and 50/60 Hz and 400 Hz to dc voltage at 12, 24, 48, and 120 V dc. The supplies are designed to meet MIL-STD-461 for EMI and MIL-STD-810 for environmental immunity. The TWM1000-XXX model is rated for 1,000 W output power, while the TWM2000-XXX is capable of 2,000 W output power. Multiple units can be run in parallel for higher power levels. Standard interface is via military circular connectors, but customized versions can be supplied with terminal-block inputs and bus-bar outputs. The power supplies are well-suited for military shipboard applications, ground command, and control rooms, as well as utility control rooms. They can be equipped with optional communications capability to monitor and control output voltage and current. The 1,000-W version measures 13 × 12 × 4 in. and weighs 7.5 kg.

TECHNOLOGY DYNAMICS INC.

100 School St., Bergenfield, NJ 07621; (201) 385-0500 www.technologydynamicsinc.com

SPDT Switch Handles 5 kW from 1.0 to 1.1 GHz

A SINGLE-POLE, DOUBLE-THROW (SPDT) switch is designed to handle 100 W average power and as much as 5 kW peak power from 1.0 to 1.1 GHz. It provides at least 40-dB isolation between ports with 0.8-dB maximum insertion loss and 1.50:1 maximum VSWR. Peak power rating is for pulsed signals with pulse width of 17 μs at pulse repetition frequency (PRF) of 600 Hz and duty cycle of 2%. The TTL-controlled switch features 2-ns typical switching speed from 50% TTL to 10%/90% RF signal. It is powered by 50 mA at +50 V dc and 350 mA at +5 V dc, and supplied with female TNC connectors. The hermetic SPDT switch measures 4.22 × 2.98 × 0.70 in. and is designed for operating temperatures from –45 to +85°C.

CORRY MICRONICS INC.

761 Commonwealth Dr., Warrendale, PA 15086; (724) 940-7556, www.cormic.com


Mini-Circuits
YAT

NEW PRODUCTS

PLL Synthesizer Covers 50 to 115 MHz

MODEL FSW511-50 2476-50 is an intelligent interactive synthesizer (I2S) with a frequency range of 50 to 115 MHz and tuning step size of 500 kHz. The synthesizer has an on-board microcontroller to simplify communications and programming for COTS applications. It provides at least +3 dBm output power across the frequency range and features low phase noise of –115 dBc/Hz offset 1 kHz from the carrier, –112 dBc/Hz offset 10 kHz from the carrier, and –127 dBc/Hz offset 100 kHz from the carrier when run with a standard 10-MHz reference. The synthesizer operates from voltage supplies of +5 V dc (15 mA maximum current) for the digital port and +5 V dc (50 mA maximum) for the VCO. It is supplied in a compact low-profile housing measuring just 0.94 × 0.94 × 0.23 in., and handles operating temperatures from –40 to +85°C.

SYNERGY MICROWAVE CORP.

201 McLean Blvd., Paterson, NJ 07504; (973) 881-8800, www.synergymwave.com

Two-Part Epoxy is Thermally Conductive

MELDING BONDING strength and thermal management into one adhesive, EP30TC is a two-component (2K) epoxy (10:1 mix ratio by weight) that contains a robust thermally conductive filler material with fine particle sizes. The epoxy is certified to NASA low-outgassing requirements for use in deep space, and can be used for bonding, coating, sealing, and encapsulating for military and aerospace applications. The epoxy is able to be applied in coats as thin as 5 to 15 μm, for a thermal resistance of 7-10 × 10-6 K-m2/W. The low-viscosity material features volume resistivity of more than 1014 Ω-cm. It can be used at operating temperatures from –73 to +149°C with excellent flow properties.

MASTER BOND

154 Hobart St., Hackensack, NJ 07601; (201) 343-8983, www.masterbond.com

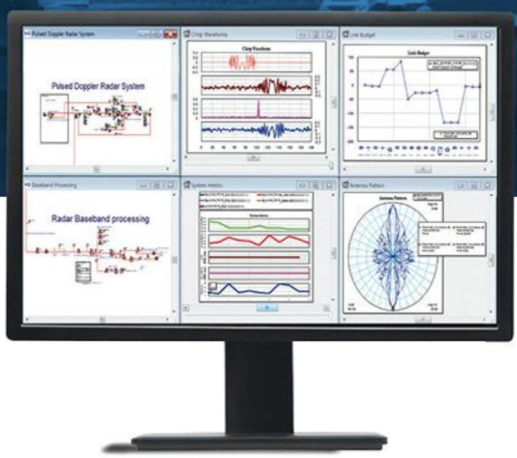

Visual System Simulator | Radar Systems Design

ENSURE SUCCESS WHEN MAKING CONNECTIONS

ALTHOUGH THEY MAY NOT seem glamorous, RF connectors play a crucial role when it comes to achieving desired system performance. Making the effort to properly install connectors thus becomes extremely important. In the white paper, "Bulletproofing the Critical Connection: What You Need to Know About RF Connectors For Critical Communications Applications," RF Industries delves into the methods that should be used to properly install and test RF connectors. The paper also explains how the requirements of future wireless networks are likely to produce new developments in connector technology.

It may seem like connectors have remained unchanged throughout the years, but the paper begins by explaining that connector technology does indeed progress over time. Moreover, connectors do not have the luxury of backup protection. Thus, a bad connection can lead to negative consequences, ranging from slight voltage-standing-wave-ratio (VSWR) changes to complete failures.

The paper details a number of parameters, processes, and procedures that apply to connector installation. Foremost, the operational status of the system must be verified to ensure proper connector operation. In terms of successful connector installation, the focus should be on cable preparation and connector preparation, with an emphasis on proper cable cutting and stripping.

RF Industries
7610 Miramar Rd.,
San Diego, CA 92126
(858) 549-6340
www.rfindustries.com

After identifying the right connector for the specific cable, the next step involves making the actual connection. A connector can be attached to a cable using one of three methods: solder/clamp, crimp, or compression. The document presents the advantages and disadvantages of each one.

Of course, after making a connection comes the testing phase. The general rule is to first conduct a physical inspection. Once a connection has been physically inspected, it must go through electrical testing.

The white paper also discusses some causes of connection failures. For instance, contamination induced by foreign substances will likely lead to failure. Moisture is another frequent nemesis of connectors. The document concludes with a look at the future connector landscape.

SATISFY TODAY'S SPECTRUM EMISSIONS DEMANDS

MEETING COMPLEX SPECTRUM emissions standards requires test solutions that can effectively perform intermodulation distortion (IMD) and RF interference measurements. The signal analyzer lies at the heart of many of these test solutions. In the application brief, "Measuring Intermodulation Distortion and RF Interference," Keysight Technologies explains how to select and optimize a signal analyzer to meet spectrum emissions standards.

Keysight Technologies
1400 Fountaingrove Pkwy., Santa Rosa, CA 95403 (707) 577-2663
www.keysight.com

The brief lists three steps that should be followed when making compliance-based spectrum emissions measurements. The first step is to simply select the correct signal analyzer. Modern signal analyzers can accommodate the complexity associated with today's signals and wireless standards. Specifically, the latest signal analyzers possess a great deal of signal-processing power and computational capabilities.

Another key aspect is to have wide digitizing bandwidths. Ultimately, the measurement capabilities of modern signal analyzers range from basic spectrum measurements to advanced digital demodulation. In addition, software simplifies measurement setup and improves speed.

For wireless spectrum emissions measurements, one must consider a number of parameters. These include spurious-free dynamic range (SFDR), IMD, frequency range, and sensitivity. In addition, measurement applications must accommodate the standards of interest. Analysis bandwidth can also be significant in terms of making fast adjacent-channel-power-ratio (ACPR) measurements, as well as locating time-varying spurious emissions.

The second step is to optimize the signal analyzer—correctly setting its attenuation value, for instance. Furthermore, when selecting the resolution bandwidth (RBW), it should allow for a sufficient displayed average noise level (DANL). The signal analyzer's noise floor can be improved through other methods that include utilizing internal or external preamplification. On top of that, advanced signal-processing technology can help enhance signal-analyzer performance.

The final step involves finding and measuring time-varying spurious and RF interference signals. Real-time spectrum-analysis (RTSA) capability enables signal analyzers to discover and measure these signals. With RTSA, thousands of overlapping spectra can be calculated each second, thereby capturing the shortest transient events. The application brief wraps up with a description of Keysight's MXA X-Series signal analyzer.

HAND FLEX™ CABLES

Hand Flex Cables conform to any shape required.

from $9.75 ea. (qty.1-9) DC to 18 GHz

Get the performance of semi-rigid cable, <u>and</u> the versatility of a flexible assembly. Mini-Circuits Hand Flex cables offer the mechanical and electrical stability of semi-rigid cables, but they're easily shaped by hand to quickly form any configuration needed for your assembly, system, or test rack. Wherever they're used, the savings in time and materials really adds up!

Excellent return loss, low insertion loss, DC-18 GHz. Hand Flex cables deliver excellent return loss (33 dB typ. at 9 GHz for a 3-inch cable) and low insertion loss (0.2 dB typ. at 9 GHz for a 3-inch cable). Why waste time measuring and bending semi-rigid cables when you can easily install a Hand Flex interconnect?

Two popular diameters to fit your needs. Hand Flex cables are available in 0.086" and 0.141" diameters, with a tight turn radius of 6 or 8 mm, respectively. Choose from SMA, SMA Right-Angle, SMA Bulkhead, SMP Right-Angle Snap-On and N-Type connectors to support a wide variety of system configurations.

Standard lengths in stock, custom models available. Standard lengths from 3 to 50" are in stock for same-day shipping. You can even get a Designer's Kit, so you always have a few on hand. Custom lengths and right-angle models are also available by preorder. Check out our website for details, and simplify your high-frequency connections with Hand Flex! *RoHS compliant*

SMA | SMA Right Angle | SMA Bulkhead | SMP Right Angle Snap-On | N-Type | N-Type Bulkhead

Mini-Circuits®

JACK BROWNE | Technical Contributor

MULTIPURPOSE TUNERS Control Impedances from 20 to 110 GHz

These versatile electromechanical tuners can create impedances using three independently adjustable wideband probes at three harmonic frequencies continuously from 20 to 110 GHz.

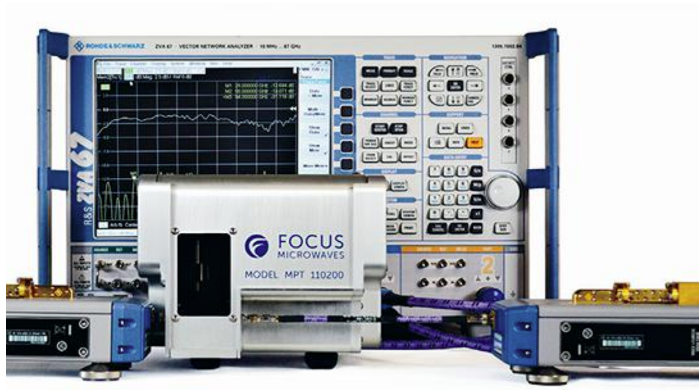

1. The MPT-110200 tuner system provides a variety of impedance tuning functions with three independent tuners that cover a frequency range of 20 to 110 GHz. The screen of the commercial VNA has markers at a fundamental frequency of 28 GHz, and second- and third-harmonic frequencies of 56 and 84 GHz, respectively.

IMPEDANCE TUNING makes it possible to determine accurately how an active device will behave under different source and load conditions. This is also becoming increasingly important at millimeter-wave frequencies, since spectrum has been largely licensed and consumed for different applications at lower frequencies.

As applications like automotive radars and Fifth-Generation (5G) wireless networks look to frequencies at 60 GHz and beyond, impedance tuners are a means of finding impedances for optimum noise and power performance of the active devices for amplifiers in those applications. To meet these needs, an extension to 110 GHz of the Multi-Purpose-Tuner (MPT) line of coaxial harmonic impedance tuners from Focus Microwaves *(www.focus-microwaves.com)* was developed for 5G applications at a fundamental frequency of 28 GHz and harmonics at 56 and 84 GHz.

This extension is a unique impedance-tuning solution with the flexibility to perform source- or load-pull on-wafer and in-fixture measurements. It enables separate changing of impedances at fundamental and harmonic frequencies at literally millions of impedance points.

The new, higher-frequency impedance tuners, such as the 20- to 110-GHz MPT-110200 tuner *(Fig. 1)*, are designed for broadband, non-50-Ω measurements on millimeter-wave devices, using three independently controlled, precision tuning probes. The three probes slide along a common slotted airline (slabline) and approach the center conductor, changing the impedance at any three user-selected harmonic frequencies from 20 to 110 GHz without external hardware interventions.

The tuner's design allows the probes to be withdrawn from the airline, for a return to a 50-Ω test environment. (Note: The MPT tuner technology is protected by U.S. patent Nos. 7,135,941; 8,188,816; 8,212,628; 8,400,238; 8,405,475; and 8,629,752.)

Such impedance tuners can vary the impedance either at the source or at the load of a device under test (DUT). When used at the source, for small-signal measurements, the noise characteristics of a DUT can be analyzed when attempting to find, say, the input impedance match that provides lowest noise figures over a bandwidth of interest.

When used at the load, for load-pull testing, impedance tuners help find which fundamental and harmonic impedances deliver the best DUT output performance. They do so in terms of such parameters as output power at 1-dB compression, gain, power-added efficiency (PAE), adjacent-channel power ratio (ACPR), and error vector magnitude (EVM).

In addition, an MPT-110200 tuner can generate the high VSWRs needed to perform prematching of an active device for optimum performance under certain conditions, such as when operating with a reduced power supply.

Some device behavior, such as output power, can be analyzed with a test setup that adds standard test instruments—e.g., a signal generator—to drive the input and a power meter and sensor to measure power at the output. However, noise analysis and more detailed load-pull measurements require a microwave vector network analyzer (VNA) to provide S-parameter displays

of amplitude and phase and Smith charts that can show the effects of changing impedance on DUT behavior.

Load-pull contours can be shown on a Smith chart to gain an understanding of device behavior at different impedances. It also makes it easier to find impedance matches for best gain, output power, compression behavior, PAE, and error vector magnitude (EVM).

In developing the MPT-110200 tuner, an upgraded (to 110 GHz) version of the ZVA 67 VNA from Rohde & Schwarz was instrumental in characterizing and calibrating the tuner system over extremely wide operating frequency ranges. The display screen of the ZVA 67 VNA in the test system of Fig. 1, for example, shows the frequency response (amplitude versus frequency) of the tuner system. Markers are set at a fundamental frequency of 28 GHz and second- and third-harmonic frequencies of 56 and 84 GHz, respectively.

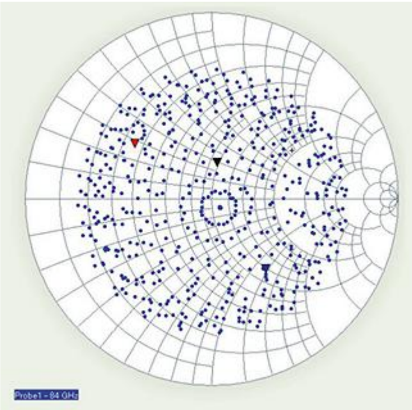

2. The VNA display screen shows a Smith chart with the tuner system's complete impedance coverage at 84 GHz.

As is often the case at higher frequencies, the excellent broadband frequency response of the probes owe a great deal to mechanical design and fabrication, and the millimeter-wave frequency response of the MPT-110200 system would not be possible without the tight machined tolerances of these slug tuners. Especially at the smaller wavelengths (λ) of millimeter-wave frequencies (λ/2 at 84 GHz = 2 mm), machined tolerances and motion control in mechanical slug tuners are critical to maintaining repeatable impedance behavior.

The design of the MPT-110200 involves cascading three separate vertically and horizontally adjustable broadband impedance probes and maintaining consistent broadband reflection factor (Γ) across the full Smith chart. The independent movement of the probes is under stepper-motor control, with the probe movements orchestrated by a computer running custom C++ and C# MPT software.

The software for the MPT tuners includes a proprietary calibration routine that enables the generation of approximately 1 billion possible combinations of impedance points for each set of harmonic frequencies in less than 30 minutes. A full calibration of an MPT system is saved in a tuner calibration structure file of typically only 60- to 120-kb memory, whereby the billions of tuning permutations occur in real time using high-speed random access memory (RAM).

A glance at the internal works of an MPT-110200 tuner system reveals the intricacy of the mechanical detail and the electronic control systems needed to achieve probe movement. It also shows the fine steps needed to provide fine resolution and control of impedances at three different frequencies and across a frequency range from 20 to 110 GHz.

While it is not trivial to incorporate three cascaded impedance tuners within a common enclosure, the relatively compact size of the tuner system achieves several goals. It reduces the signal transmission path between the impedance tuner and the DUT; it helps to increase the tuning range; and it simplifies the placement of the tuner system when it must be mounted onto an automated on-wafer measurement system.

As with other MPT systems, the MPT-110200 tuner can be set in a high-VSWR mode or in a harmonic mode, providing choices in impedance tuning ranges for flexibility in impedance tuning and matching at fundamental frequencies and at harmonic frequencies. The millimeter-wave frequency range of this particular tuner system *(Fig. 2)* makes it a candidate for behavioral modeling of active devices that will be needed for signal amplification in many emerging millimeter-wave applications.

WHY USE HARMONIC TUNING?

Wireless communications have undoubtedly become a staple of many modern lives, whether for personal entertainment or military applications. The complex demands of modern communications systems have pushed a growing number of circuit designers toward impedance tuners as a means to gain optimum performance from discrete devices and integrated circuits (ICs).

By understanding the behavior of an active device in non-50-Ω environments, the impedance matching circuitry around the device, and even the manner in which the device is biased, can be fine-tuned for best performance.

Circuit designers have learned how to use device energy produced at second- and third-harmonic frequencies to improve PAE and EVM. This feeds back the energy at the harmonic frequencies with changes in phase to help cancel unwanted spurious signals and improve the efficiency of the active device, in an operation known as "waveform engineering." This also reduces operating power requirements. This design trend becomes even more critical at higher frequencies.

Harmonic impedance tuners should become increasingly more common in microwave test labs as the move to using higher frequencies continues. Admittedly, the MPT-110200 tuner is just one step in that direction. Nevertheless, the broadband tuner system will provide essential insights into device behavior through 110 GHz and offer a sound starting place for many active circuit designers. mw

FOCUS MICROWAVES INC., 1603 St. Regis, Dollard-des-Ormeaux, Quebec H9B 3H7, Canada; (514) 683-4554, www.focus-microwaves.com

WALT STRICKLER | Product Marketing Manager, Anritsu
www.anritsu.com

VNAs Prove to Be Essential Tools for 5G Communications

The ultimate success of next-generation 5G communication systems will rely heavily on the measurement capabilities of vector network analyzers.

VECTOR NETWORK ANALYZERS (VNAs) are general-purpose measurement instruments that can be used in a wide variety of applications. A perfect example is exemplified in their role in the 5G space, which has become hotbed of activity for VNAs. *Figure 1* presents a basic description of a 5G communication system.

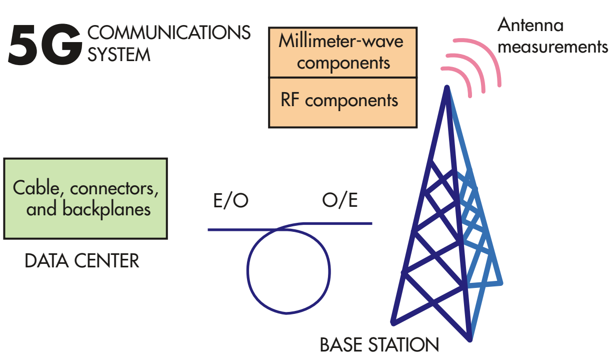

1. This diagram offers a simplified view of a 5G communications system.

To achieve the data rates desired for 5G communications, it is critical that the channels through which the data is passed do not constrain or degrade the data rate. While the information being conveyed is digital, the signals are fundamentally analog. As data rates increase, analog behavior becomes more critical.

VNAs are excellent tools for measuring signal integrity and diagnosing issues when data rates fall short of expectations. For example, VNAs are good for analyzing real-world channel defects, like exceeded tolerances on printed-circuit-board (PCB) artwork, as well as plating and dielectric thickness variations. They are able to evaluate connector performance, construction, and how well connectors are mounted. VNAs can also analyze multi-layer PCB stackups and find imperfect vias or ground-plane issues.

Converting frequency measurements to the time domain, VNAs can even measure the distance to a fault to pinpoint where issues occur. Some VNAs, such as the Anritsu ShockLine MS46500B series, offer an Advanced Time Domain option that enables signal-integrity engineers to measure parameters such as time-domain reflection (TDR), time-domain transmission (TDT), and crosstalk. Furthermore, these analyzers are able to display an eye diagram based on simulated data being transmitted over a measured channel.

To move the massive amounts of data traffic expected in 5G communication systems between data centers and base stations, digital signals will often be converted from electrical to optical signals and back. VNAs can be used to help determine the efficiency at which these conversions happen. When combined with a well-characterized optical modulator or photodiode, VNAs can determine the transfer function of optical transmitters, receivers, and transceivers, including key parameters such as bandwidth, flatness, phase linearity, and group delay.

TESTING 5G BASE-STATION COMPONENTS

At the base station, unparalleled performance will be required of 5G radios and their RF components. Getting the most out of these components requires a deeper understanding of their behavior. Vector network analyzers are used to make measurements as early in the design process as the wafer stage, where S-parameter measurements can be conducted on devices to ensure expected performance or to build device models.

Combined with historically more expensive microwave and millimeter-wave instrumentation, there is a need for dramatic reductions in cost for measurement equipment, such as VNAs. As a result, dedicated cost-effective VNAs have emerged.

Wafer-level measurements pose a unique set of challenges—VNAs need to de-embed the effects of fixtures and probes that enable the measurements. More accurate models lead to shorter design cycles as everyone races to be the first to offer 5G radio solutions. VNAs that cover frequency ranges from 70 kHz to 145 GHz in a single coaxial connection and utilize a wide range of standard embedding/de-embedding techniques allow signal-integrity engineers to realize the most accurate device models.

LOWER-COST SOLUTIONS

Among the performance requirements being placed on 5G radios is the need to handle much wider bandwidths, requiring radios to operate at higher frequencies than traditional communication systems. The move to microwave and millimeter-wave frequencies will require many more cell sites to account for the greater path losses at these frequencies.

Combined with historically more expensive microwave and millimeter-wave instrumentation, there is a need for dramatic reductions in cost for measurement equipment, such as VNAs. As a result, dedicated cost-effective VNAs have emerged (*Fig.* 2). It addresses a market need by offering an unprecedented price point for an E-band VNA, covering frequencies from 55 to 92 GHz in an instrument ready to use right from the box for mass production of E-band components.

The last stage performed by 5G communication systems is the transmission of microwave and millimeter-wave signals to the devices that will utilize them. To achieve 5G's required data rates,

many infrastructure companies are employing multiple-input, multiple-output (MIMO) technologies with antenna systems utilizing large numbers of array elements, known as massive MIMO. This poses challenges for VNAs, which have been historically used to characterize antenna systems.

The geometries associated with microwave and millimeter-wave components are much smaller than traditional RF components. This makes it difficult to do connectorized measurements, forcing companies to instead perform over-the-air (OTA) measurements. Combined with the large number of array elements and the significantly greater path losses at the high frequencies, the VNAs used to characterize the antenna systems must be much smaller and account for the multiple array elements.

To address this issue, there has been an emergence of small microwave/millimeter-wave measurement modules tethered to a base VNA model to get closer to the devices-under-test (DUTs). One such module is shown in *Figure 3*—it enables measurements up to 145 GHz and is about the size of a deck of playing cards.

2. This VNA is able to perform measurements at E-band frequencies.

3. Approximately the size of a deck of playing cards, this module enables measurements up to 145 GHz.

LEVERAGING NEW TECHNOLOGY

To address the numerous aforementioned challenges facing VNAs and the world of 5G, VNA suppliers must take advantage of innovative technologies. For example, Anritsu's application of nonlinear-transmission-line (NLTL) technology in vector network analysis and other test instrumentation has proven to provide high performance, robust, frequency scalable, and cost-effective test solutions.

NLTL technology redefines the level of performance and size of instrumentation while lowering the cost usually associated with high-frequency test and measurement equipment, helping to usher in the next wave of microwave/millimeter-wave instruments. It accelerates next-generation product development and lowers production costs with the portability to install and maintain next-generation radio systems.

VNAs are an essential tool for enabling 5G communication systems. They can be used in applications ranging from data-center signal-integrity measurements, through characterization of the devices and components incorporated in fiber connectivity and millimeter-wave radios in next-generation base stations, to OTA measurements required to address massive-MIMO technologies. mw

JACK BROWNE | Technical Contributor

Scopes Check Coms Signals to 6 GHz

With outstanding measurement power, this family of oscilloscopes provides frequency- and time-domain functionality and flexible triggering for analysis of complex signals.

The R&S RTO2000 family of oscilloscopes includes models with two and four channels and analog bandwidths from 0.6 to 6.0 GHz, along with a host of functions that show signals in frequency and time domains.

WHEN IS AN OSCILLOSCOPE more than "just" a scope? When it is a member of the R&S RTO2000 oscilloscope family from Rohde & Schwarz, with the capabilities to capture and show signals in the time and frequency domains at bandwidths to 6 GHz. With their high performance levels, multiple-domain flexibility, large display screens, and intuitive functionality, these oscilloscopes can reveal the finest details about signals within their capture ranges—be they analog, digital, or powerline *(see photo)*.

The R&S RTO2000 scope family includes two- and four-channel models with 3-dB analog bandwidths from 600 MHz to 6 GHz). The highest-frequency model is the R&S RTO2064, with maximum bandwidth of 4 GHz when four channels are used and 6 GHz when two channels are used. The maximum sampling rate is 10 GSamples/s on each channel for all models.

The only exceptions are the R&S RTO2044 and R&S RTO2064 oscilloscopes, which provide maximum sampling rate of 10 GSamples/s on each channel for all four channels and 20 GSamples/s per channel in two-channel measurement mode. The combination of a low-noise front end and 10-GSamples/s analog-to-digital conversion enables the oscilloscopes to capture and display 1 million waveforms/s.

The vertical resolution is 8 b, with 16-b resolution available for some reduction in sampling rate. A high-resolution option (the R&S RTO-K17 option) is also available, which provides 16-b vertical resolution while preserving the highest sampling rate. The 50-Ω and 1-MΩ input ports for each oscilloscope are rated for maximum input voltages of 5 and 150 V RMS, respectively.

The input sensitivity can be set from 1 mV/div to 10 V/div for the entire analog bandwidth of an instrument. The isolation between channels is better than 60 dB to 2 GHz, better than 50 dB to 4 GHz, and better than 40 dB to 6 GHz.

The R&S RTO2000 family of oscilloscopes is built around a 12.1-in. capacitive touch-sensitive color display screen, with integrated spectrum analysis and spectrogram display functions for performing signal analysis in the frequency and time domains. Each instrument includes an application cockpit with icons for direct access to all applications, such as trigger and decoding functions.

The scopes include color-coded controls to simplify operation. In addition, a unique digital zone trigger function assists in isolating captured signal events in the frequency and time domains to facilitate analysis of signals with complex modulation formats, protocol signals, and precise timing signals. As many as eight zones can be defined to separate different events shown on the screen.

A handy trigger time stamp can be used to label historical measurements and save them for future reference. The oscilloscopes incorporate enough memory (2 GSamples) to capture and analyze even long data sequences and pulse trains.

To further simplify operation, the R&S RTO2000 series includes more than 90 measurements in internal software, allowing users to perform tests automatically with the push of a few buttons. The measurements include amplitude-related, time-domain-related, and jitter measurements, along with the creation of eye diagrams and histograms. Numerous trend, track, and math functions are included to dig deep into signal analysis. mw

ROHDE & SCHWARZ GMBH & CO., P.O. Box 80 14 69, 81614 Munich, Germany; 888-TEST-RSA (1-888-837-8772); www.rohde-schwarz.com

USB & Ethernet

POWER SENSORS

Turn Smart Power Sensors into Low-Cost RF Power Meters!

1 to 8000 MHz -45 to +20 dBm from $745 ea. qty. (1-4)

Mini-Circuits' smart RF power sensors turn almost any Windows® or Linux® based computer into a low-cost testing platform for all kinds of RF components and systems. To give you even more capabilities, our lineup now features models for high-sensitivity measurement of CW, multi-tone and modulated signals at levels as low as -45 dBm!

With 8 different models in stock offering USB and Ethernet control options, measurement speeds as fast as 10 ms*, dynamic range options from -45 to +20 dBm, and measurement capability for continuous wave and modulated signals, chances are, we have a power sensor to meet your needs and fit your budget!

Our user-friendly GUI provides a full range of measurement tools including measurement averaging, time-scheduled measurements, multi-sensor support, and measurement applications supporting RF testing of couplers, filters, amplifiers and more! View data and graphs on-screen or export to Excel® for reporting and data analysis.

All Mini-Circuits power sensors fit in your pocket and come supplied with all the accessories you need for immediate use right out of the box. Visit minicircuits.com and place your order today for delivery as soon as tomorrow.

RoHS compliant

Model	Power Measurement	Frequency MHz	Dynamic Range (dBm)	Control Interface	Price $ ea. (Qty1-4)
NEW! PWR-6LRMS-RC	True RMS	50 to 6000	-45 to +10	USB & Ethernet	1595.00
NEW! PWR-6LGHS	CW	50 to 6000	-45 to +10	USB	895.00
NEW! PWR-6RMS-RC	True RMS	50 to 6000	-35 to +20	USB & Ethernet	1595.00
PWR-4RMS	True RMS	50 to 4000	-35 to +20	USB	1169.00
PWR-2.5GHS-75 (75Ω)	CW	0.1 to 2500	-30 to +20	USB	795.00
PWR-4GHS	CW	0.009 to 4000	-30 to +20	USB	795.00
PWR-6GHS	CW	1 to 6000	-30 to +20	USB	745.00
PWR-8GHS	CW	1 to 8000	-30 to +20	USB	869.00
PWR-8GHS-RC	CW	1 to 8000	-30 to +20	USB & Ethernet	969.00
PWR-8FS	CW	1 to 8000	-30 to +20	USB	969.00

*Measurement speed as fast as 10 ms for model PWR-8-FS. All other models as fast as 30 ms.

Excel is a registered trademark of Microsoft Corporation in the US and other countries.
Neither Mini-Circuits nor Mini-Circuits Power Sensors are affiliated with or endorsed by the owners of the above-referenced trademarks.

Mini-Circuits®

www.minicircuits.com P.O. Box 350166, Brooklyn, NY 11235-0003 (718) 934-4500 sales@minicircuits.com

JACK BROWNE | Technical Contributor

Wideband Mixer Integrates Programmable IF Amplifiers

This dual-channel mixer provides adjustable gain and the wide bandwidth needed for the multiple-antenna and complex-modulation schemes of modern communications systems.

MODERN WIRELESS RECEIVERS, working with complex digital modulation formats and the wide bandwidths needed for high data rates, rely on such techniques as digital modulation and multiple-input, multiple-output (MIMO) antenna schemes to operate effectively. But to achieve optimum performance with diversity receivers and MIMO approaches, signal amplitude control is needed.

Fortunately, the dual-channel LTC5566 downconversion mixer from Linear Technology has that amplitude control built in, taking the form of two intermediate-frequency (IF) variable-gain amplifiers (VGAs) that contribute to a wide conversion-gain range for the dual-channel mixer, across a wide RF input range of 300 MHz to 6 GHz.

The dual-channel downconversion mixer *(see figure)* surrounds of pair of broadband frequency mixers with many of the components needed for a MIMO receiver, all on a single packaged integrated circuit (IC). The LTC5566 features two active mixers, fixed-gain local-oscillator (LO) amplifier for each channel, IF VGAs for each channel, and a serial peripheral interface (SPI). The SPI, or a parallel interface, can control mixer conversion gain as well as other functions.

The LTC5566 dual-channel downconversion MIMO mixer provides programmable frequency-conversion loss/gain for an RF range of 300 MHz to 5 GHz (and usable to 6 GHz), an LO range of 150 MHz to 6 GHz, and an IF range of 1 to 500 MHz.

The LTC5566 offers conversion gain from −3.5 to 12.0 dB, programmable in 0.5-dB steps. Both on-chip mixers are optimized for use from 300 MHz to 5 GHz, but can be used to 6 GHz with degraded performance. Single-ended RF input ports are matched to 50 Ω by means of integrated RF transformers. Differential LO input ports can be driven with single-ended or differential signals. Differential IF output ports can be connected to differential IF filters and amplifiers in support of in-phase (I) and quadrature (Q) modulation schemes.

The two downconversion channels and their mixers are well isolated, with 50-dB channel-to-channel isolation from 300 MHz to 3.6 GHz. The isolation drops somewhat at higher frequencies, although it is still 40 dB at 4.5 GHz. The phase shift between channels is minimal across the frequency-conversion gain-control range.

A real benefit of the LTC5566 is its integrated LO buffers, requiring only 0 dBm power to attain its specified performance. The LO power can vary by as much as ±6 dB with minimal effect on IP3 performance. Also, its RF inputs are rated to withstand as much as +20 dBm power for each channel.

The differential IF gain error between any two 0.5-dB steps in the full 15.5-dB conversion loss/gain range is typically ±0.06 dB. The IF phase is also tightly controlled for the full 15.5-dB gain control range, with typical IF phase error of 2.4 deg. at IF of 150 MHz and 5.5 deg. at an IF of 350 MHz. The LO port input return loss is better than 10 dB from 150 MHz to 6 GHz.

The LTC5566 operates from a single +3.3-V dc supply; nominal current consumption is 384 mA with both channels active. Individual mixers can be turned on or off independently with separate control lines. In the LTC5566's low-power mode, the current draw is reduced to 294 mA, although with some decrease in IIP3 performance. mw

LINEAR TECHNOLOGY Corp., 1630 McCarthy Blvd., Milpitas, CA 95035-7417; (408) 432-1900; www.linear.com

JACK BROWNE | Technical Contributor

Terminations Maintain Security on SMA Ports

A trio of terminations provides ultra-secure protection to 26.5 GHz for coaxial test ports.

COAXIAL TERMINATIONS PROVIDE valuable functions in various systems and test setups, protecting against damage from high-level reflected signals. Unfortunately, they are sometimes mistakenly removed from an application, resulting in damage to expensive test gear.

But while mistakes will happen, a line of coaxial security terminations from Midwest Microwave, part of Cinch Connectivity Solutions *(www.cinchconnectivity.com)*, will help to avoid them. Three different male SMA security terminations are available for use at frequencies through 26.5 GHz, with low VSWR and a foolproof method for staying in place on the test ports they are meant to protect. These low-cost additions to a test setup can provide invaluable protection against costly errors.

Measurement systems often have a number of test ports in addition to the main input port and a reference port for a reference oscillator. For the sake of measurement accuracy, any unused port in a measurement system, such as auxiliary test ports, should be terminated in the system's characteristic impedance—normally 50 Ω at microwave frequencies. Also, damage can occur when high-power reflected signals essentially have nowhere to go, or reach a transmission "dead end" because of an unterminated, resistive signal port that turns the incident signal power into heat.

The potential problem of unterminated test ports can be eliminated through the use of the ingenious Midwest Microwave TRM-244x series of security terminations *(see photo)*. In terms of performance, they work like other coaxial terminations, with one large difference: They can only be removed by using a special tool.

The security terminations are based on the company's standard TRM-244x series of terminations, modified with a passivated stainless-steel shell around the terminations as a protective mechanism. They provide the electrical performance of their TRM-244x series counterparts, with the outer shell preventing accidental removal from sensitive test ports.

The Midwest Microwave TRM-244x series of security terminations provide practical protection for unused test signal ports at frequencies to 26.5 GHz, with removal possible only through the use of a special tool.

SIMPLE ATTACHMENT

The terminations can be attached by hand—fingers, specifically—with the final amount of torque applied by means of the company's TLS-0017-ST-SMA-02 tool and an SMA torque wrench (clockwise to tighten). Once fully torqued and properly attached, they can only be removed by using the same tool and an SMA torque wrench (counterclockwise to loosen).

Three different dc-coupled terminations are available—models TRM-2444-MS-SMA-02, TRM-24440MS-SMA-02, and TRM-24430MS-SMA-02—with respective high-end frequency limits of 8.0, 18.0, and 26.5 GHz. The respective maximum VSWRs are 1.11:1, 1.19:1, and 1.30:1. The SMA male terminations have a characteristic impedance of 50 Ω and will mate to standard SMA female connectors. The terminations are rated for 0.5-W (+27 dBm) nominal power-handling capability at room temperature (+25°C) and slightly less power at elevated temperatures.

Overall, the terminations are designed for operating temperatures from −55 to +125°C. They are available for frequency ranges that accommodate most standard microwave spectrum analyzers and other test equipment in need of signal port protection, and provide a simple but effective means of keeping a termination in place where needed. Just don't lose the special tool. mw

CINCH CONNECTIVITY Solutions Waseca, 299 Johnson Ave. SW, Ste. 100, Waseca, MN 56093; (507) 833-8822, www.cinch.com

Highpass Filters Extend to 30 GHz

Reflectionless 50-Ω MMIC filters in Mini-Circuits' XHF2 Series absorb and terminate stopband signals internally rather than reflecting them back to the source. Covering a total frequency range of DC to 30 GHz, with cutoff frequencies to 18.3 GHz, the MMIC filters are stable to within ±0.3 dB for operating temperatures of -55 to +105°C. The filters can be cascaded and are usable in both transmit and receive applications. As an example, model XHF2-153+ has a stopband of DC to 12 GHz with cutoff of 14.2 GHz and passband of 15.3 to 30.0 GHz. The RoHS-compliant filter is suitable for aerospace and military systems, Wi-Fi, WiMax, and microwave radios and is supplied in a 2 × 2 mm QFN package.

DC Pass Splitter/Combiner Handles 5 W from 680 to 6000 MHz

Mini-Circuits' model SEPS-2-63+ is a two-way, 0-deg. surface-mount power divider/combiner with frequency range of 680 to 6000 MHz. It can handle as much as 5 W input power as a splitter and exhibits low insertion loss (above nominal 3-dB splitting loss) of typically 0.8 dB to 5000 MHz and 1.0 dB to 6000 MHz. The typical isolation between ports is 17 dB to 1200 MHz and 22 dB from 1200 to 6000 MHz. The splitter/combiner can pass as much as 1500 mA current, 750 mA at each port. It is designed for operating temperatures from -40 to +85°C and supplied in a shielded package measuring 1.25 x 1.00 x 0.20 in. with wrap-around terminations. The splitter/combiner is well suited for satcom, wireless, and test and measurement applications.

75-Ω Diplexer Splits Signals to 1220 MHz

Mini-Circuits' model DPLB-2025A0+ is a 75-Ω diplexer that is usable from DC to 1220 MHz. It has a low passband of DC to 204 MHz and a high passband of 258 to 1220 MHz with low typical insertion loss of 1 dB in both passbands. The diplexer delivers high co-channel rejection and excellent out-of-channel rejection, with stopband isolation of typically 50 dB from 258 to 1200 MHz for the low passband and typically 55 dB from DC to 204 MHz for the high passband. The return loss is typically 20 dB or better across the full frequency range. The RoHS-compliant diplexer can be used in multiband radios and cable-television (CATV) applications, including DOCSIS® 3.1 systems and equipment. The surface-mount filter measures 1.181 × 1.181 × 0.280 in. and is designed for operating temperatures from -40 to +85°C.

Coaxial Adapter Mates 2.92-mm Female Connectors

Mini-Circuits' model KM-KM50+ is a low-cost, high-performance DC-to-40-GHz coaxial adapter with 2.92-mm male connectors at both ends for interconnecting cables and components with 2.92-mm female connectors. The RoHS-compliant adapter features low typical insertion loss of 0.13 dB across the full bandwidth with VSWR of typically less than 1.03:1 across the full bandwidth. It provides flat amplitude response with frequency and over operating temperatures from -55 to +100°C. The rugged coaxial adapter features passivated stainless-steel construction and is built for high reliability and long operating lifetime. The 2.92-mm-to-2.92-mm adapter is only 0.74 in. long and 0.28 in. in diameter.

Tiny Surface-Mount LTCC Package Houses Dual Lowpass Filters

Mini-Circuits' model DLFCV-1000+ is a dual lowpass filter with each filter providing passband of DC to 1000 MHz and stopband of 1700 to 5000 MHz. The passband insertion loss is typically 1.2 dB, reaching 3.0 dB at a cutoff frequency of 1280 MHz. The passband VSWR is typically 1.40:1, with passband amplitude unbalance maintained to 0.1 dB and passband phase unbalance within 3 deg. The stopband rejection is typically 27 dB. The passband group delay is closely matched for both filters, and typically less than 0.9 ns at 1000 MHz. The dual lowpass filter is supplied in a ceramic surface-mount package that measures 0.126 x 0.98 x 0.059 in. and is designed for operating temperatures from -40 to +85°C.

Rugged SP8T Electromechanical Switch Channels DC to 12 GHz

Mini-Circuits' model MSP8TA-12-12D+ is an absorptive failsafe single-pole, eight-throw (SP8T) switch constructed for long operating lifetime for applications from DC to 12 GHz. It employs a patented design with few frictionless moving parts for a lifetime rating of more than 5 million switching cycles when hot switching 0.1 W power. With reliable "sleep-time" switching, it features a break-before-make configuration with 20-ms switching that is a good fit for ATE applications. The switch operates with low insertion loss of typically 0.2 dB from DC to 8 GHz and 0.4 dB from 8 to 12 GHz. Isolation is typically 100 dB from DC to 8 GHz and 90 dB from 8 to 12 GHz. The rugged switch is supplied with SMA connectors and is designed for operating temperatures from -15 to +45°C.

CHRIS DeMARTINO | Technical Editor

Modeling and Simulation Software Adapts to Today's Needs

This modeling and simulation tool can prove highly beneficial for engineers across a wide range of disciplines.

RF/microwave engineers today can choose from among a range of currently available simulation tools to meet their specific design needs. One company that specializes in modeling and simulation is COMSOL (*www.comsol.com*). The company's software platform, COMSOL Multiphysics, is a tool designed for physics-based modeling and simulation. On top of that, COMSOL Multiphysics can be expanded with a large number of add-on products that target specific areas, such as electrical, mechanical, acoustic, fluid, thermal, and chemical applications.

One add-on of particular note is the RF Module. This software allows for modeling and simulation of various RF/microwave components, including filters, power dividers, and couplers. Antenna design is another main area targeted by the software. Other applications supported by the RF Module include microwave heating and metamaterials.

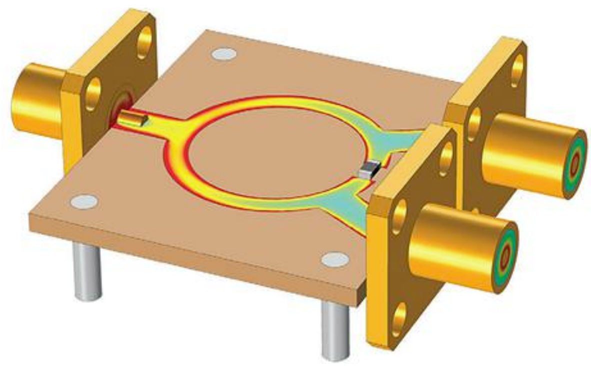

1. This is an image of a Wilkinson power-divider simulation model.

OVERVIEW

I recently had the opportunity to spend some time with the RF Module and get a better sense of its capabilities. Those who have no prior experience with COMSOL Multiphysics ought to know that the RF Module is based on the finite-element method (FEM), which is used to solve Maxwell's equations.

Once a model is simulated, users can observe predefined plots of electric and magnetic fields. Users can also view S-parameter plots, as well as other results from a particular simulation. In addition, the capabilities of the RF Module extend beyond traditional electromagnetic (EM) modeling—the created models can include effects like temperature rise and structural deformations.

APPLICATION GALLERY

The Application Gallery is COMSOL's own library of demo models. Most of these demos include the actual model file, as well as a step-by-step guide that explains how to build the model from scratch. The library contains a variety of microstrip designs, such as a connectorized Wilkinson power divider *(Fig. 1)*, a branchline coupler, and a rat-race coupler.

Moreover, various filter designs are provided, including a lumped-element lowpass filter, a coupled-line bandpass filter, and several waveguide filters. COMSOL also supplies a large number of antenna models, among them dipole, microstrip patch, and Vivaldi antennas. Many other demo models can be found on COMSOL's website—more than 80 specific to the RF Module are currently available.

The step-by-step instructions can be highly beneficial to someone new to COMSOL. By following these guides, one will be able to learn how to create geometries, add materials, specify input/output (I/O) ports, and more. For example, users can become familiar with the various transform options, such as *Array, Copy, Mirror,* and *Rotate*. These functions are intended to streamline the task of creating geometries.

Of course, the ultimate goal of creating a model is to obtain simulation results. The guides demonstrate how to configure different kinds of I/O ports, like coaxial and waveguide types. Readers are further instructed on how to define a mesh, perform a simulation, and ultimately view the simulation results (e.g., electric field distribution and S-parameter plots).

One major benefit of the Application Gallery is that it enables users to create their own designs using an existing demo model as a baseline. In essence, users can identify a demo model similar to their intended design. That model can then be modified in whatever manner necessary to create the desired model. Alternatively, one could follow the step-by-step guide, with the exception of using the actual project parameters in place of those presented in the documentation. In any case, the Application Gallery becomes a major advantage for users.

APPLICATION BUILDER

The Application Builder is another significant feature of COMSOL Multiphysics. It essentially makes it possible to create models that can then be used as customized applications. This capability allows a simulation specialist to build a model that can be customized by other designers without the time and effort needed to return to the original design process. One example is the Slot-Coupled Microstrip Patch Antenna Array Synthesizer found in the Application Gallery *(Fig. 2)*.

USER PRESENTATIONS

The COMSOL Conference 2016 featured a number of user presentations pertinent to RF/microwave engineering. They included “Electromagnetic Modeling of a Millimeter-Wave-length Resonant Cavity,” “Modeling Post Convection Cooling of High Power Waveguide,” “Multiphysics Analysis of RF Cavities for Particle Accelerators: Perspective and Overview,” and many others. Anyone who is interested in learning about the research areas enabled by COMSOL should take a look at these presentations.

FINAL THOUGHTS

The RF Module can benefit anyone involved with designing antennas, filters, waveguide components, and more. For one, the Application Gallery is a good resource for both experienced and new users. New users can become acquainted with the software by taking advantage of the various demo models. The step-by-step guides offer a practical approach to explain the process of building a model. Moreover, the Application Builder is primed for emerging needs like 5G wireless networks. Those who have yet to use COMSOL Multiphysics should give it a try. mw

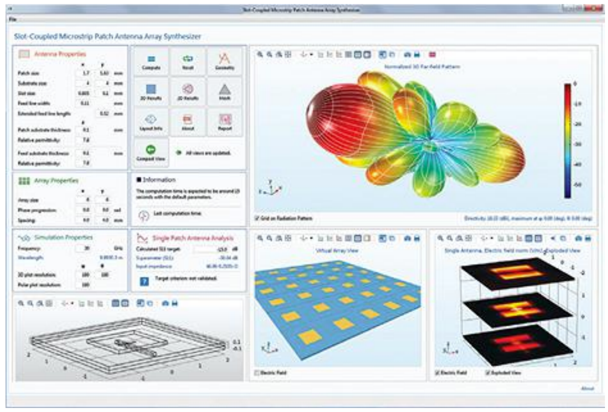

2. This image shows an app, which was built, that simulates a single slot-coupled microstrip patch antenna fabricated on a multi-layered low-temperature co-fired ceramic (LTCC) substrate.

CHRIS DeMARTINO | Technical Editor

Evaluation Kit Supports Move from IR to RF

This evaluation kit helps manufacturers of remote-control products transition to an RF testing environment.

REMOTE CONTROLS HAVE traditionally utilized infrared (IR) technology. However, a change is now underway, as RF technology is increasingly being used in remote controls. In fact, according to industry estimates, almost 50% of TV and set-top-box remote controls currently entering the market are based on RF technology.

One company that is supporting the utilization of RF-based remote-control products is RedRat. The firm's RF Module Evaluation Kit is intended for RF4CE and Bluetooth testing *(Fig. 1)*. Manufacturers of set-top boxes and consumer electronics can take advantage of the evaluation kit's components and software to allow RF testing scripts to be incorporated into current IR test processes. This capability enables evaluation before manufacturers and vendors move to a testing environment that is either mixed or fully RF-based.

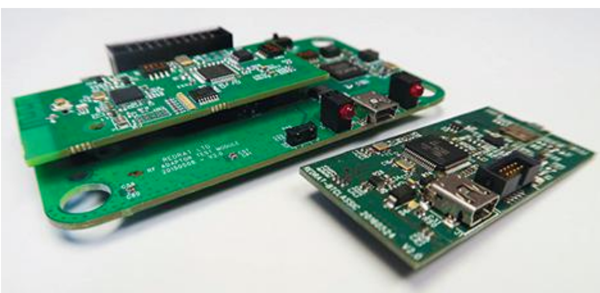

1. This evaluation kit supports both RF4CE and Bluetooth set-top-box testing environments.

With RedRat's evaluation kit, set-top-box manufacturers can examine various factors associated with automated set-top-box control via RF protocols. Such factors include pairing with multiple boxes, the impact of interference in a test facility, and how rapidly commands can be sent. The company says its evaluation kit has been successfully incorporated into RF4CE and Bluetooth set-top-box testing environments of several large set-top-box manufacturers and broadband companies, both in the U.S. and Europe.

The evaluation kit contains a USB module adapter, which can be connected to a laptop or PC via USB. Both Windows and Linux operating systems are supported. Customers can also request Mac-compatible evaluation kits. Moreover, firmware updates are delivered via the RedRat Device Manager.

2. The kit's evaluation software allows for target discovery, pairing, and control.

In addition, the evaluation kit contains an RF module for RF4CE and Bluetooth testing. RF4CE capability is enabled by Texas Instruments' (TI) CC2533 system-on-a-chip (SoC) solution for 2.4-GHz IEEE 802.15.4 and ZigBee applications. The driving force behind the module's Bluetooth capability is TI's CC2564 dual-mode Bluetooth controller.

The kit also consists of evaluation software and associated scripting tools. The evaluation software includes a Windows "Toolbox" application to experiment with target discovery, pairing, and control *(Fig. 2)*. Additional features include an HTTP REST application programming interface (API) for integration with third-party software, as well as a .NET API for direct use in third-party applications.

Although many newer set-top boxes utilize both IR and RF technologies, IR is expected to be phased out over time. With that being said, this evaluation kit appears primed to meet future needs in this arena. mw

REDRAT LTD., +44 1799 520092; www.redrat.co.uk

Coaxial Splitter/Combiner Passes DC from 10 to 40 GHz

MODEL ZN2PD-K44+ is a wideband two-way, 0-deg. power splitter/combiner with a frequency range of 10 to 40 GHz. It is an example of the company's move toward developing a growing number of products for millimeter-wave frequencies. The splitter/combiner can pass as much as 600 mA current, 300 mA at each port. The 50-Ω power splitter/combiner features low insertion loss, with typical loss of 0.6 dB to 18 GHz, 0.9 dB to 26.5 GHz, and 1.0 dB to 40 GHz. The isolation between ports is typically 20 dB, and the component can handle as much as 10 W input power as a splitter. The two-way divider/combiner, well-suited for terrestrial wireless systems, satellite communications (satcom) systems, and radar systems, measures 3.5 × 2.0 × 0.5 in. with 2.92-mm coaxial connectors. It exhibits typical VSWR of 1.50:1 at all ports at the highest frequencies. It is designed for operating temperatures from –55 to +100°C.

MINI-CIRCUITS, P. O. Box 350166, Brooklyn, NY 11235-003; (718) 934-4500, Fax: (718) 332-4661, *www.minicircuits.com*

Continuously Variable Attenuator Spans 1 to 2 GHz

THE MODEL 3814-10, a compact, continuously variable attenuator, provides 0- to 10-dB attenuation from 1 to 2 GHz.

Attenuation resettability is 0.1 dB or better for use in the most challenging applications, such as measurement and military electronic systems. It exhibits maximum insertion loss of 0.5 dB across the full bandwidth and can handle input signals to 5 W average power and as much as 3 kW peak power for short pulses. Maximum VSWR is 1.80:1. The attenuator, which weighs less than 3 oz., is supplied with stainless-steel, female SMA connectors and designed for operating temperatures from –55 to +85°C.

ARRA INC., 15 Harold Ct., Bay Shore, NY 11706-2296; (631) 231-8400, e-mail: sales@arra.com

Planar Resonator VCO Tunes 110 to 330 MHz

MODEL DCM01129 is a planar-resonator voltage-controlled oscillator (VCO) with broad frequency range of 110 to 330 MHz. It provides at least +3 dBm output power over the frequency range, with typical tuning sensitivity of 7 to 16 MHz/V. It achieves its full frequency range with tuning voltages from 0.5 V (for 110 MHz) to 24 V (for 330 MHz). The low-noise oscillator features typical single-sideband (SSB) phase noise of –12 dBc/Hz offset 10 kHz from the carrier with typical harmonics of –10 dBc. The VCO draws no more than 27 mA current from a supply of +5 to +12 V dc. The oscillator, which is designed for operating temperatures from –40 to +85°C, comes in a RoHS surface-mount-technology (SMT) housing measuring just 0.5 × 0.5 × 0.180 in.

SYNERGY MICROWAVE CORP., 201 McLean Blvd., Paterson, NJ 07504; (973) 881-8800, *www.synergymwave.com*

FEM Helps ISM Applications from 902 to 931 MHz

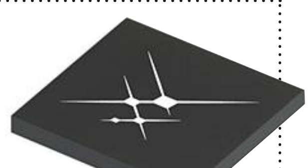

MODEL SKY66105-11 is a compact, front-end module (FEM) designed for industrial-scientific-medical (ISM) band applications from 902 to 931 MHz. A good fit for smart meters, sensors, and machine-to-machine (M2M) applications, the module squeezes a power amplifier, output impedance matching, logic control, and switchable lowpass harmonic filters into a 12-pin multichip-module (MCM) package measuring 8 × 6 × 1.05 mm. It provides +30 dBm (1 W) output power with on/off-time switching time of 1 to 2 µs. Typical small-signal gain is 29 dB. The FCC-compliant FEM runs on battery supplies of +2.0 to +4.8 V dc and draws less than 10 µA sleep-mode current.

SKYWORKS SOLUTIONS INC., 20 Sylvan St., Woburn, MA 01801; (781) 376-3000, e-mail: sales@skyworksinc.com, *www.skyworksinc.com*

Isolators and Circulators Channel L-Band Signals

FAMILIES OF high-performance coaxial isolators and circulators cover L-band frequencies from 0.8 to 2.0 GHz with high power-handling capabilities. Available with SMA and Type N female coaxial connectors, the isolators and circulators handle forward power levels to 50 W with typical insertion loss of 0.9 dB. The isolation is typically better than 15 dB and VSWR is typically 1.45:1.

MECA ELECTRONICS INC., 459 E. Main St., Denville, NJ 07834; (866) 444-6322, *www.e-MECA.com*

ADVERTISER	PAGE
A	
ARRA INC.	c3
www.arra.com	
C	
CALIFORNIA EASTERN LAB	11
www.cel.com/switches	
CIAO WIRELESS INC	17
www.ciaowireless.com	
COILCRAFT	c4
www.coilcraft-cps.com	
COPPER MOUNTAIN TECHNOLOGIES	6
www.coppermountaintech.com/testimonials	
CPI BEVERLY MICROWAVE DIVISION	96
www.cpii.com/bmd	
CTT	87
www.cttinc.com	
D	
DBM CORP	64
www.dbmcorp.com	
DELTA SIGMA INC	42-43
www.111rfpower.com	
E	
ECLIPSE MICROWAVE	106
www.eclipsemdi.com	
EQUIPTO MANUFACTURING	84
www.equiptoelec.com	
F	
FAIRVIEW	26, 27
www.fairviewmicrowave.com	
H	
HEROTEK INC	13
www.herotek.com	
HOLZWORTH INSTRUMENTATION	62
www.holzworth.com	
HUBER+SUHNER INC	80, 105
www.hubersuhner.com	
I	
INTEGRA TECHNOLOGIES	115
www.integratech.com	
INTERNATIONAL MICROWAVE SYMPOSIUM	49
www.ims2017.org	
J	
JFW INDUSTRIES INC	47
www.jfwindustries.com	
K	
KOAXIS INC	48
www.koaxis.com	
KRYTAR INC	83, 104
www.krytar.com	
L	
L-3 NARDA-MITEQ	3
www.nardamiteq.com	
LINEAR TECHNOLOGY CORPORATION	19
www.linear.com/SmartMesh	

ADVERTISER	PAGE
M	
M/A COM TECHNOLOGY SOLUTIONS, INC	8-9
www.macom.com/mmics	
MECA ELECTRONICS INC	7
www.e-MECA.com	
MICRO CIRCUIT LABORATORIES LLC	75
www.microcircuitlabs.com	
MINI-CIRCUITS/SCI COMPONENTS	12, 14-15, 23, 29, 30-31, 35, 41, 53, 59, 67, 73, 81, 85, 89, 91, 93, 95, 99, 101, 109, 111, 113, 119
www.minicircuits.com	
N	
NEXYN CORPORATION	16
www.nexyn.com	
NI AWR	97
www.ni.com/radar	
NI MICROWAVE COMPONENTS	18
www.ni-microwavecomponents.com/quicksyn	
P	
PASTERNACK ENTERPRISES	32
www.pasternack.com	
PLANAR MONOLITHICS INDUSTRIES	1
www.pmi-rf.com	
R	
ROHDE&SCHWARZ GMBH&CO KG	c2
www.rohde-schwarz.com/ad/IoT	
S	
SAGE MILLIMETER INC	60-61
www.sagemillimeter.com	
SKYWORKS SOLUTIONS INC	2
www.skyworksinc.com	
SMITHS MICROWAVE	4
www.smithsinterconnect.com	
SR TECHNOLOGY CORPORATE	115
www.srtechnology.com	
STANFORD RESEARCH SYSTEMS (SRS)	38
www.thinkSRS.com	
SYNERGY MICROWAVE	37, 55
www.synergymwave.com	
T	
TAIYO YUDEN USA INC	74
www.yuden.co.jp/ut/solutions	
TELEDYNE MICROWAVE SOLUTIONS	78
www.teledynemicrowave.com	
W	
W.L. GORE & ASSOCIATES INC	44
www.gore.com/test	
WAMICON	77
www.wamicon.org	
WRIGHT TECHNOLOGIES, INC	63
www.wrighttec.com	

This index is provided as an additional service by the publisher, who assumes no responsibility for errors or omissions.

Subscription Assistance and Information:
(ISSN 0745-2993)
Microwaves & RF is published monthly. Microwaves & RF is sent free to individuals actively engaged in high-frequency electronics engineering. In addition, paid subscriptions are available. Subscription rates for U.S. are $95 for 1 year ($120 in Canada, $150 for International). Published by Penton Media, Inc., 9800 Metcalf Ave., Overland Park, KS 66212-2216. Periodicals Postage Paid at Kansas City, MO and additional mailing offices. POSTMASTER: Send change of address to Microwaves & RF PO Box 2100, Skokie, IL 60076-7800. For paid subscription information, please contact Microwaves & RF at PO Box 2100, Skokie IL 60076-7800. Canada Post Publications Mail agreement No. 40612608. Canada return address: IMEX Global Solutions PO Box 25542, London ON N6C 6B2.

Get a piece of the ARRA pie...

We've said a mouthful with these pie à la mode units . . . A truly time-tested ARRA product. Modified along the way into a lightweight rugged, dependable product. Practically shockproof (can stand up to any environmentals). ***Broadband, linear phase slope, great specs!***

- **Three sized units for maximum, medium, or trim-type phase adjustments**
- **Low insertion loss & excellent VSWR**
- **Completely enclosed sliding mechanism offers maximum protection**

Visit our website at www.arra.com
E-Mail: sales@arra.com

- **Available with micrometer or locked shaft**
- **Unique matching structure**
- **RF power, 100 W average**

Some of the best darn component recipes you can find are cooking at ARRA right now! Send for your copy today and get a piece of the ARRA pie.

. . . the last word in variable attenuators

ARRA INC.
15 Harold Court • Bay Shore NY 11706-2296

Tel 631-231-8400 **Fax 631-434-1116**